CHARACTERIZATION OF THE ROLE OF *ZEA MAYS* BURP DOMAIN-CONTAINING GENES IN MAIZE DROUGHT RESPONSES

By
Kyle Phillips

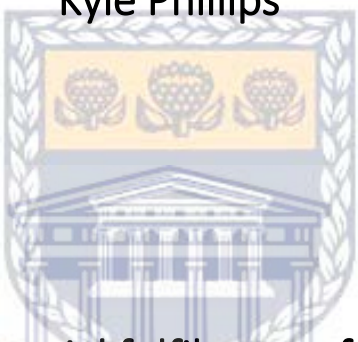

A thesis submitted in partial fulfilment of the requirements for the degree of Philosophiae Doctor (Biotechnology) in the Department of Biotechnology, University of the Western Cape

Supervisor: Prof Ndiko Ludidi
January 2016

CHARACTERIZATION OF THE ROLE OF *ZEA MAYS* BURP DOMAIN-CONTAINING GENES IN MAIZE DROUGHT RESPONSES

Kyle Phillips

KEYWORDS

BURP-domain containing protein

RD22-like proteins

Water deficit stress

Abscisic Acid

Transcript accumulation

Maize

ABSTRACT

Global climate change has resulted in altered rainfall patterns, causing annual losses in maize crop yield due to water deficit stress. Therefore, it is important to produce maize cultivars which are more drought-tolerant. This not an easily accomplished task as plants have a plethora of physical and biochemical adaptation methods. One such mechanism is the drought-induced expression of enzymatic and non-enzymatic proteins which assist plants to resist the effects of water deficit stress. The RD22-like protein subfamily is expressed in response to water deficit stress. Members of the RD22-like subfamily include AtRD22, GmRd22 and BnBDC1 which have been identified in *Arabidopsis thaliana*, *Glycine max* and *Brassica napus* respectively. This study aims at characterising two putative maize RD22-like proteins (designated ZmRd22A and ZmRd22B) by identifying sequence/domain features shared with characterised RD22-like proteins. Semi-quantitative and quantitative PCR techniques were used to examine the spatial and temporal expression patterns of the two putative maize Rd22-like proteins in response to, water deficit stress and exogenously applied abscisic acid in the roots and 2nd youngest leaves of maize seedlings. Using an *in silico* approach, sequence homology of the two putative maize Rd22-like proteins with AtRD22, GmRD22 and BnBDC1 has been analysed. Online bioinformatic tools were used to compare the characteristics of these Rd22-like proteins with those of the two maize proteins. It was shown that the putative maize RD22-like proteins share domain organisation with the characterised proteins, these common features include a N-terminal hydrophobic signal peptide, followed by a region with a conserved amino acid sequence, a region containing several TxV (x is any amino acid) repeat units and a C-terminal BURP domain-containing the conserved

X_5-CH-X_{10}-CH-X_{23-27}-CH-X_{23-26}-CH-X_8-W motif. The putative maize Rd22-like protein appears to be localized in the apoplast, similarly to AtRD22, GmRD22 and BnBDC1. Analysis of the gene's promotor regions reveals *cis*-acting elements suggestive of induction of gene expression by water deficit stress and abscisic acid (ABA). Semi-quantitative and quantitative real time PCR analysis of the putative maize RD22-like gene revealed that the genes are not expressed in the roots. Exposure to water deficit stress resulted in an increase of ZmRD22A transcript accumulation in the 2nd youngest leaves of maize seedlings. ZmRD22A was shown to be non-responsive to exogenous ABA application. ZmRD22B was highly responsive to exogenous ABA application and responded to water deficit stress to a lesser degree. Transcript accumulation studies in three regions of the 2nd youngest leaves in response to water deficit stress showed that ZmRd22A transcripts accumulate mainly at the base and tips of the leaves. A restricted increase in ZmRD22A transcript accumulation in the middle of the leaves was observed. ZmRD22B showed a similar, but weaker transcript accumulation pattern in response to water deficit stress. However, ZmRD22B showed increased transcript accumulation in the middle region of the leaves. In response to exogenous ABA application, ZmRd22B exhibited high transcript accumulation at the base of the 2nd youngest leaves, with the middle showing higher transcript accumulation than the tip of the leaves. It was concluded that ZmRD22A and ZmRD22B share the domain organisation of characterised RD22-like proteins as well as being responsive to water deficit stress, although only ZmRD22B was shown to be responsive to exogenous ABA application.

DECLARATION

I declare that "*CHARACTERIZATION OF THE ROLE OF ZEA MAYS BURP DOMAIN-CONTAINING GENES IN MAIZE DROUGHT RESPONSES*" is my own work and that it has not been submitted for any degree or examination at any other university, and that all the sources I have used or quoted have been indicated and acknowledged by complete references.

Full name: Kyle Phillips

Signed at: The University of the Western Cape Signature: 

Date: 31 January 2016

ACKNOWLEDGMENTS

I would like to thank my principal investigator Prof. Ndiko Ludidi for all his advice and demonstration. What I have learnt from you will be invaluable to furthering my career. To all the members of the Plant Biotechnology Research Group, especially Zintle Kolo, thank you for your support and friendship.

I would also like to thank my family for their support and encouragement throughout my postgraduate career, without them I would not have been able to complete this daunting task.

In conclusion I would like to thank the University of the Western Cape for hosting me during my doctoral studies and the National Research Foundation for funding my work, without your support none of my work would have been possible.

Table of Contents

KEYWORDS i

ABSTRACT ii

DECLARATION iv

ACKNOWLEDGMENTS v

LIST OF ABBREVIATIONS ix

LIST OF FIGURES x

LIST OF TABLES xii

AIM AND HYPOTHESIS xiii

Chapter 1: Literature review 1

1.1. Introduction 1

1.2. Plant responses to drought (abiotic) stress 5

1.2.1. The production of reactive oxygen species 5

1.2.2. The peroxidation of lipid membranes during abiotic stress 10

1.2.3. Cell death as an indicator of abiotic stress 13

1.2.4. Enhanced lignin biosynthesis as a sign of abiotic stress 15

1.3. Plant defense responses to water deficit stress 17

1.3.1. Abscisic acid biosynthesis 17

1.3.2. The induction of stress-responsive genes by ABA signaling 19

1.3.3. Induction of water deficit responsive gene via ABA-independent signaling 22

1.4. BURP domain-containing proteins 25

1.4.1. RD22-like proteins 28

1.5. Conclusion 31

Chapter 2: In silico analysis of GRMZM2G446170 and GRMZM5G800586; two putative maize RD22-like proteins. 32

2.1. Introduction 32

2.2. Methods and materials 34

2.2.1. Construction of a phylogenetic tree 34

2.2.2. Determining subcellular localization of reference and target genes 34

2.2.3. Determining transit peptide cleavage sites 35

2.2.4. Identification of BURP domains 35

2.2.5. Sequence alignment of BURP-domain contain RD22 proteins 35

1.2.6. Promoter analysis for ZmRD22 36

2.3. Results 36
2.3.1. Phylogenetic analysis of five BURP-domain containing proteins 36
2.3.2. Determining the subcellular localization of ZmRD22A and ZmRD22B 38
2.3.3. Determining signal peptide cleavage sites 39
2.3.4. Identification of the BURP-domain 42
2.3.5. Sequence alignment of five BURP-domain containing proteins 44
2.3.6. Promoter analysis of GRMZM2G446170 and GRMZM5G800586. 46
2.4. Discussion 48
Chapter 3: Spatial and temporal transcript accumulation patterns of GRMZM2G446170 and GRMZM5G800586 in response to water deficit stress 52
3.1. Introduction 52
3.2. Methods and Materials 54
3.2.1. Plant Growth and Water Deficit Stress Treatment 54
3.2.2. Measurement of Relative Water Content 56
3.2.3. Measurement of Cell Viability 57
3.2.4. Determination of H_2O_2 and Malondialdehyde Contents 57
3.2.5. Evaluation of the effect of water deficit stress on the transcript accumulation of ZmRD22A and ZmRD22B 58
3.2.6. Statistical analysis of results 62
3.3. Results 62
3.3.1. Morphological comparison between maize seedlings grown in well-watered and water-deprived conditions 62
3.3.2. Measuring relative water content and abiotic stress indicators 64
3.3.3. Semi-quantitative PCR analysis of ZmRD22A and ZmRD22B transcript accumulation levels in response to water deficit stress 66
3.3.4. Relative quantitative RT-PCR analysis of ZmRD22A and ZmRD22B transcript accumulation in response to water deficit stress 67
3.3.5. Relative quantitative RT-PCR analysis of ZmRD22A and ZmRD22B transcript accumulation in response to water deficit stress in defined sections of maize leaves and roots 70
3.4. Discussion 73
Chapter 4: Examining the spatial and temporal expression pattern of GRMZM2G446170 and GRMZM5G800586 in response to exogenous ABA application 79
4.1. Introduction 79
4.2. Methods and materials 81
4.2.1. Plant growth and exogenous ABA treatment 81

4.2.2. Measurement of Cell Viability 82
4.2.3. Determination of H_2O_2 and Malondialdehyde Contents 82
4.2.4. Lignin content assay 83
4.2.5. Evaluation of the effect of exogenous ABA applications on the transcript accumulation of ZmRD22A and ZmRD22B 84
4.2.6. Statistical analysis of results 85
4.3. Results 86
4.3.1. Examining the effect of exogenous ABA application of the stress status of maize seedlings 86
4.3.2. Semi-quantitative RT-PCR analysis of the effect of exogenous ABA application on GRMZM2G446170 and GRMZM5G800586 transcript accumulation 88
4.3.3. Quantitative RT-PCR analysis of GRMZM2G446170 and GRMZM5G800586 transcript accumulation in response to exogenous ABA application 89
4.3.4. Determination of spatial and temporal changes in the transcript accumulation of GRMZM5G800586 in leaf regions by Quantitative RT-PCR in response to exogenous ABA treatments 92
4.4. Discussion 93
Chapter 5: General conclusion 96
Chapter 6: References 100

LIST OF ABBREVIATIONS

AAO	Aldehyde Oxidase
ABA	Abscisic Acid
ABF	Abscisic Acid Binding Factors
ABRE	Abscisic Acid Response Element
ANOVA	One-Way Analysis Of Variance
Au	Absorbance units
bZIP	Basic Region Leucine Zipper
CAD	Cinnamyl Alcohol Dehydrogenase
CAT	Catalase
ChIP	Chromatin immunoprecipitation
COMT	Caffeate O-methyltransferase
cTP	Chloroplast Transit Peptide
DREB	Drought Regulation Factor
DRIP1	DREB2-inactivating protein 1
GHS	General House Survey
GPX	Glutathione Peroxidase
GRF7	Growth Regulating Factor 7
HNE	4-hydroxy-2-nonenal
LB	Leaf Base
LEA	Late Embryogenesis Associated
LM	Leaf Middles
LT	Leaf Tip
MCSU	MoCo Sulfurase
MDA	Malondialdehyde
MnSOD	Manganese Superoxide Dismutase
mTP	Mitochondrial Transit Peptide
NAD(P)H	Nicotinamide Adenine Dinucleotide Phosphate
NCED	9-cis-epoxycartenoid dioxygenase
PCD	Programmed Cell Death
PCR	Polymerase Chain Reaction
Pfam HHMs	Protein Families Hidden Markov models
PPB	Potassium Phosphate Buffer
PUFA	Polyunsaturated Fatty Acid
RC	Reliability Class
ROS	Reactive Oxygen Species
RWC	Relative Water Content
SADC	Southern African Development Community
SDS	Sodium Dodecyl Sulphate
Semi-q-RT-PCR	Semi-quantitative Reverse Transcription Polymerase Chain Reaction
SnRK2	SNF1-Related Protein Kinase
SOD	Superoxide Dismutase

SP	Secretary Pathway
TBA	Thiobarbituric Acid
TTC	2,3-5 triphenyltetrazolium chloride
V3	Vegetative growth stage 3
WFP	World Food Programme
ZEP	Zeaxanthin Epoxidase
Zm	Maize

LIST OF FIGURES

Figure 1.1: South African maize production regions. 2

Figure 1.2: South African seasonal rainfall patterns for July 2014-January 2015. 3

Figure 1.3: The production of $^1O_2$ and O_2^- in the chloroplast. 6

Figure 1.4: The production of superoxide radicals and the functioning of antioxidant systems in leaf peroxisomes. 7

Figure 1.5: Depiction of the mitochondrial electron transport chain and the associated ROS producing site. 8

Figure 1.6: Mechanism of ROS induced lipid peroxidation. 12

Figure 1.7: The induction of programmed cell death by ROS-dependent pathways. 15

Figure 1.8: The induction of ABA biosynthesis by water deficit stress. 18

Figure 1.9: Induction of abiotic stress responses via ABA-dependent and independent pathways. 22

Figure 1.10: Crosstalk between ABA-independent pathway and ABA-dependent pathway. 25

Figure 2.1: Phylogenetic tree depicting the relationship between five BURP-domain containing genes. 37

Figure 2.2: Prediction of the presence of signal peptides and their cleavages sites. 41

Figure 2.3: Determining the presence of a BURP-domain in five proteins suspected of being BURP-domain containing. 43

Figure 2.4: Sequence alignment and domain organization of five BURP-domain containing proteins. 45

Figure 3.1: Morphological comparison of maize seedling grown in the absence and presence of sufficient water supply. 63

Figure 3.2: The degree of abiotic stress experienced in maize seedling grown under well-watered and water-deprived conditions. 65

Figure 3.3: Relative gene expression, expressed as the ratio of pixel intensity of the target and reference genes. 67

Figure 3.4: Relative quantitative RT-PCR analysis of ZmRD22A and ZmRD22B in relation to Zm 18s rRNA and Zm β-tubulin in response to water-deprivation. 69

Figure 3.5: Relative RT-PCR quantification of ZmRD22A and ZmRd22B expression in leaf section in response to drought stress. 72

Figure 4.1: Measuring the stress status of maize seedlings after exogenous application of 50 µM ABA. 87

Figure 4.2: Semi-quantitative RT-PCR analysis of the effect exogenous ABA application has on transcript accumulation of ZmRD22A and ZmRD22B in the 2nd youngest leaves of maize seedlings. 89

Figure 4.3: Quantitative RT-PCR analysis of ZmRD22A and ZmRD22B transcript accumulation in response to the exogenous application of ABA. 91

Figure 4.4: qRT-PCR measurement of ZmRD22B transcript accumulation in leaf sections in response to ABA treatments. 93

LIST OF TABLES

Table 2.1: Subcellular localization prediction for ZmRD22A and ZmRD22B generated using TargetP V1.1 39

Table 2.2: Percentage identity matrix for the alignment of five BURP-domain containing protein sequences 45

Table 2.3: Identification of transcription factor binding sites involved in drought and abscisic acid induced gene expression in the promoter regions of ZmRD22A and ZmRD22B 45

Table 2.3: Identification of transcription factor binding sites involved in drought and abscisic acid induction. 47

AIM AND HYPOTHESIS

The aim of this study is to examine the effect water-deficit stress and exogenous ABA application has on the transcript accumulation of two putative maize RD22-like proteins. Based on literature it is hypothesised that water-deficit stress and exogenous ABA application will result in increased levels of transcript accumulation for both ZmRd22A and ZmRd22B.

The aim of this thesis will be achieved by completing the following objectives:

- *In silico* analysis of ZmRD22A and ZmRD22B in reference to three experimentally characterized RD22-like proteins.
- Examining spatial and temporal expression patterns of ZmRD22A and ZmRD22B.
- Semi-quantitative and quantitative analysis of ZmRD22A and ZmRD22B transcript accumulation in response to water deficit stress.
- Semi-quantitative and quantitative analysis of ZmRD22A and ZmRD22B transcript accumulation in response to exogenous ABA application.

Chapter 1: Literature review

1.1. Introduction

South Africa has several different climatic zones, with the majority of the agriculturally productive provinces receiving summer rainfall. According to the South African Weather Service (2015), there have been eight summer rainfall seasons in which less than 80% of normal rainfall was measured. The United Nations Food and Nutrition working group (2015) indicates that South Africa is faced with a water shortage due to the uncharacteristic and erratic rainfall experienced during the 2014/2015 summer rainfall season, which has reduced the productivity capacity of the affected areas. Persisting drought conditions in South Africa's maize production belt (the North-West Province, the Free-State, KwaZulu-Natal, Gauteng, Mpumalanga and the Northern Province) has resulted in a crop failure rate of over 50%. In May of 2015 (the middle of the South African maize harvesting season), crop yield dropped a third as compared to the same period in 2014 resulting in an estimated crop yield of 9.665 million tons, the worst yield in eight years (WFP 2015). The damage caused by reduced rainfall patterns extends beyond reducing the yield and quality of maize. This is because maize is an important staple food that is a source of carbohydrates for approximately 200 million people living in the Southern African Development Community (SADC). The price of food in South Africa has increased by 4.40% in July 2015, this is in conjunction with an average of 6.36% food inflation from 2009 to 2015 (Trading Economics 2015). The Basic Needs Basket Project, which has undertaken the task of monitoring the price of 39 basic goods and services per month on a national scale, shows that the prices of staple food items such as maize have increased by 37% in urban areas of the Free-State, 34% in the North

West Province and 29% in Gauteng. In rural areas the price of maize has increased by 39% in the Free-State and 25% in Gauteng (SPII 2015).

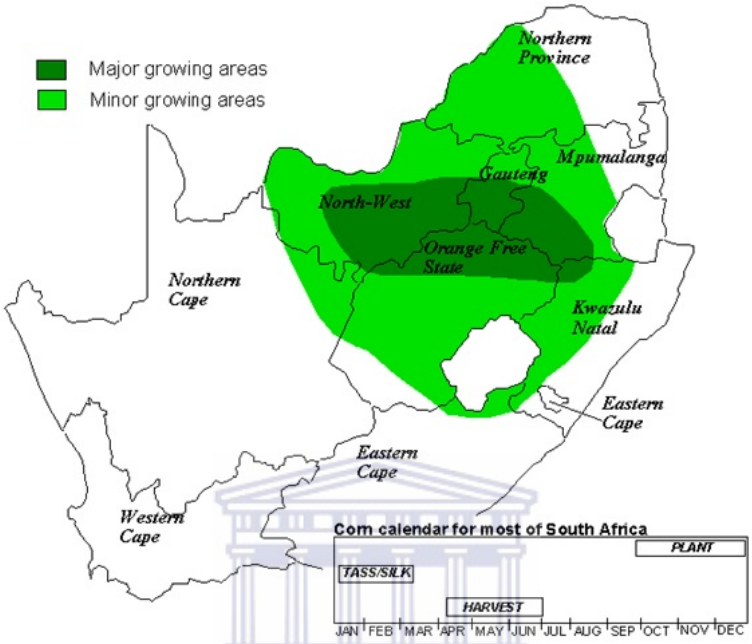

Figure 1.1: South African maize production regions. Graphic depiction of the major and minor maize production areas in South Africa. The major production areas are shaded with dark green and the minor production areas are shaded with light green. The key in the low right corner of the figure provides a timeline for the planting, growing and harvesting of maize. This figure was adapted from the Joint Agriculture Weather Facility(USDA 2004).

In spite of the high cost of staple food, South Africa is deemed to be a food secure country due to its capacity to import staple foods in order to supplement the reduced crop yield consequent to poor rainfall. The finding of a 2009 general household survey (GHS) conducted by Statistics South Africa provides a more realistic picture of South African food security. The GHS reported that approximately 20% of South African household have inadequate or severely inadequate access to food. Areas in which inadequate access to food is most severe include the Free-State in which 33.5% of households have limited access to food, while 23% of households in KwaZulu-Natal, 21% of household in Eastern Cape, 21.5% of household in Mpumalanga, 11.9% of

households in Limpopo and 14.5% of households in the Western Cape have in adequate access to food (Statics South Africa 2009). Aside from being a source of carbohydrates for both humans and livestock , maize is also used in the production of biofuels and starch from maize is enzymatically converted into sorbitol, dextrin as well as sorbic and lactic acids. These products are in turn used in the production of household items which include: beer, ice cream, syrup, shoe polish, glue, ink, batteries, cosmetics, aspirin and paint. Poor maize harvests therefore not only increase the price of food products but also all the products derived from maize.

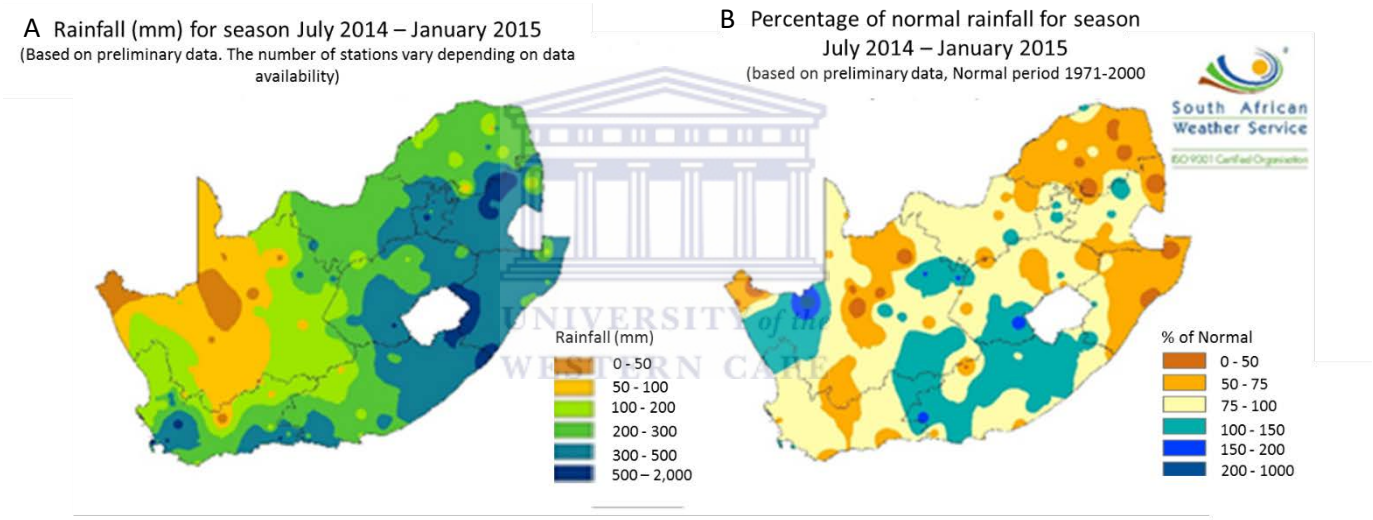

Figure 1.2: South African seasonal rainfall patterns for July 2014-January 2015. (A) The amount of rainfall in mm is illustrated in this map for the time period of July 2014-January 2015 which covers the planting period for maize as well as the start of the tasseling period. The map shows that Gauteng, Mpumalanga and KwaZulu-Natal have received the minimal required water in mm for maize growth, while large portions of the Northern-Province, Northwest-Province and the Free State are receiving rainfall below the minimal requirements for maize growth. (B) The percentage rainfall for the same time period is below normal expected rainfall patterns for the maize growth belt as compared to percentage rainfall from 1971-2000.(South African Weather Services 2015).

The dependence on rain-fed cultivation has been reduced by increasing the area of maize-producing land that is irrigated. The major problem with irrigation is the use of ground water which has a high mineral salt content, these mineral salts accumulate in the soil increasing soil

salt concentrations and imposing further abiotic stress. On the other hand, water is a limited resource in South Africa and drought compounds the problem. Maize is a relatively water efficient crop, producing approximately 15 kg of grain for each milliliters of water consumed and needs between 450 and 600 mm of water per growth season. Exposure of maize to water-stress during vegetative and tasselling growth stages result in short plants with a reduction in green leaf number, leaf dimension, leaf area index and dry mass. Water-stress which extends from the tasselling stage to the cob formation stages results in reductions in grain yield as it affects the weight and number of cobs per plant as well as the weight and number of kernels per cob.

Maize cultivars differ in their sensitivity to water-stress. The tolerance of certain maize cultivars may be attributed to a consortium of physical and biochemical adaptations ranging from leaf curling and regulation of stomatal movement to increased biosynthesis of hormones and stress-defense proteins. Abscisic acid (ABA) is a plant hormone which is known to play a crucial role in the response of plants to water- stress. One such response is a change in expression patterns of dehydration responsive genes such as genes that encode RD22-like proteins. These proteins contain a BURP-domain which to date has been isolated exclusively from plants, indicating a plant specific function. The specificity of RD22-like proteins to plant functioning is further instilled by its response not only to water deficit but also to ABA. This review will look at the physical and biochemical effects of drought on maize plants as well as provide an overview of the synthesis and role of ABA under drought conditions. The characteristics and functioning of RD22-like proteins in drought response will also be included in the review.

1.2. Plant responses to drought (abiotic) stress

1.2.1. The production of reactive oxygen species

Drought can be described as a prolonged absence of precipitation, resulting in a lack of atmospheric and soil moisture. Water deficit (drought) results in changes to habitual plant metabolism. These metabolic changes initiate the overproduction of reactive oxygen species (ROS), which at low concentrations act as signaling molecules that promote the induction of abiotic stress responsive gene expression. When ROS concentration increases above threshold values, redox homeostasis is perturbed and the plant suffers oxidative stress (Gill and Tuteja 2010). Reactive oxygen species result from the acquisition of individual electrons by atmospheric oxygen, due to the molecule's two unpaired electrons and their identical spin quantum numbers (del Río, Sandalio *et al.* 2006). In this way, several reactive oxygen species, including molecules such as superoxide radicals (O_2^-), singlet oxygen ($^1O_2$), hydrogen peroxide (H_2O_2) and hydroxyl radicals (•OH) are produced as by-products of regular plant metabolism in cellular components such as chloroplast, mitochondria and peroxisome (Navrot, Collin *et al.* 2006). Reactive oxygen species are produced in the chloroplast as the production of triose phosphate during photosynthesis requires the transfer of electrons along a transfer chain at photosystem II. Singlet oxygen is generated from this electron transfer when oxygen acts as the final electron acceptor (Gill and Tuteja 2010). Alternatively, diversion of electrons from ferredoxin to oxygen due to overloading of the electron transfer chain leads to the generation of singlet oxygen (Rinalducci, Murgiano *et al.* 2008). Superoxide radicals are also produced in the chloroplast as the result of photo-reduction of O_2 at photosystem I via the Mahler reaction (Makino, Miyake *et al.* 2002).

Hydrogen peroxide is then produced as a by-product of the disproportionation of superoxide anions into H_2O_2 by the antioxidant enzyme superoxide dismutase (SOD). The detoxification of H_2O_2 to H_2O and O_2 is then carried out by enzymes such as catalase and ascorbate peroxidase (Asada 1999). The production of singlet oxygen, superoxide and the generation of H_2O_2 from superoxide, make the chloroplast a major site for ROS production under stress conditions.

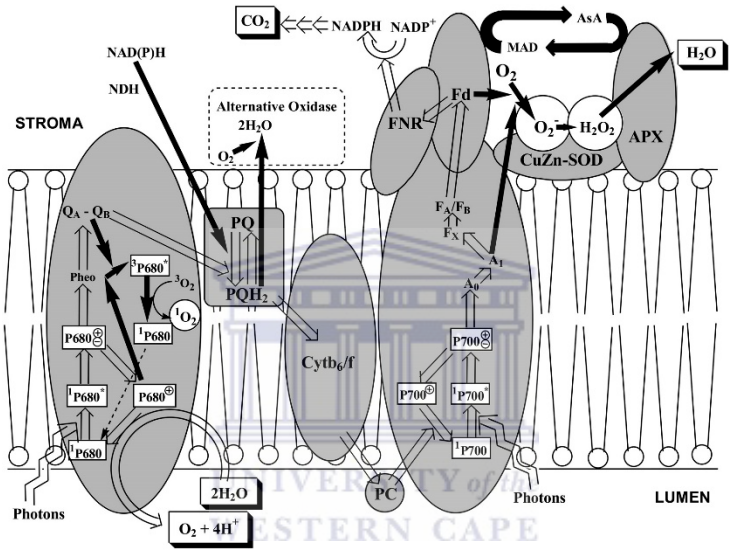

Figure 1.3: The production of $^1O_2$ and O_2^- in the chloroplast. This figure shows the production of $^1O_2$ at PS II and O_2^- at PS I, the white arrows indicate the flow of electrons and excitation of Chloroplast reaction centers under normal light intensity with all the electrons generated being used for the fixation of CO_2. Under conditions where light intensity exceeds capacity the electron flow is diverted resulting in the production of ROS indicated by the black arrows. The top right corner shows the dismutation of superoxide to hydrogen peroxide by Cu/Zn superoxide dismutase and the detoxification of hydrogen peroxide into water by Ascorbate peroxidase (figure adapted from Asada 2006).

Reactive oxygen species are also produced to a lesser extent in the peroxisome due to the oxidative degradation of branched amino acids, which generates superoxide and by extension H_2O_2. The direct production of H_2O_2 occurs in the peroxisome due to the reaction of glycolate oxidase (Hofmann 2011) and the metabolism of triacylglycerols by fatty acid β-oxidation (Hayashi, Nito *et al.* 2002).The main sites of ROS production in the peroxisome are the organelle's matrix and the peroxisomal membrane. In the organelle matrix, the activity of xanthine oxidase

result in the generation of O_2^-. Dismutation of xanthine oxidase generated O_2^- by the activity of superoxide dismutase results in the progentation of H_2O_2 and O_2^- Under stable homeostatic conditions the H_2O_2 generated in the organelle matrix will be scavenged by catalase, however under stress conditions catalase is unable to effectively scavenge H_2O_2 (del Río, Sandalio *et al.* 2006). At the peroxisomal membrane O_2^- is produced due to oxygen acting as an electron acceptor for NAD(P)H- dependent electron transport chains. Aside from H_2O_2 being produced as a by-product of O_2^- detoxification it is also directly produced in the peroxisome via the glycolate oxidase (photorespiratory) reaction, which is required for the oxygenation of ribulose-1.5-biphosphate (Hofmann 2011). Other sources of peroxisomal H_2O_2 production include the metabolism of triacylglycerols in storage organs such as endosperms and cotyledons (Hayashi, Nito *et al.* 2002).

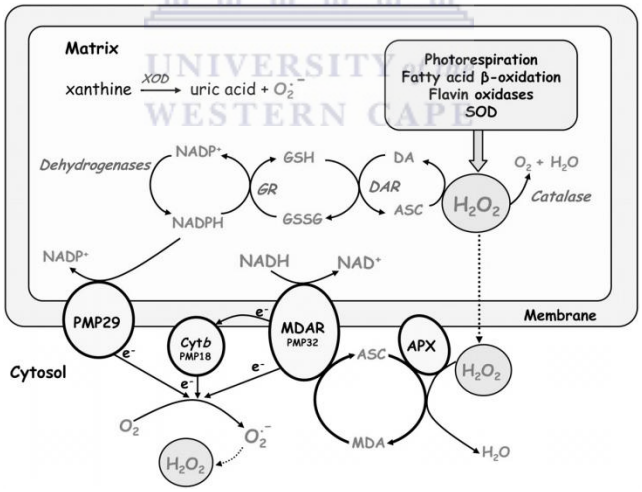

Figure 1.4: The production of superoxide radicals and the functioning of antioxidant systems in leaf peroxisomes. The production of ROS occurs at two sites in the peroxisome, namely the organelle's matrix where the oxidation of xanthine by xanthine oxidase (XOD) liberates uric acid and O_2^-. At the peroxisomal membrane a small ETC composed of three membrane polypeptides namely PMP29, Cytochrome b and monodehydroascorbate reductase (MDAR) contribute to peroxisomal ROS production. (Figure adapted from del Rio et.al 2006)

The electron transfer chains of the mitochondria, which are high in free energy and capable of facilitating the reduction of oxygen, make the mitochondria another potent producer of ROS (Rhoads, Umbach *et al.* 2006). The respiratory activity of the mitochondria is known to generate superoxide under normal respiratory conditions, due to the presence of an electron transport chain in the mitochondria. ROS production becomes aggravated under biotic and abiotic stress conditions and O_2^- is produced at an increased rate at mitochondrial complex I and III. Once O_2^- is generated it is then disproportionated by SOD to form H_2O_2. It is estimated that between 1-5% of oxygen consumed by the mitochondria results in the production of H_2O_2. The accumulation of H_2O_2 in the mitochondria is extremely dangerous due to the presence of divalent metals in the mitochondria with which H_2O_2 can react and generate the highly reactive •OH (Moller 2001).

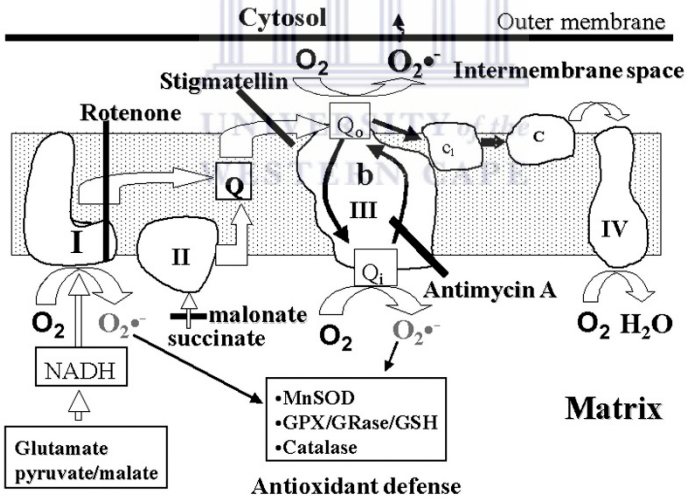

Figure 1.5: Depiction of the mitochondrial electron transport chain and the associated ROS producing site. There are three sites for O_2^- production along the mitochondrial ETC. These include the site at complex I and the Q_1 site at complex III which release ROS into the mitochondrial matrix where they are detoxified by manganese superoxide dismutase (MnSOD), Glutathione peroxidase (GPX) and catalase (CAT). The alternate site for O_2^- generation is the Q_0 site on complex III, at which the O_2^- produced is released away from the matrix antioxidant defenses and is more likely to leave the mitochondria (figure adapted from Chen et.al 2003).

The overproduction of ROS is dangerous to plants as it causes the plant to suffer lipid peroxidation, protein oxidation, DNA fragmentation and inevitably PCD-like cell death, all of which are symptomatic of oxidative stress. Hydrogen peroxide molecules are moderately reactive and have a relatively long cellular half-life (1 ms) and, due to their uncharged state, are able to travel across membranes (Bhattacharjee 2012). The properties of H_2O_2 make it the main cause of lipid peroxidation and subsequently the production of aldehydes such as 4-hydroxy-2-nonenal (HNE) and malondialdehyde (MDA), which damage DNA and proteins by forming conjugates with these molecules (Gill and Tuteja 2010). The reaction of ROS or MDA (and other by-products of oxidative stress) with proteins cause the proteins to become oxidized. Protein oxidation occurs when multiple amino acids in a polypeptide chain are oxidized, generating free carbonyl groups, inhibition or altering of protein activity (Ghezzi and Bonetto 2003). According to Moller, Jenson and Hansson (2007) protein oxidation increases their susceptibility to proteolytic attack. The alkylation and oxidation of DNA also occurs as a result of reaction with ROS. •OH reacts not only with the deoxyribose backbone of DNA but also with both the purine and pyrimidine bases, causing the formation of pyrimidine dimers, cross-linking and strand breaks (Tuteja, Singh *et al.* 2001). The cumulative effects of ROS-induced oxidative stress on plants causes a reduction in protein synthesis, damage to cell membranes and photosynthetic apparatus which culminates in overall retardation of plant growth and development (Atkinson and Urwin 2012).

The ability of H_2O_2 to diffuse across cellular membranes and it's relatively long half-life, makes it dangerous at high concentrations, however these same characteristics also make it suitable to act as a signaling molecule at low concentrations (Gough and Cotter 2011). Grether-Beck and

colleagues (2000) showed that ROS are capable of altering the activity of certain transcription factors, thereby regulating the expression of certain genes. Gene expression may also be altered by the products of oxidative damage such as biologically active lipid peroxidation products, which are able to act as secondary messengers. An example in which ROS acting as signaling molecules is the induction of antioxidant enzymes which detoxify ROS and help maintain redox homeostasis (Gill and Tuteja 2010). Other examples of ROS acting as signaling molecules are seen in both tomato and commelina, where oligogalacturonide elicitor or chitosan was used to induce the propagation of H_2O_2. The elevated levels of H_2O_2 were shown to act as a signal for stomatal closure, this was proven by scavenging of the H_2O_2 with catalase, which reducing both stomatal closure and H_2O_2 levels (Desikan, Cheung *et al.* 2004). H_2O_2 has been implicated in the induction of cell death and the induction or repression of ABA/abiotic stress responsive genes in Arabidopsis. These include sti1-like proteins, LEA-related proteins, cor15a (cold regulated protein precursor) and the BURP domain-containing protein RD22 (Gechev, Minkov *et al.* 2005). The involvement of H_2O_2 in signaling pathways that influence ABA/abiotic stress responses together with RD22 is of interest to research aimed at elucidating the responses of plants to drought.

1.2.2. The peroxidation of lipid membranes during abiotic stress

The first biochemical change that occurs in plants suffering from oxidative stress is the accumulation of aldehydes, hydroxyl and keto fatty acids. These small hydrocarbons result from the interaction of ROS (in particular H_2O_2, O_2^- and •OH) with the polyunsaturated fatty acids (PUFA) which make up lipid membranes (Kotchoni, Kuhns *et al.* 2006, Anjum, Sofo *et al.* 2015). The peroxidation of lipids, as this phenomenon is known, is considered to be one of the most

damaging processes which occur in living organisms during stress conditions. This is evident in the use of lipid peroxidation levels (membrane damage) as an indicator of the degree of oxidative stress the organism is suffering (Garg and Manchanda 2009). Lipid peroxidation levels are an effective indicator of oxidative stress as it occurs when ROS levels exceed threshold concentrations, as is known to occur under abiotic stress (Sharma, Jha *et al.* 2012). The peroxidation of lipids occurs in both organellar and cellular membranes, causing disruption of habitual cellular function as well as intensifying the effects of oxidative stress by producing lipid-derived radicals (Montillet, Chamnongpol *et al.* 2005). The destruction of lipid membranes via peroxidation is a three step process which involves the initiation of peroxidation, the progression of the peroxidation chain reaction and the termination of the reaction. Lipid peroxidation is initiated by the removal of hydrogen atoms from unsaturated fatty acyl chains of the membrane PUFAs. The abstraction of hydrogen atoms are a result of transition metal complexes (iron and copper in particular) and ROS (H_2O_2, $O_2^{\cdot-}$ and •OH) interacting with the PUFAs to give rise to ROO•. This occurs under aerobic conditions as oxygen is added to fatty acids at the carbon-centered radical. Once the formation of ROO• occurs, lipid peroxidation progresses via a peroxidation chain reaction caused by ROO• interacting with adjacent PUFA side chains. Termination most often occurs when a peroxyl radical reacts with α-tocopherol, giving rise to a relatively stable peroxide bridged dimer (ROOR) (Davies 2000, Fam and Morrow 2003, Gill and Tuteja 2010). The chained nature of lipid peroxidation events means that a single initiation has the potential to cause massive membrane damage. The effects of lipid peroxidation include decreased membrane fluidity, which allows free exchange of phospholipid between the two halves of the lipid bi-layer and increased membrane leakage, allowing unrestricted crossing of substances from

one side of the membrane to the other. Macromolecules such as membrane proteins, enzymes as well as other membrane-associated molecules such as receptors and ion channels are also damaged by lipid peroxidation (Møller, Jensen *et al.* 2007). One of the aldehydes that arise from lipid peroxidation is MDA, Changes in MDA levels are easily measurable and these changes are used as a widely accepted indicator of the degree of oxidative stress in higher plants (Shulaev and Oliver 2006). The detection of lipid peroxidation in this way is possible due to the colorimetric reaction of MDA with thiobarbituric acid (TBA) which results in a reddish product referred to as a TBA reactive substance. The degree of lipid peroxidation can then be determined by measuring TBA reactive substance concentrations spectrophotometrically (Hodges, DeLong *et al.* 1999, Taulavuori, Hellström *et al.* 2001).

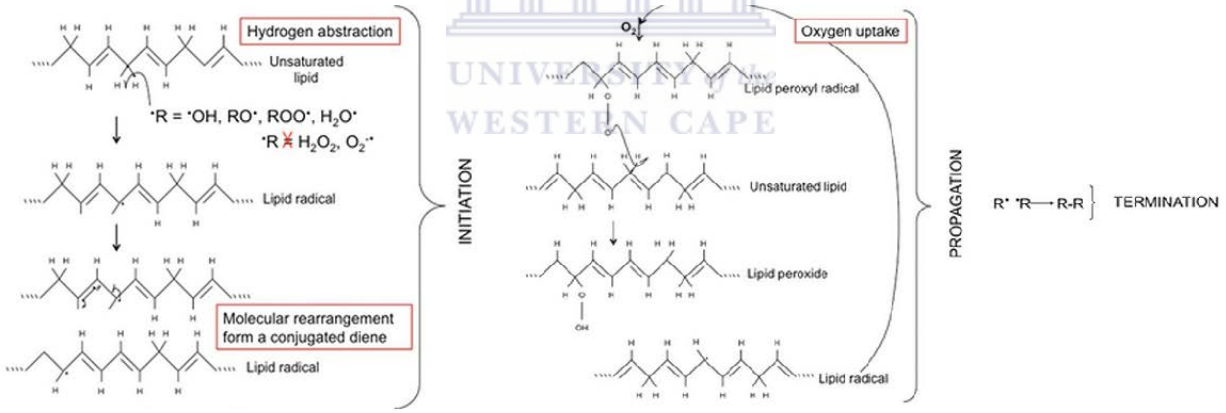

Figure 1.6: Mechanism of ROS induced lipid peroxidation. Lipid peroxidation induced by ROS occurs in three stages, in the initiation stage a hydrogen atom is abstracted from an unsaturated lipid. Hydrogen atom abstraction occurs at methylene groups and results in the formation of lipid radical, a conjugated diene (two double bonds separated by a single bond) is formed through molecular rearrangement. Once initiation has occurred the lipid peroxidation chain is propagated by the formation of a lipid peroxyl radical (lipid radical prior to oxygen uptake) which interacts with the adjacent unsaturated lipid causing a hydrogen abstraction and lipid peroxide formation. The lipid peroxidation chain reaction will continue until terminated by the formation of a peroxide bridged dimer occurs as a consequence of the reaction of a lipid peroxyl radical with an α- tocopherol molecule. (Vatansever, de Melo et al. 2013)

1.2.3. Cell death as an indicator of abiotic stress

Cell death is an integral part of plant growth and development as well as proper responses to environmental stresses, however extensive cell death during unfavorable environmental conditions such as abiotic stress is detrimental to the survival of the plant (Gechev, Van Breusegem *et al.* 2006). Dat and Van Breusegem (2006) suggest that two form of cell death occur in plants, namely apoptosis and necrosis which are distinguished by the presence or absence of hallmarks such as DNA laddering, release of cytochrome c, caspase involvement, ATP depletion, cytoplasmic swelling and loss of membrane integrity (Pennell and Lamb 1997). Cell death which occurs in response to abiotic stress is most likely programmed cell death (PCD) as it is characterized as an active processes involving a single or a series of molecular signals mediated by intracellular death programs (Van Breusegem and Dat 2006). The first experimental evidence for the involvement of ROS in plant cell death was shown by Levine *et al.* (1994) by demonstrating inhibition of ROS-induced cell death by cyclohexamide and protease inhibitors. The involvement of ROS in PCD was also shown by Lam (2004), in this study cellular lesions were identified which possessed several hallmarks of PCD. These included chromosome condensation, DNA laddering and the release of cytochrome c. These PCD-characteristic lesions were observed preceding a biphasic oxidative burst induced by ozone exposure. The relationship between ROS and PCD allows for the use of cell viability as an indicator of oxidative stress-induced cell death. Various instances of ROS-induced damage trigger PCD events. These include damage of choroplastic photosystem II By $^1O_2$ (Krieger-Liszkay, Fufezan *et al.* 2008), H_2O_2 induced oxidation of protein kinases, phosphatases and transcription factors containing thiolate residues (Dat, Vandenabeele *et al.* 2000), the inability of plants to enzymatically detoxify •OH means that its excess production

inevitably induces PCD (Pinto, Sigaud-kutner *et al.* 2003). Measuring changes in cell viability can be achieved assaying physical or metabolic changes to the cell. Using metabolic changes such as the reduction of 2,3-5 triphenyltetrazolium chloride (TTC) to measure cell viability (Chang, Chen *et al.* 1999) is not reliable as changes to enzymatic pathways may be temporary or reversible and some enzymes may still be present after the death of the cells. Measuring physical changes to cells is thus a more reliable determinant of cell viability as physical damage to the cell is irreversible (Castro-Concha, Escobedo *et al.* 2006). Various physical changes can be measured to determine cell viability. These include cytoplasmic streaming, electrolyte leakage and uptake of vital stains (neutral red, Evans Blue, trypan blue and Fluorescein diacetate) into living cells. These methods tend to be more tedious as in the case of cytoplasmic streaming or ineffective as in the case of electrolyte leakage, as stressed cells may have a large transient electrolyte flux. The disadvantage of measuring the number of living cells using vital stain uptake is that changes in cell membrane permeability due to experimental treatments reduce the accuracy of the assay (Jacyn Baker and Mock 1994). An effective measure for measuring cell viability is the non-permeating dyes such as Evans Blue which cannot permeate intact cell membranes but are capable of leaking into ruptured cells and staining the contents of the dead cell. The dye can then be extracted from the dead cells using a detergent such as SDS. The amount of dye taken up by the tissue being studied can then be spectrophotometrically determined.

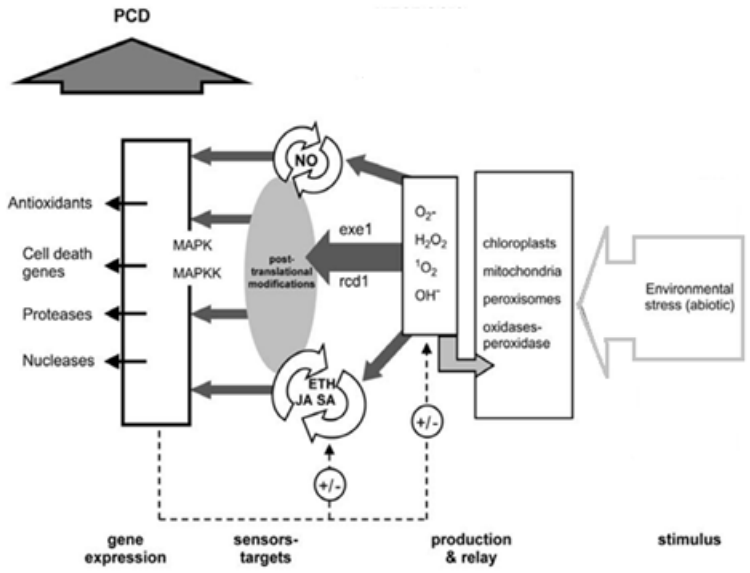

Figure 1.7: The induction of programmed cell death by ROS-dependent pathways. Environmental changes stimulated the production of ROS a several site in the organelles and through enzymatic reactions. The sustained production of ROS at elevated levels initiates signal transduction cascades which involve cross talk between salicylic acid, jasmonate, ethylene and nitric oxide. This cross talk may diminish the stress response of amplify and redirect it down a more specific signal transduction cascade via specific transducer sensors and toward ROS-dependent and cell-death related gene expression. Adapted from Van Breusegem and Dat (2006).

1.2.4. Enhanced lignin biosynthesis as a sign of abiotic stress

Lignin is a phenylpropanoid composed of branched polymers and is abundant in plant cell walls, where it functions as mechanical support allowing plants to grow upright. Lignin also functions in the transport of water via xylem vessels and as a defense mechanism against pests and pathogenic microorganisms (Boudet 2000, Boerjan, Ralph *et al.* 2003). The biosynthesis of lignin has been shown to be altered in maize by abiotic stress, water deficit in particular. In maize roots, deposition of lignin occurs in response to water deficit. However the deposition of lignin in the roots differs between the mature region and elongation region, as observed in both rice (Yang, Wang *et al.* 2006) and wild watermelon (Yoshimura, Masuda *et al.* 2008). The differential deposition of lignin in roots under water deficit results in a greater reduction of growth in the mature region of the root in comparison with the elongation region. The reduction in growth

consequent to lignin deposition is in part due to the increased expression of cinnamoyl-CoA reductase 1 and 2 (lignin biosynthesis associated enzymes), the stiffening of cell walls and reduction in cell wall expansion (Fan, Linker *et al.* 2006). As explained by Yang *et al.*(2006), the expression of cell growth and extensibility genes is upregulated in rice roots during the initial stages of water deficit, this allows increased growth of the roots in the early stages of water deficit stress. Once the intermediate to final stages of water deficit stress is reached, an increase in the expression of lignin biosynthesis genes and reduction in root growth is observed. This suggests that plants increase proliferation of their root system in an attempt to tap into water sources which are located deeper in the soil. Failure to access water sources leads to root growth restriction by lignin deposition in an attempt to conserve resources and outlast the water deficit conditions as seen with *Citrullus lanatus sp.* (watermelon), which exhibits remarkable water deficit resistance (Yoshimura, Masuda *et al.* 2008). The deposition of lignin in the intermediate to late stages of water deficit stress is also observed in the leaves. In a study carried out by Hu *et al.*(2009), two drought-induced genes encoding cinnamyl alcohol dehydrogenase (CAD) and caffeate *O*-methyltransferase (COMT), involved in lignin biosynthesis were identified. The expression of these genes was examined in three drought tolerant and one drought sensitive maize cultivars and expression was found to be down-regulated in the early stages of drought in all four cultivars. The expression of CAD and COMT was up-regulated in the three drought tolerant cultivars during intermediate water deficit stress while the expression of CAD and COMT in the drought sensitive cultivar was unrecovered. Changes in lignin deposition under water deficit conditions mean that lignin content can be used as an indication of water deficit stress (Le Gall, Philippe *et al.* 2015).

1.3. Plant defense responses to water deficit stress

1.3.1. Abscisic acid biosynthesis

The overproduction of ROS during water deficit is indicative of stress in plants. The simulation of abscisic acid (ABA) biosynthesis is another indicator of water deficit. ABA is a phytohormone that is maintained at low levels in plant cells and is required for normal functioning of the cell, this is evident in the loss of vigor observed in ABA-deficient mutants. The requirement of ABA for optimal growth was further proven by the restoration of wild-type growth rates to ABA-deficient mutant upon addition of exogenous ABA (Wasilewska, Vlad *et al.* 2008). Elevation of ABA levels under non-stress conditions have detrimental effects on plant growth and development. However, an increase in ABA biosynthesis under wate-deficit stress is beneficial. The levels of ABA increase in vegetative tissue when plants experience water deficit stress promoting the closure of stomata and reducing water loss from transpiration. The increased levels of ABA are also responsible for the induction of stress-responsive genes which encode enzymes active in stress damage mitigation (Bray 2002, Finkelstein and Rock 2002). The importance of ABA biosynthesis was further established in work carried out by Xiong, Shumaker and Zhu (2001), who showed that ABA-deficient mutants were more prone to water deficit stress than their wild-type counterparts.

It was previously believed that ABA was derived directly from farnesyl diphosphate, a C_{15} sesquiterpene precursor. However, this theory for ABA formation was disproved (Hirai, Yoshida *et al.* 2000, Kasahara, Takei *et al.* 2004). The current theory for biosynthesis of ABA in higher plants is believed to be an indirect pathway in which a C_{40} carotenoid precursor is cleaved to yield

a C_{15} molecule (xanthoxin) followed by the two-step conversion of xanthoxin to ABA by the activity of aldehyde oxidase (Seo and Koshiba 2002, Schwartz, Qin *et al.* 2003). The first reactions in the biosynthesis of ABA occur in the plastid where carotene (C_{40}) gives rise to zeaxanthin. Violaxanthin is then formed by the epoxidation of zeaxanthin by zeaxanthin epoxidase (ZEP). This is followed by several structural modifications culminating in the conversion of violaxanthin to 9-cis-neoxanthin. Xanthoxin is then generated via the oxidative cleavage of 9-cis-neoxanthin by 9-cis-epoxycartenoid dioxygenase (NCED). Xanthoxin is then exported from the plastid to the cytosol where it is converted to ABA-aldehyde and finally ABA (Xiong and Zhu 2003). The importance of ZEP in ABA biosynthesis was shown by the isolation of Arabidopsis mutants that were ZAP-deficient, which showed accumulation of zeaxanthin and drastic reductions in ABA content. These mutants were found to have a wilting phenotype and produced non-dormant seeds (Merlot, Mustilli *et al.* 2002, Xiong, Lee *et al.* 2002).

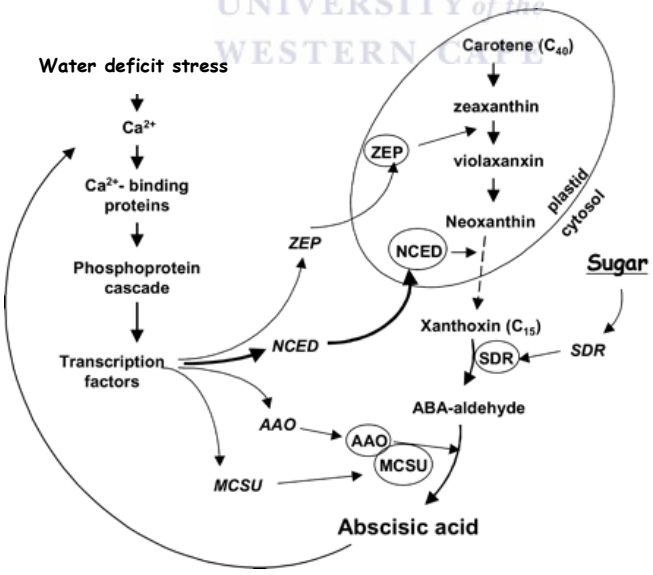

Figure 1.8: The induction of ABA biosynthesis by water deficit stress. The biosynthesis of ABA is induced by water deficit stress and ABA feedback through a Ca^{2+}-dependent phosphorelation cascade as shown on the left. Induction of ABA biosynthesis requires the activation of zeaxanthin epoxidase (ZEP), 9-cis-epoxycaroteniod dioxygenase (NCED), aldehyde oxidase (AAO) and MoCo sulfurase (MCSU). The conversion of the C_{40} carotene percursor occurs in the plastid and involves the epoxidation of zeaxanthin by ZEP to violaxanxin. Following several structural conversions and the oxidative cleavage of neoxanthin by NCED, xanthoxin (C_{15}) is produced and moves into the cytosol where it is converted into ABA via a two-step reaction (Xiong and Zhu 2003).

1.3.2. The induction of stress-responsive genes by ABA signaling

The biosynthesis of ABA is regulated by certain environmental queues, this is believed to occur via transcriptional regulation of the genes involved in ABA biosynthesis. It is believed that many dehydration responsive genes are regulated by the ABA that accumulates during water deficit (Shinozaki and Yamaguchi-Shinozaki 2000). The increase in cellular ABA concentrations is accomplished by an increase in *de novo* production of ABA, coupled with suppression of ABA degradation (Xiong and Zhu 2003). The accumulation of ABA via drought-stress induction is mainly regulated by transcription factors that induce the expression of ABA biosynthesis genes (Xiong, Lee *et al.* 2002) The importance of ABA in water deficit responses was explained by the work of Quin and Zeevaart (1999) as well as Luchi *et al.* (2001) who showed that water deficit results in the potent induction of 9-cis-epoxycarotenoid dioxygenase (NCED); an essential enzyme in ABA biosynthesis. Water deficit responsive gene that are not ABA-responsive have also been identified via the analysis of expression of water deficit responsive genes in Arabidopsis mutants which are ABA-deficient or ABA-insensitive (Bray 1997, Ingram and Bartels 1996). Further analysis of ABA-induced genes unveiled that some genes require the biosynthesis of proteins in order for ABA induction to occur. Shinoazki and Yamaguchi-Shinozaki (1997) hypothesized that four independent pathways facilitate the activation of stress-induced genes during water deficit: two which are dependent on ABA (pathways I and II) and two which are independent of ABA (pathways III and IV).

Water deficit responsive genes which are responsive to ABA; but do not require protein biosynthesis for induction, have been shown to contain Abscisic Acid Response Elements (ABREs) in their promoter regions (pathway II). These ABREs have a conserved sequence, PyACGTGGC and function as *cis*-acting DNA elements in the regulation of ABA-regulated gene expression (Guiltinan, Marcotte *et al.* 1990, Abe, Yamaguchi-Shinozaki *et al.* 1997). ABREs were initially identified in wheat *EM* and rice *rab* genes which were shown to contain a basic region leucine zipper (bZIP) structure. The binding specificity of these ABREs is attributed to the ACGT at the core of the conserved motif, and coupling elements are required to specify the function of the ABREs, resulting in an ABA-responsive complex (Menkens, Schindler *et al.* 1995, Shen and Ho 1995). Currently the molecular mechanism involved in the activation of bZIP proteins by ABA and the binding to ABREs and subsequent initiation of ABA-induced gene transcription is still unknown and further study is required to elucidate the mechanism behind the expression of ABA-responsive genes that are regulated by ABRE *cis*-acting elements.

In some cases, the biosynthesis of protein factors is required for the expression of water deficit inducible genes. This is seen in the induction of RD22 from *Arabidopsis thaliana* (Shinozaki and Yamaguchi-Shinozaki 1997). The ABA-responsive expression of RD22 is governed by a 67-bp region located between position -207 and -141 of the promoter which contains conserved motifs for DNA-binding protein, such as MYC (CACATG) and MYB (CTAACCA). The RD22 promoter however does not contain an ABRE (Iwasaki, Yamaguchi-Shinozaki *et al.* 1995). The ability of MYC and MYB to act as a cis-acting elements in the ABA-induced transcription of RD22 was examined by Abe and Yamaguchi-Shinozaki *et al.* (1997). This was accomplished by designing a wild type (wt) and six mutated 67 bp fragments, with base substitutions in the MYC and MYB sites. Tandem

repeated dimers of the wt and mutant fragments were then fused at position -118 upstream of the rd22 TATA promoter-GUS fusion construct. The construct was then integrated into tobacco via *Agrobacterium*-mediated transformation. Analysis of the transformed tobacco plants showed that the wt 67 bp sequence resulted in a 24.8-fold increase in induction of the GUS reported gene after exposure to water deficit. The mutant 67 bp sequences showed a 3.2-fold decrease with substitutions in both MYC sites, a 9.3-fold decrease with substitutions in the first MYC site and a 6.2-fold decrease with substitutions in the MYB site. A 108.4-fold increase in GUS activity compared to the wt, was observed when the base substitutions were made in the second MYC site only. This suggests that the second MYC site acts a negative regulator of RD22 expression. Fragments with mutations in both the MYC and MYB sites exhibited no expression in response to water deficit; while substitutions outside of the MYC and MYB sites resulted in a 47-fold increase in expression. This suggests that both the first MYC site and MYB site function as positive *cis*-acting elements in the water deficit responsive expression of RD22. The importance of these DNA-binding proteins in the ABA-induced expression of RD22 is illustrated by the inhibition of RD22 expression by cycloheximide an inhibitor of protein synthesis (Yamaguchi-Shinozaki and Shinozaki 1993). Whether the induction of gene expression is direct or indirect, ABA is an important factor in the adaptation of tolerance of plants to water deficit stress.

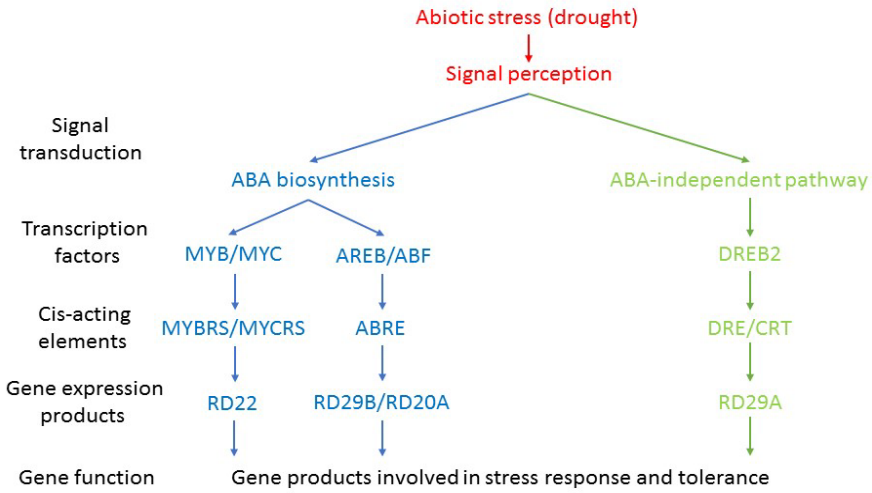

Figure 1.9: Induction of abiotic stress responses via ABA-dependent and independent pathways. Three signal transduction pathways are shown for induction of gene expression under drought, two which are ABA-dependent and one ABA-independent pathway. The induction of gene expression via the ABA-dependent pathway occurs most often in response to the interaction between AREB/ABF and ABRE. Examples of genes induced by this pathway include RD29B and RD20A. The alternative pathway for ABA-dependent induction involves the interaction of MYB/MYC with the cis-acting elements MYBRS and MYCRS. RD22 is one of the drought responsive gene which is induced via this pathway. The interaction of the transcription factor DREB2 and the cis-acting element DRE/CRT is known to induce the expression of drought responsive genes such as RD29A. Adapted from (Shinozaki and Yamaguchi-Shinozaki 2007)

1.3.3. Induction of water deficit responsive gene via ABA-independent signaling

Aside from the induction of abiotic stress genes being induced in an ABA-dependent fashion, several plant genes have been identified which are induced independently of ABA. One such ABA-independent gene is MbDREB1 isolated from dwarf apples. This gene has been implicated in enhancing plant tolerance to low temperatures, drought and high soil salinity (Yang, Liu *et al.* 2011). Another example of a ABA-independent stress induced gene is ERD1, which encodes a chloroplast-targeted Clp protease which functions in both water deficit stress response and senescence (Shinozaki and Yamaguchi-Shinozaki 2007). The expression of genes in an ABA-independent manner is chiefly regulated by DREB2 (Drought-Responsive Element Binding site)

proteins which are members of the APS/ERF family of plant-specific transcription factors. In Arabidopsis DREB2A and DREB2B have been implicated in the plant's responses to drought, high salinity and heat stress as evident by their over expression when Arabidopsis is exposed to these conditions (Sakuma, Maruyama *et al.* 2006b). DREB2 proteins are only able to activate other drought responsive gene after they have under gone post-transcriptional modification, this is shown by their inability to confer drought tolerance when overexpressed in transgenic plants. Furthermore an active from of DREB2 was shown to activate stress-induced genes and improve the drought tolerance of transgenic Arabidopsis cultivars (Zhu 2002, Sakuma, Maruyama *et al.* 2006a). In spite of its active role in enhancing water deficit stress tolerance DREB2 expression is tightly regulated, due to its adverse effect on plant growth. The regulation of DREB2 is carried out by growth-regulating factor7 (GRF7) a transcriptional repressor of several osmotic-stress responsive genes. GRF7 suppresses DREB2 expression by binding a short region of DREB2's promoter, preventing its expression under non-stress conditions. The suppression of ABA-independent activation of DREB2 by GRF7 was shown experimentally in GRF7 knock down/out mutants which show enhanced DREB2A expression, these GRF7 mutants exhibited increased drought tolerance as well as retardation in growth, both consistent with over expression of DREB2A (Yoshida, Mogami *et al.* 2014). The expression of DREBs under normal growth conditions is not only suppressed at a transcriptional level, an ubiquitin-proteasome pathways is proposed for the degrading of DREBs expression that overcomes GRF7 suppression. DREB2A-inactivating protein1 (DRIP1) is a ubiquitin E3 ligase containing a C3HC4 ring domain which is active in the degradation of DREAB2A (Qin, Sakuma *et al.* 2008). The overexpression of DRIP1 was shown to delay the expression of drought responsive genes which were shown to be induced by DREB2A,

while in DRIP1/DRIP2 double knockout mutants the expression of these proteins are increased, this provides evidence of the role of DRIP1 in the regulation of DREB2A activity (Morimoto, Mizoi *et al.* 2013).

The induction of several dehydration responsive gene via exogenous ABA application is indicative of some cooperation between ABA-dependent and ABA-independent signal transduction pathways. Although genes are either induced via an ABA-dependent or ABA-independent pathway the transcriptional network which is active in response to drought/salinity stress requires crosstalk between the two signaling pathways (Yamaguchi-Shinozaki and Shinozaki 2006). The crosstalk between ABA-dependent and ABA-independent signal transduction pathways is believed to be facilitated by three SNF1-related protein kinase 2 (SnRK2) enzymes belong to subclass III. The role of these enzymes in ABA-dependent/independent crosstalk is illustrated by the activation of these proteins by both osmotic stress and ABA (Fujita, Nakashima *et al.* 2009, Fujita, Yoshida *et al.* 2013). The involvement of SnRK2.2/3/6 in osmotic stress and ABA responses were shown in a study carried out by Fuji, Verslues and Zhu (2011). Arabidopsis SnRK2 mutants were exposed to both exogenous ABA and osmotic stress and the mutant in which SnRK2.2/3/6 were intact proved the most responsive to the treatments. Further evidence of crosstalk between the two pathways was shown by Kim *et al.*(2011). An ABRE-motif was identified on a short region of the DREB2A promoter and was shown to be required for the dehydration-responsive expression of DREB2A. In addition to this transient expression and chromatin immunoprecipitation (ChIP) analysis carried out on DREB2A has revealed the involvement of AREB1/ABF2, AREB2/ABF4 and ABF3 in its regulation during ABA signaling under osmotic stress.

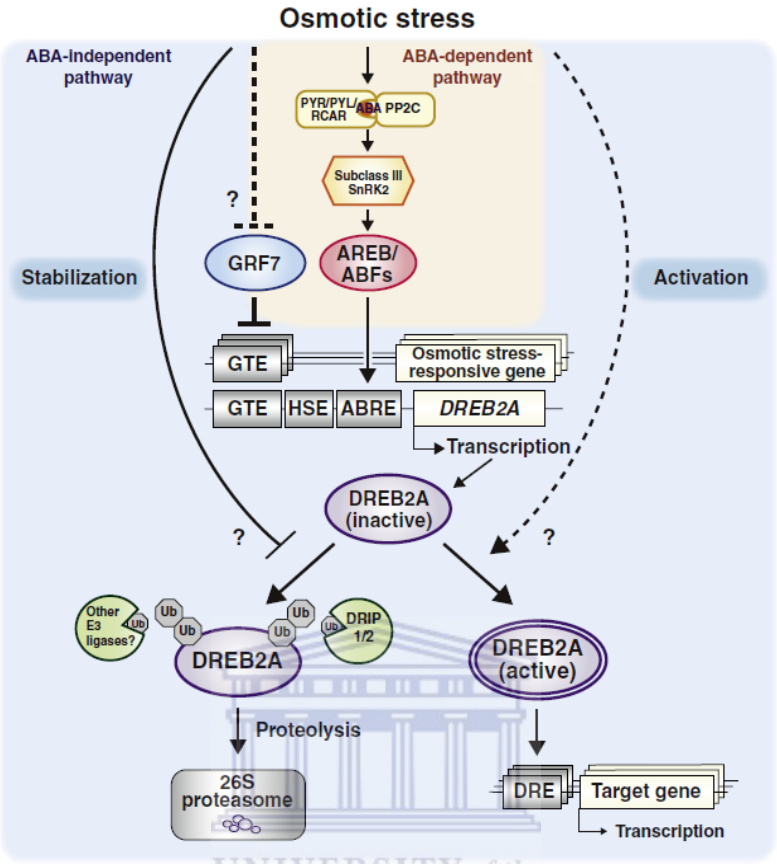

Figure 1.10: Crosstalk between ABA-independent pathway and ABA-dependent pathway. DREB2A is an important transcription factor involved in the ABA-independent expression of stress responsive genes. Due to its adverse effects on plants growth it is regulated on two fronts, By GRF7 and DRIP1/2. Crosstalk between the two pathways is suggested based on the involvement of GRF7 in the suppression of both ABA-dependent and ABA-independent stress responsive genes and the induction of DREB2A by AREB/ABFs. Transcription factors and DNA-binding proteins are shown in colored ellipses. Dashed lines indicate possible although unconfirmed routes. PYR/PYL/RCAR, pyrabactin resistance1/PYR1-like/regulatory components of ABA receptor; PP2C, protein phosphatase 2C; GTE, GRF7-targeting cis-element; HSE, heat shock element; Ub, ubiquitin (Yoshida, Mogami et al. 2014).

1.4. BURP domain-containing proteins

The identification of proteins which contain a BURP domain has to date been restricted to plants, which suggests that these proteins have a plant specific function. Proteins belonging to this family are recognized by their C-terminal BURP domain (Xu, Li *et al.* 2010a). BURP domain-containing proteins are then further divided into seven subfamilies: BNM2-like proteins; USP-like proteins; RD22-like proteins; PG1β-like proteins; BURP V; VI and VII (Granger, Coryell *et al.* 2002, Gan, Jiang

et al. 2011). BURP domain-containing proteins perform a wide range of functions and their subcellular localization is diverse. BURP domain-containing proteins identified in *A. thaliana* (AtUSPL1) and *V. Faba* (VfUSP) have been shown to function in seed development. These seed associated BURP domain-containing proteins are localized in Golgi cisternae, dense vesicles, prevacuolar vesicles as well as protein storage vacuoles (Van Son, Tiedemann *et al.* 2009). GhRDL1, a BURP domain-containing protein identified in cotton, has been implicated in fiber development. GhRDL1, predominantly expressed in elongating fiber cells, is localized to the cell wall where it interacts with GhEXPA1, an α-expansin involved in the loosening of cell walls. Overexpression of GhRDL1 in *Arabidopsis* caused a substantial increase in seed size, while the joint overexpression of GhRDL1 and GhEXPA1 in cotton plants led to increased numbers of cotton bolls producing 40% more fiber and had no adverse effects on either fiber quality or vegetative growth (Xu, Gou *et al.* 2013). BURP domain- containing proteins which are associated with the cell wall have been isolated in tomato and soybean. PG1β is the β-subunit of polygalacturonase isolated from tomato. This BURP-domain protein is cell wall- associated and is active in limiting pectin solubilization. The suppression of PG1β accumulation results in tomatoes which are softer than their wild-type counterpart, this suggests that PG1β is involved in fruit firmness (Brummell and Harpster 2001). Another example of cell wall-associated BURP domain-containing protein is SCB1. This protein in covalently bound to the cell wall matrix in soybean seed coats. A study conducted by Batchelor *et al.*(2002) provides evidence that SCB1 play a role in cellular differentiation. BURP domain-containing proteins are not only active in seed/fruit growth and development but play a protective role as well, as explained by Yamaguchi-Shinozaki and Shinozaki (1993), who identified a BURP domain-containing protein designated AtRD22 whose

expression is induced in response to ABA, water deficit and salinity stress. The role of RD22-like proteins in stress response was also observed in *B. napus*, where the expression of BnBDC1 (a RD22-like protein) is induced by NaCl exposure (Shunwu, Zhang *et al.* 2004). The expression of BgBDC3, a mangrove RD22-like protein, is suppressed by exposure to desiccation and exogenous ABA application (Banzai, Sumiya *et al.* 2002). In spite of the work done demonstrating the

response of RD22-like genes to phytohormones associated with stress response and with abiotic stresses such as water-deprivation and salinity stress, the role of RD22-like proteins in stress response is largely unknown (Wang, Zhou *et al.* 2012). All BURP domain-containing proteins share similar characteristics, which include the C-terminal domain containing four conserved cysteine-histidine repeats and a conserved tryptophan reside in the following motif: X_5-CH-X_{10}-CH-X_{23-27}-CH-X_{23-26}-CH-X_8-W ,where X is any amino acid (Ding, Hou *et al.* 2009). Other identifiable features of BURP-domain containing proteins include an N-terminal Hydrophobic domain, a transit peptide, a variable internal region, and an optional segment with subfamily specific repeat units (Hattori, Boutilier *et al.* 1998). The optional segment can be used to differentiate between the subfamilies: for example, proteins belonging to the BMN2-like subfamily lack the optional segment entirely but have a short conserved segment that succeeds the transit peptide and is directly linked to the C-terminal domain (Ding, Hou *et al.* 2009). RD22-like and USP-like subfamily proteins can be identified by a variable region preceded by a region containing approximately 30 amino acids. The two subfamilies can be distinguished from each other as RD22-like proteins have 3-5 TXV repeats in the variable region while USP-like proteins have no repeats in the variable region (Granger, Coryell *et al.* 2002, Zheng, Heupel *et al.* 1992). The presence of numerous copies of a 14 amino-acid repeat sequence is the characteristic used to recognize PGβ1-like subfamily.

Of the various functions performed by BURP domain-containing proteins, the role of RD22-like proteins in response to abiotic stress is of significance and understanding the process involved in stress response will aid in producing crop cultivars which can withstand harsher growth conditions.

1.4.1. RD22-like proteins

In plants, water deficit stress may occur as a result of transpiration rates that are higher than water uptake from the environment. This phenomenon can be caused by various environmental factors which include low temperatures, high soil salinity and drought. Water deficit has detrimental effects on the growth and development of seedlings and mature plants. The pernicious effects of water deficit include loss of cellular turgor, obstruction of water potential gradients, and loss of cell membrane integrity and protein denaturation. The survival of plants that suffer water deficit is dependent on the plants' ability to respond to the stress, which may occur within seconds of the onset of water deficit by changes being made in the phosphorylation status of proteins or over a long period of time in the form of changes in gene expression which could occur within minutes or hours of water deficit (Bray 1997). One such gene subfamily that undergoes water deficit-induced changes in expression encodes RD22-like proteins. As explained by Yamaguchi-Shinozaki and Shinozaki (1993), the *Arabidopsis thaliana* RD22 (AtRD22) gene contains three introns which are 93, 369 and 457 bp in length, respectively and AT-rich while the coding region of the gene is GC-rich. The ATG codon is located 44 nucleotides from the transcription initiation site and is bordered by the plant consensus sequence AACA ATG GC (Joshi 1987, Burton, Zhang *et al.* 1999) with a TATA box sequence at position -30 (Yamaguchi-Shinozaki

and Shinozaki 1993). The AtRD22 gene sequence contains four cis-acting elements, two of which are MYB recognition elements at positions -144 and -666 and two basic loop-helix-loop recognition elements at positions -200 and -191.

The AtRD22 gene encodes a 42259 Da protein which is 392 amino acids long and has high sequence homology with USP from *Vicia faba* (BäUmlein, Boerjan *et al.* 1991). The presence of an N-terminal hydrophobic region which is composed of 109 amino acid with five repeat sequence suggests that like USP, AtRD22 is translocated across the endoplasmic reticulum membrane (Yamaguchi-Shinozaki and Shinozaki 1993). Due to the similarities between USP and RD22 Northern blot analysis was carried out by Bassuner *et al*. (1988) in which the analysis detected AtRD22 mRNA in developing seeds 3 to 6 days after anthesis, after which the mRNA levels decrease to the point of being non-existent in matured seeds, similar expression pattern is also observed for USP. Using the β-glucuronidase reporter gene system, Iwasaki *et al*. (1995) identified a *cis*-regulating region in the AtRD22 promoter that is responsive to water deficit as well as ABA. A stress responsive RD22-like protein was also identified in soybean and designated GmRD22. This protein was shown to exist in two forms, a larger version which is cytoplasm-specific and a smaller version which was shown to be localized to the apoplast. Localization of GmRD22 was confirmed using confocal microscopy together with the fusion of GFP to the C-terminus of GmRD22 as well as localization of GmRD22 in a native system using immuno-gold electron microscope analysis in soybean leaves. Localization to the apoplast suggests that GmRD22 may play a regulatory role in cell wall metabolism via interaction with other cell wall proteins (Wang, Zhou *et al.* 2012). Once localization of the protein was validated, functional analysis was conducted and it was found that GmRD22 interacts with five cell wall/apoplast

localized proteins. Two of the proteins were branded acid phosphatase of the HAD III subfamily, enzymes which are active in the acquisition of phosphorous by plants (Olczak and Wątorek 2003). One of the GmRD22 interacting proteins was identified as a member of the subtilase family, members of this family may function in control of development, protein turnover or act as downstream components of signaling cascades (Rautengarten, Steinhauser *et al.* 2005). The third class of proteins which GmRD22 was shown to interact with were identified as class III peroxidases, a large family made up of genes involved in a range of stress-responsive functions including lignin and suberin formation, cross-linking of cell wall components, the synthesis of antimicrobial metabolites and participation in both ROS and RNS (reactive nitrogen species) metabolism (Almagro, Gómez Ros *et al.* 2009). The interaction of GmRD22 and GmPer1 (class III peroxidase) was confirmed using a Co-IP (Co-immunoprecipitation) assay and the role of GmRD22 and GmPer1 interaction in response to abiotic stress was assayed. Transgenic rice and Arabidopsis plants which over express GmRD22 were generated, and shown to have a significantly higher lignin content than their wild type counterparts in the case of the rice plants. In the Arabidopsis transgenic line, lignin content was not found to be significantly different. This discrepancy in increasing lignin content is believed to be due to differences in basal lignin content between rice and Arabidopsis. The rice seedlings using in this experiment had a much lower basal lignin content than that measured in the Arabidopsis seedlings (Wang, Zhou *et al.* 2012). The involvement of RD22-like proteins in stress response of Arabidopsis and soybean is a strong indication of these proteins performing a similar function in other plant species. Studying the response of putative RD22-like proteins in crop species could provide important insight in

understanding stress responses and using this knowledge in the generation of stress tolerant crop cultivars.

1.5. Conclusion

The importance of drought tolerant crops for food security is paramount in current times, with the looming threat posed by global warming and all the negative environmental changes that are associated with this phenomenon. The generation of crops that are able to yield sufficient amounts of produce under harsh conditions will only be possible through an in-depth understanding of the effects of drought and other abiotic stresses on the biochemistry of plants on a cellular and holistic level. The dual nature of ROS production, ABA biosynthesis and induction of stress responses by ABA are only three pieces of a larger puzzle which has multiple missing pieces. It is only by illuminating these blank spots in our knowledge that stress tolerant crops can be produced. A good deal is known about ROS and ABA and how they participate in the initiation of stress response, however not a lot is known about many of the protein that are expressed under these conditions. RD22-like proteins are a prime example of a stress responsive protein with unknown properties, much research must still be conducted on this subfamily of proteins in order to elucidate its function during water deficit and other abiotic stresses. The knowledge that the expression of RD22-like proteins are dehydration inducible only provide insight into the "when", now the "why" needs to be elucidated.

Chapter 2: In silico analysis of GRMZM2G446170 and GRMZM5G800586; two putative maize RD22-like proteins.

2.1. Introduction

The computational analysis of biological molecules and biochemical pathways has in recent years become a valuable tool in preliminary elucidation of protein localization, domain organisation and identification of several other features. Bioinformatics tools allow for fast analysis of structural components as well as allowing the grouping of proteins based on these structural components. The picture provided by computational analysis is, however a theoretical one and should always be corroborated by experimental data. The classing of uncharacterised proteins using *in silico* tools is particularly useful as it provides a starting point for experimental characterisation. This can be accomplished by using proteins which have been experimentally characterised as reference points for the characterisation of putative members of the protein class being assessed. As the name suggests, RD22 (responsive to dehydration) genes are inducible by drought stress. It has also been shown that RD22 expression is influenced by abscisic acid (ABA) a phytohormone whose biosynthesis is enhanced under drought stress (Shinozaki and Yamaguchi-Shinozaki 2007). As such, promoter region analysis should provide information on the possible responses of two RD22-like genes, namely ZmRD22A (GRMZM2G446170) and ZmRD22B (GRMZM5G800586) to drought and ABA signals. All BURP-domain proteins have similar characteristics which can be used to identify them as members of this protein family as well as characteristics which indicate the subfamily they belong to. The definitive characteristics of RD22 proteins include a hydrophobic N-terminal domain containing a putative signal peptide, a short segment which is conserved in all BURP-domain proteins, an inconstant internal region consisting

of repeat units. This variable region can be used to distinguish which subfamily a BURP-domain containing protein belongs to, for example proteins belonging to the RD22 subfamily have between 3-5 TxV repeats (where X represents any amino acid) (Ding, Hou *et al.* 2009) and the BURP domain which is located at the C-terminal end of the protein. The BURP domain contains a conserved motif, which is as follows $X_5CHX_{10}CHX_{23\text{-}27}CHX_{23\text{-}26}CHX_8W$ (Matus, Aquea *et al.* 2014). Maize is an important agricultural crop and its yield and crop quality is dependent on receiving enough rain (Rogé and Astier 2015). In spite of this, not much work has been conducted to isolate BURP-domain containing proteins in maize even though these proteins have been shown to function in withstanding the effect of water deficit stress in several other plant species (Gan, Jiang *et al.* 2011). In this study, three experimentally characterised BURP-domain containing proteins, namely Glyma6G081100 (GmRD22) (Wang, Zhou *et al.* 2012), AT5G25610 (AtRD22) (Harshavardhan, Seiler *et al.* 2014) and AY293830 (BnBDC1) (Shunwu, Zhang *et al.* 2004) will be used to analyse two putative RD22-like proteins from maize, namely GRMZM2G446170 and GRMZM5G800586, which are designated ZmRD22A and ZmRD22B respectively. The reference proteins have been shown to belong to the RD22 subfamily of BURP-domain containing proteins. As such similarity between their domain organisation and that of ZmRd22A and ZmRD22B will be an indication of their being RD22-like proteins.

2.2. Methods and materials

2.2.1. Construction of a phylogenetic tree

Sequence data was obtained from phytozome V10.3 (http://phytozome.jgi.doe.gov/pz/portal) and Genbank (http://www.ncbi.nlm.nih.gov/genbank/). The nucleotide sequences (in fasta format) for GmRD22, AtRD22, BnBDC1, GRMZM2G446170 and GRMZM5G800586 were then imported into Geneious V8.1.7. A phylogenetic tree was then constructed by geneious tree builder using a Global alignment with a Blosum62 scoring matrix. The Jukes-Cantor model was used to determine genetic distance and the neighbour-joining method was used to build the tree with AtUSPL1 (*Arabidopsis thaliana* unknown seed protein) acting as an outgroup.

2.2.2. Determining subcellular localization of reference and target genes

The subcellular localization of the proteins encoded by GRMZM2G446170 and GRMZM5G800586 was determined by uploading the protein sequence (in Fasta format) of the target genes onto the TargetP1.1. server (http://www.cbs.dtu.dk/services/TargetP/). TargetP1.1. predicted the subcellular localization of the target proteins based on the predicted presence of an N-terminal signal sequence which may be specific to the chloroplast, mitochondria or secretory pathways. The prediction of subcellular localization was determined using plant networks and a specificity of >0.95. The analysis was carried out based on a method described by Emanuelsson and Nielsen *et al.*(2000).

2.2.3. Determining transit peptide cleavage sites

The cleavage site for signal peptide removal was determined by uploading the protein sequences (in Fasta format) of GRMZm2G446170, GRMZm5G800586 and the proteins encoded by the reference genes onto the SignalP4.1 server (http://www.cbs.dtu.dk/services/SignalP/). Identification of signal peptide cleavage sites was carried out using eukaryotic organism grouping and default D-cut-off values which are optimised for correlation. The cleavage sites were identified using the method described by Petersen and Brunak *et al.*(2011).

2.2.4. Identification of BURP domains

The presence of a BURP domain in GRMZM2G446170 and GRMZM5G800586 was determined by inputting the protein sequences (in Fasta format) into myhits SIB motif scan (http://myhits.isb-sib.ch/cgi-bin/motif_scan). The protein sequences GMRD22, AtRD22 and BnBDC1 were input as well to determine how accurate the domain identification provided by motif scan was. The protein sequences were compared to Pfam HMMs (global models) to identify all known motifs which were present in the protein sequences being analysed.

2.2.5. Sequence alignment of BURP-domain contain RD22 proteins

The nucleotide sequence of GRMZM2G446170, GRMZM5g800586 and three RD22 reference genes AtRD22, GmRD22 and BnBDC1 were obtained from phytozome V10.3 (http://phytozome.jgi.doe.gov/pz/portal.html) and genbank (http://www.ncbi.nlm.nih.gov/genbank/). The nucleotide sequences were then imported to Geneious V8.1.7. and a global pairwise alignment using scoring matrix Blosum62 was carried out.

The sequence alignment was then used to highlight structural component and domain organisation which was similar across the five gene sequences.

1.2.6. Promoter analysis for ZmRD22

A 2000 bp region upstream of the transcription start site of GRMZM2G446170 and GRMZM5G800586 was obtained using phytozome V10.3 (http://phytozome.jgi.doe.gov/pz/portal). These sequences were then inserted into the PlantPan 2.0 plant promoter analysis tool (http://plantpan2.itps.ncku.edu.tw/promoter.php). Using the PlantPan transcription factor library specific for maize, possible transcription factor binding sites were identified.

2.3. Results

2.3.1. Phylogenetic analysis of five BURP-domain containing proteins

A phylogenetic tree was constructed to infer the evolutionary relationship between five RD22-like genes, two of which were identified in *Zea mays (*ZmRD22A and ZmRd22B*)* , whereas the remaining three were identified in *Arabidopsis thaliana (*AtRD22), *Brassica napus* (BnBDC1) and *Glycine max* (GmRD22). The gene encoding the *Arabidopsis thaliana* unknown seed protein (AtUSPL1) was used as an outgroup in the construction of this tree as it is encodes a protein from the BURP-domain containing protein family, however it is not a member of the RD22 subfamily. Two branching events have occurred to produce the current versions of the maize genes ZmRD22A and ZmRD22B. Firstly, genetic change events resulted in 0.27 base substitutions in every 100 bases between the ancestor at the root of the tree and the ancestor at node A. The two maize genes have diverged from a common ancestor at node A and have undergone 0.07

(ZmRD22A) and 0.06 (ZmRD22B) base substitutions in every 100 bases of the ancestral sequence. All of the nucleotide sequences identified in dicot plant species share the same root ancestor as the nucleotide sequences originating from the monocot plants, however the genetic change event at node B resulted in 0.04 base substitutions per 100 bases causing the formation of two separate braches in the dicot section of the tree. After a further 0.2 base substitutions per 100 bases, the current version of GmRD22 was formed as seen at node D. The branching at node C occurred after genetic change in the ancestor at node B, 0.22 base substitution per 100 bases resulted in the branching event at node C which, represents the common ancestor shared by AtRD22 and BnBDC1. Both sequences differ from their common ancestor by 0.08 and 0.06 base substitution per 100 bases respectively.

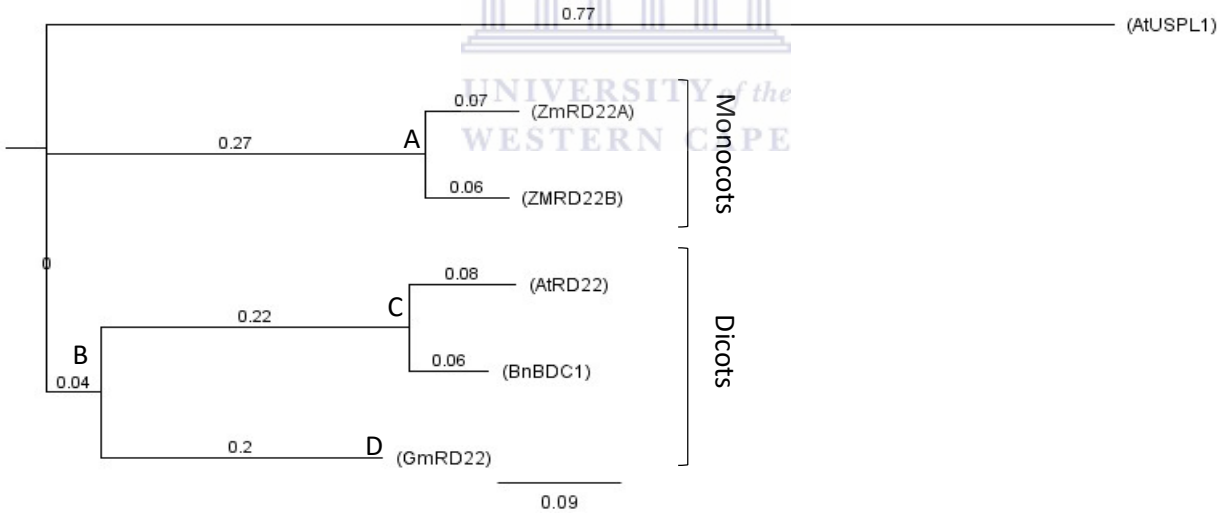

Figure 2.1: Phylogenetic tree depicting the relationship between five BURP-domain containing genes. The scale for genetic change is indicated as 0.09. The values indicate branch length providing a measure for nucleotide substitutions per site in relation and the branch points/nodes are labelled A to D. The tree used AtUSPL1 as an outgroup, the brackets indicate which class the plants enclosed by those bracket belong too.

2.3.2. Determining the subcellular localization of ZmRD22A and ZmRD22B

Predictions were made regarding the subcellular localization of ZmRD22A and Zmrd222B using TargetP V1.1. Table 1 is the output generated by TargetP and depicts the results of the analysis. The names and lengths of each sequence analyses are provided in the first and second columns. The score received for each of the possible subcellular locations are shown in columns 5-6, and are labelled cTP (chloroplast transit peptide), mTP (mitochondrial transit peptide), SP (secretary pathway) and other (any location other than those previously described). The location (Loc) indicates the location for which the protein has the highest score, i.e. its predicted subcellular location. The last column RC shows the reliability class of the prediction, where 1 indicates the strongest prediction and 5 the weakest. The RC value is a measure of the difference between the highest location score and lowest location score of each protein sequence analysed. A RC value of 1 indicates that the difference in highest and lowest location scores is >0.800 as seen with the protein sequences for At5G25610.1 (AtRD22), Ay293830.1 (BnDCB1) and Glyma.06G081100.1 (GmRD22). A lower RC value like 4, as seen with the protein sequences for GRMZm2G446170 (ZmRD22A) and GRMZm5G800586 (ZMRD22B), indicates a difference in the highest and lowest location scores of between 0.400 and 0.200. The cut-off value for each subcellular localization is provided in the bottom row. These values are the result of a specificity >0.95. Assignment of a subcellular location requires the target protein to have the highest score for the assigned

location, the score for the assigned location also has to be higher than the cut-off values for that location.

Table 2.1: Subcellular localization prediction for ZmRD22A and ZmRD22B generated using TargetP V1.1

Name	Length	cTP	mTP	SP	Other	Loc	RC
AT5G25610.1	392	0,02	0,033	0,969	0,025	SP	1
AY293830.1	387	0,057	0,064	0,917	0,026	SP	1
Glyma06G81100.1	343	0,008	0,04	0,979	0,052	SP	1
GRMZM2G446170_T01	375	0,04	0,229	0,554	0,014	SP	4
GRMZM5G800586_T01	456	0,031	0,038	0,579	0,023	SP	4
cut-off		0,73	0,86	0,43	0,84		

2.3.3. Determining signal peptide cleavage sites

The presence and locations of the signal peptides and there cleavage sites of the putative maize Rd22 proteins and that of characterised Rd22 proteins was determined using SignalP. SignalP produces three output scores for each position in the input sequence; namely a C-score represented by the red vertical lines, an S-score represented by the green curve and a Y-score represented by the blue peak, the graph also indicates a cut-off value represented by a horizontal red line. The graph in Figure 2.2.A suggests that the signal peptide in AtRD22 is located between position 1 and 20, as indicated by the drastic drop in the S-score after position 20. Cleavage of the signal peptide to produce the matured protein occurs between positions 21 and 22 as shown by the C-score and Y-score values at these positions. Figure 2.2.B, which was generated for BnBDC1, has the shortest signal peptide spanning from position 1 to 18 as indicated by the drop in the S-score at this point. Four peaks in C-score values are shown in Figure 2.2.B all of which are under the cut-off. However the C-score at positions 19 and 20 are the highest. Confirmation that signal peptide cleavage occurs between these positions is provided by the Y-score which peaks

above the cut-off value of 0.450 at these positions. Figure 2.2.C shows the signal output for GmRD22, illustrating two peak one at position 22 and another at position 30. The Y-score at position 22 is above the cut-off values while the Y-score at position 30 is under the cut-off value, suggesting that the signal peptide of GmRD22 spans from position 1-21 and that cleavage of the signal peptide occurs between position 22 and 23. Figure 2.2.D, which represents the signalP output for ZmRD22A, shows two possible signal peptide cleavage sites at position 22 and 24 respectively. Cleavage of the signal peptide at position 22 is unlikely as there is a small peak in S-score after this position and the C-score is below the cut-off. Cleavage of the ZmRd22A signal peptide is more likely to occur at position 24, due to the combination of the drop in S-score after this position, a C-score value above cut-off and a Y-score value which is higher than that at position 22. The signal output generated for ZmRD22B (Figure 2.2.E) is not as definitive as the previous outputs. The signal peptide clearly spans from position 1 to 21 as suggested by the drop in the S-score after this position. The location of the signal peptide cut site at position 22 is precarious as both the C-score and Y-score are below the cut-off value of 0.450. However this is the most likely cleavage site as the other possibility is at position 26, which has even lower C- and Y-scores.

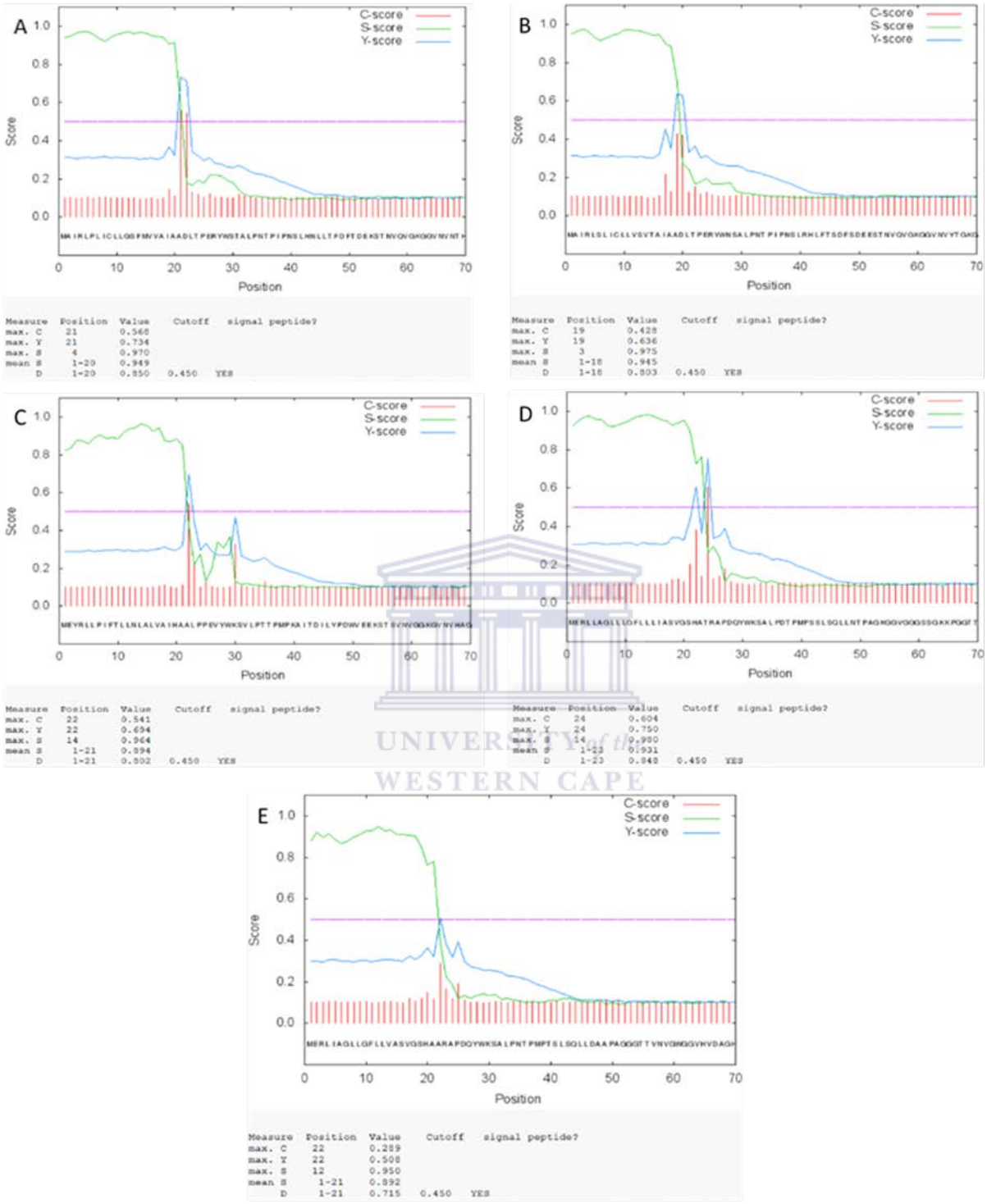

Figure 2.2: Prediction of the presence of signal peptides and their cleavages sites. SignalP was used to predict the presence of signal peptides and their cleavage sites in the sequences of five proteins sequences. The graphic outputs were labelled A (AtRd22), B (BnBDC1), C (GmRD22), D (ZmRD22A) and E (ZmRD22B). The three scores produced by signalP are presented on the graph these include the C-score (Red vertical lines), the S-score (Green curve) and the Y-score (blue peak). The data on each of the graphs are tabulated under the corresponding graph, these tables include the score measured (column 1) the relevant nucleotide base positions (column 2), the score calculated (column 3), the cut-off value and whether or not a signal peptide is present is also indicated in the table.

2.3.4. Identification of the BURP-domain

The presence of a BURP-domain in the five query sequences was detected by analysis with motif scan an online bioinformatics tool which identifies domains in the query sequence using a target sequences which have been characterised. The output of this analysis is an alignment between the query and target sequences as seen in figure 2.3.A which shows the output of the alignment of AtRD22 with the motif scan data base. A strong match was made between the query and target sequences as indicted by the "!", A BURP-domain was identified in the AtRD22 sequence and was shown to be located between amino acid 174 and 392. The validity of this result is indicated by a raw-score and N-score which are higher than the default threshold values for positive results and a low E-value, which eliminates the possibility of false positives. The same is true for BnBDC1 (figure 2.3.B) in which a BURP-domain was located at the same position as the BURP-domain in AtRD22, the two alignments also share the same status, raw score, N-score and E-value. The presence of a BURP-domain (amino acid position 128-343) in the GmRD22 (Figure 2.3.C) sequence was shown by an alignment with a strong match status and an above threshold raw-score ad N-score of 483.1 and 150.382 respectively and an E-value of 8.8^{-144}. Analysis of the ZmRd22A and ZmRd22B sequences resulted in alignment with strong match statuses for both sequences, the position of the BURP-domain was between amino acids 160-374 in the ZmRd22A (Figure 2.3.D) sequence and between amino acids 236-455 in the ZmRd22B sequence (Figure 2.3.E). Validation of the alignments were indicted by above threshold raw and N-score for both sequences 446.7 and 139.428 (ZmRd22A), 465.2 and 144.984 (ZmRd22B). The E-values for these sequences were 7.9^{-133} and 2.2^{-138} respectively.

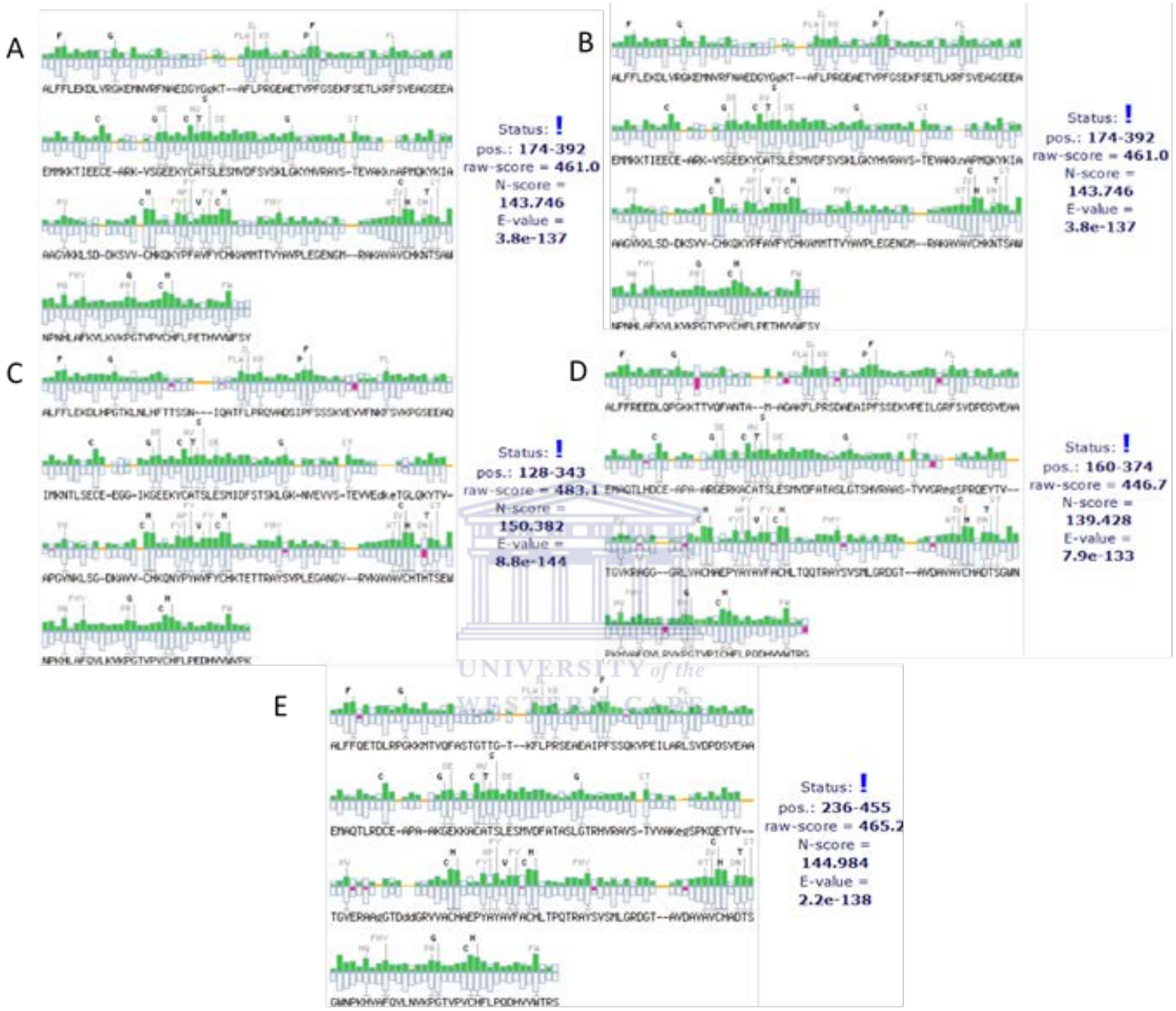

Figure 2.3: Determining the presence of a BURP-domain in five proteins suspected of being BURP-domain containing. The motif scan graphs exhibit the similarity between the five query sequences and the BURP-domain sequences in the Pfam HMMs local and global model data base. The graphic outputs were labelled A (AtRd22), B (BnBDC1), C (GmRD22), D (ZmRD22A) and E (ZmRD22B). Status is an indication of the strength of the match the ! symbolises a strong match, the raw score is an indication of how well the query and data base sequences align, the E-value is an estimation of the number of false positives and the N-score is the raw score normalised based on the size of the data base selected for the analysis.

2.3.5. Sequence alignment of five BURP-domain containing proteins

Five sequences of BURP-domain containing proteins were aligned and the percentage identities calculated, as seen in Table 2.2. The sequences of AT5G25610.1 (ATRD22) and AY293830.1 (BnBDC1) are very similar as they share 87.34% sequence identity. The protein sequences for GRMZM2G446170_T01 (ZmRD22A) and GRMZM800586_T01 (ZmRD22B) are similar as well, sharing an 86.06% sequence identity. The protein sequence for Glyma06G081100.1 seems to be the most divergent of the five sequences, showing only limited similarity with the other sequences. It shares the highest percentage similarity with the BnBDC1 and AtRD22 protein sequences, having 59.53% and 58.02% of amino acids in common. Over all the five sequences share a percentage sequence similarity of between 50.24% and 59.53%. Several conserved regions were identified, which are shared by the five protein sequences. The first of these spans from amino acid position 1 to ± 20 and is highlighted in Figure 2.4 in blue. In the short region following this, a section of the protein sequence which is conserved across all five sequences exists. Conserved amino acid bases in this region are highlighted with green in on Figure 2.4. The subsequent region varies between the five protein sequences. However TxV (where x is any amino acid) repeats have been identified as a conserved motif (encased in red on Figure 2.4). These TxV units are repeated between 3 and 5 times in this variable region. In the case of Glyma06G081100.1, TxV is only repeated twice. The final conserved region present in all five protein sequences is the region perceived to be the BURP domain (encased in yellow in Figure 2.4), this region starts with an AFL amino acid triplet, is highly conserved and contains a X_5-CH-X_{10}-CH-$X_{23\text{-}27}$-CH-$X_{23\text{-}26}$-CH-X_8-W motif in all the protein sequences (underlined in yellow in Figure 2.4).

Table 2.2: Percentage identity matrix for the alignment of five BURP-domain containing protein sequences

target sequence	Query sequence				
	1	2	3	4	5
1 AT5G25610.1	100.00%	87.34%	58.02%	50.42%	51.83%
2 AY293830.1	87.34%	100.00%	59.53%	50.42%	52.52%
3 Glyma.06G081100.1	58.02%	59.53%	100.00%	53.33%	53.71%
4 GRMZM2G446170_T01	50.42%	50.42%	53.33%	100.00%	86.06%
5 GRMZM5G800586_T01	51.83%	50.42%	53.71%	86.06%	100.00%

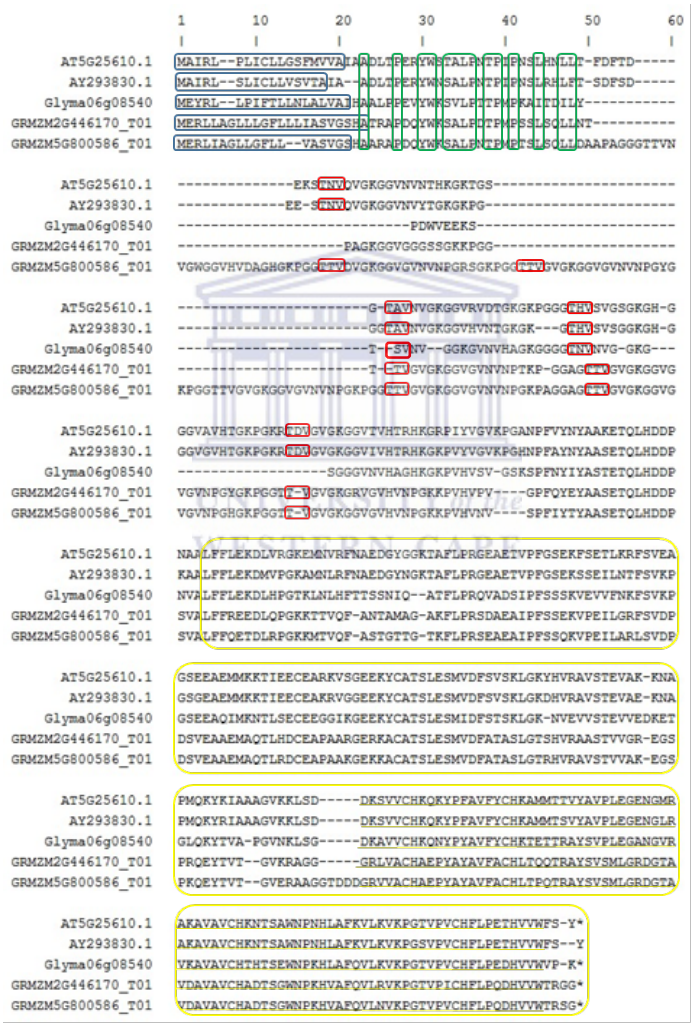

Figure 2.4: ***Sequence alignment and domain organization of five BURP-domain containing proteins.*** *Five BURP-domain containing proteins At5G25610 (AtRD22), AY293830.1 (BnBDC1), Glyma06g08540 (GmRD22), GRMZM2G446170_T01 (ZmRd22A) and GRMZM5G800586_T01 (ZMRD22B) were aligned resulting in 136 identical sites (29% identity) and a pairwise identity of 52.4 %. Similar domains and structural components were identified and are indicated as follows: the hydrophobic signal peptides are encircled in blue, the conserved amino acids in the conserved region are shown in green, The TxV (x is any amino acid) repeats are shown in red, the BURP-domains are shown in yellow and the conserved motif of the BURP-domain is underlined with yellow.*

2.3.6. Promoter analysis of GRMZM2G446170 and GRMZM5G800586.

Analyses of the promoter region 2000 nucleotide bases upstream of the transcription start site of GRMZM2G446170 (ZmRD22A) and GRMZM5G800586 (ZmRD22B) have revealed the presence of several transcription factor binding sites which are involved in the induction of gene expression by drought and ABA signals. These transcription factor binding sites are listed in Table 2.3; column 1 indicates the family the transcription factor belongs to, while column 2 provides the identity of the transcription factor. Other information on the transcription factors such as the position in the nucleotide sequence and the strand on which it resides is, provided in columns 3 and 4 respectively. The hit sequences used to identify the transcription factor binding sites are listed in column 6, and the similarly of the query sequence to the hit sequence is provided in column 5. From Table 2.3, it can be seen that the majority of the transcription factor binding sites present in the GRMZMG446170 (ZmRD22A) sequence belong to the AP2 family of transcription factors. These sites have been shown to allow the binding of DREB1-A and DREB2-A transcription factors. The ZmRD22A promoter region also contains bZip and MyB family transcription factor binding sites. The analysis of the GRMZM5G800586 (ZmRD22B) promoter region shows a distribution of transcription factor binding sites which are the antithesis of that seen in the promoter region of ZmRD22A. In the promoter region of ZmRD22B the majority of the transcription factor binding sites belong to the bZIP family of transcription factors, with all of them having been identified as AREB2s, while AP2 and MyB family transcription factor binding sites were also identified.

Table 2.4: Identification of transcription factor binding sites involved in drought and abscisic acid induction.

	Family	TF name	Position	strand	similarity score	hit sequence
GRMZM2G446170	AP2	DREB2;DREB2A	1549	-	1,00	tggCGGTGc
	AP2	DREB1	1711	+	0,99	cagCCGACg
	AP2	DREB1	1851	-	0,99	cGTCGGctt
	AP2	DREB1A	1712	+	0,98	agCCGACggc
	AP2	DREB1A	1849	-	0,98	gtcGTCGGct
	AP2	DREB1	1711	+	0,90	cagCCGACgg
	AP2	DREB1	1850	-	0,90	tcGTCGGctt
	bZIP	AREB2	392	+	0,96	caaACGTGgg
	MyB/SANT	ASG4	183	+	0,97	taGATATtgc
	MyB/SANT	ASG4	183	-	0,99	taGATATtgc
GRMZM5G800586	AP2	DREB2C	255	+	0,87	cgCGGCCgac
	AP2	DREB2C	255	-	0,87	cgcGGCCGac
	MYB/SANT	ARR14	592	-	1,00	taGAATCaca
	bZIP	AREB2	230	-	0,95	ttggcCACGTgtc
	bZIP	AREB2	233	+	1,00	gccACGTGtcgcg
	bZIP	AREB2	232	+	0,95	ggcCACGTgtc
	bZIP	AREB2	233	-	1,00	gccACGTGtcg
	bZIP	AREB2	506	+	0,75	ACAAGtat
	bZIP	AREB2	607	-	0,75	gcaCTTGT

2.4. Discussion

The bioinformatic analysis of two putative maize RD22-like proteins encoded by GRMZM2G446170_T01 and GRMZM800586_T01 was carried out in conjunction with three experimentally characterised RD22-like proteins identified in *Arabidopsis thaliana (AtRD22), Brassica napus* (BnBDC1) and *Glycine max* (GmRD22). These proteins were characterised by Harshavardhan and Van Son, *et al.* (2014), Shunwu and Zhang, *et al.* (2004) and Wang and Zhou, *et al.* (2012) respectively. In this study, the three characterised RD22-like proteins were used as references for *in silico* analysis of this subfamily of proteins. Completion of phylogenetic relationship analysis of the five sequences releveled they all share an ancestral sequence. However genetic change events resulted in the formation of an ancestral monocot and dicot sequence as seen in Figure 2.1. The ZmRD22 gene sequences differ from their shared ancestral sequence by 0.07 (ZmRD22A) and 0.06 (ZmRD22B) residue changes per 100 residues. This suggests that ZmRD22B is more closely related to the original RD22-like sequence. Dicot and monocot RD22 gene sequences were found to be derived from different ancestral sequences. The dicot ancestral sequence was found to be 0.04 residues/100 residues different from the plant RD22 ancestral sequence (clad B in Figure 2.1). The RD22-like sequence identified in *Arabidopsis thaliana* and *Brassica napus* diverged from the ancestral sequence which is different from the ancestral sequence at clad B by 0.22 residues/100 residues (clad C in Figure 2.1). These sequences differ from the clad C ancestor by 0.08 (AtRD22) and 0.06 (BnBDC1) residues/100 residues respectively. The GmRD22 protein sequence differs from the ancestral protein sequence at clad B by 0.2 residues/ 100 residues. The divergence of these five sequences from a common ancestor

suggests possible structural similarities which can be used to preliminarily characterise GRMZM2G446170_T01 and GRMZM800586_T01 as RD22-like protein encoding genes.

The localization of proteins provide insight to their functions and as such *in silico* analysis was carried out on ZmRD22A and ZmRD22B. It was found that both are secreted into the apoplast as shown in Table 2.1. The localization of these proteins were determined as such due to the scores for the other locations being low and being below the designated cut-off value, as described by Peterson and Brunak (2011) in an article which explains how signalP distinguishes subcellular localization of proteins. In an attempt to show the accuracy of the signalP prediction, the subcellular localization of three "reference" RD22-like proteins were determined. The localization of the reference proteins which was apoplastic as seen in Table 2.1, was confirmed experimentally by Wang and Zhou *et al.*(2012), Tang and Ou *et al.*(2014) and Shunwu and Zhang *et al.*(2004). The correctness of the prediction for each of the reference proteins is an indication of the reliability of the prediction that ZmRD22A and ZmRD22B are localized to the apoplast. The N-terminal domain of BURP domain-containing proteins has been identified as a signalling peptide (Xu, Li *et al.* 2010a) as such it plays a role in determining the localization of its protein, using signalP (signal peptide identification tools) signal peptides were identified in the two query protein sequences as well as the reference protein sequences. The signal peptides were all found to be ± 20 amino acids in length as shown in Figure 2.2. The maturation of the proteins requires the cleavage of these signal peptides as all of the sequences had a cleavage site identified 1-2 amino acid residues from the end of the signal peptide. All proteins in this family contain a BURP domain at their C-terminal ends (Jamoussi, Elabbassi *et al.* 2014). The BURP-domains of the query proteins were found to be 214 (ZmRD22A) and 219 (ZmRD22B) amino acids in length. In

comparison to the reference proteins, in which the BURP-domain was ± 220 amino acids in length as seen in figure 2.3. Alignment of the five protein sequences (Figure 2.4) shows that AtRD22 and BnBDC1 shared the most sequence similarity. The two sequences share 87.34% sequence identity, which agrees with the relationship established by the phylogenetic tree in Figure 2.1. Similarly, the protein sequences for ZmRD22A and ZmRD22B share a high percentage sequence identity of 86.06%. From the alignment of the sequences, it can be seen that the signal peptides of the proteins share a similar sequence, which may contribute to their shared subcellular localization (Yu, Chen *et al.* 2006). The TxV repeat units, which are specific to the variable region of the RD22 subfamily were identified in all five sequences. The X_5-CH-X_{10}-CH-$X_{23\text{-}27}$-CH-$X_{23\text{-}26}$-CH-X_8-W motif, found in all BURP domain-containing proteins, was also present in all five protein sequences. This confirms that the proteins present here are BURP domain-containing proteins and that the two maize proteins belong to the RD22 subfamily of BURP domain-containing proteins. Promoter region analysis (Table 2.3) has revealed the presence of transcription factor binding sites which are involved in induction of gene expression under both drought and ABA signals. From the presence of more DREB-A and DREB2-A in the promoter region of ZmRD22A, it can be assumed that the expression of this gene is directed by drought signals. The induction of drought-responsive gene expression by DREB1-A transcription factors has been shown by Sakuma and Maruyama *et al.*(2006a) while DREB2 has been shown to be involved in the negative-regulation of gene expression in response to drought (Qin, Sakuma *et al.* 2008). ZmRD22B appears to be inducible by ABA signaling as shown by the presence of several AREB sites in the promoter region of the gene's nucleotide sequence, it was shown by Nakashima and Yamaguchi-Shinozaki *et al.*(2014) that ABREs are a major cis-acting element in ABA-induced gene expression.

Furthermore, the presence of MyB family transcription factor binding sites are another indication of ABA-induced gene expression, as shown in (2003), in work conducted by Abe and Urao *et.al*.

In summery the phylogenetic analysis and sequence alignment has revealed that, ZmRD22A and ZmRD22B share common ancestral sequence with three experimentally characterized RD22-like proteins. The proteins also have similar domain organizations and are localized to the same subcellular compartment. Promotor analysis suggests that the expression of ZmRD22A and ZmRD22B is induced by different signaling pathways, namely ABA-independent in the case of ZmRD22A and ABA-dependent in the case of ZmRD22B. The *in sillico* characterization of ZmRD22A and ZmRD22B has provided a frame of reference for the experimental characterization of these protein

Chapter 3: Spatial and temporal transcript accumulation patterns of GRMZM2G446170 and GRMZM5G800586 in response to water deficit stress

3.1. Introduction

Plants grown under conditions of water deficit experience disruption in photosynthetic efficiency and gas exchange (Chaves, Pereira *et al.* 2002). This occurs as dehydration damages the photosynthetic apparatus culminating in a reduction of carbon cycling, accumulation of carbohydrates, peroxidation of lipids, premature senescence of leaves and perturbation of water balance (Anjum, Xie *et al.* 2011). Plants which are unable to adapt to this altered state of photosynthesis suffer physiological and biochemical changes which affect growth and yield (Bita and Gerats 2013). Plants suffering from water deficit exhibit reductions in relative water content and increases in cellular concentrations of compatible solutes in an attempt to maintain cell turgor (Shao, Chu *et al.* 2009). The biochemical response of plants to water deficit stress is initiated by an oxidative burst caused by the over production of oxygen ions, free radicals and peroxides which are referred to as reactive oxygen species or ROS (Gill and Tuteja 2010). These reactive oxygen molecules are produced by normal oxygen metabolism and act as signalling molecules. However ROS is overproduced when plants are exposed to drought stress, resulting in the oxidative damage to proteins, lipids, DNA and ultimately cell death (Sharma, Jha *et al.* 2012). The ability of ROS to act as signalling molecules or cause damage to plants depends on the balance between ROS production and antioxidant enzyme activity. Water deficit may be directly perceived by stress-sensors located on the plasma membrane, resulting in the inhibition of protein kinases and protein phosphatases. These kinases and phosphatases are in turn

responsible for the activation of transcription factors which interact with *cis*-acting elements and induce the expression of drought-responsive genes (Xiong, Schumaker *et al.* 2001). The expression of stress-responsive genes is an adaptation to negative environmental conditions. Several such stress responsive genes have been identified in maize. This study will focus on two maize genes which encode putative RD22-like proteins. This subfamily of the BURP domain-containing protein family is active in conferring drought tolerance (Harshavardhan, Seiler *et al.* 2014). The expression of RD22-like proteins is induced under water deficit conditions. RD22-like proteins have been characterised on a genetic level in *Arabidopsis thaliana*. The actual mechanism by which it aids plants to tolerate the effects of drought stress is still unknown (Liu, Ding *et al.* 2014). This study will aim to assay the effect of water deficit on the expression of two putative maize RD22-like proteins using a combination of quantitative and semi-quantitative PCR techniques. *In silico* analysis of these two putative maize RD22-like proteins has revealed structural components shared with experimentally characterised RD22 proteins. It is, therefore hypothesised that the expression of ZmRD22A and ZmRD22B encoded by GRMZM2G446170 and GRMZM5G800586 respectively, will be up-regulated in leaves and roots of maize seedlings grown under water deficit conditions.

3.2. Methods and Materials

3.2.1. Plant Growth and Water Deficit Stress Treatment

The plant growth media (Promix® Organic; Windell Hydroponics, Cape Town, South Africa) was prepared by filling a clear acrylic tube (dimensions as follows: inner diameter 19 cm, outer diameter 19.5 cm, wall thickness 0.5 cm, circumference 63.5 cm, height 100 cm) half way. The growth media was then weighed and its volume determined. In order to obtain the desired water potential for each experimental condition, the growth media was mixed with a calculated volume of nutrient solution. The growth media was mixed with nutrient solution at a ratio of 1:1 (v/v). The nutrient solution used was a maize-specific blend of macro and micro nutrients with concentrations as follows: 1mM K_2SO_4, 2 mM $MgSO_4$, 5 mM $CaCl_2$, 5 mM KNO_3, 10 mM NH_4NO_3, 1 mM K_2HPO_4 buffer at pH 7.2, 5 µM H_3BO_3, 5 µM $MnSO_4$, 1 µM $ZnSO_4$, 1 µM $CuSO_4$, 2 µM Na_2MoO_4, 1 µM $CoSO_4$, 100 µM Fe-NaEDTA and 10 mM 2-(N-morpholino) ethanesulfonic acid (MES) at pH 6.2. After the growth media and nutrient solution was thoroughly mixed the growth media was dried at 80°C until the growth media was completely dry (approximately 4 days). The growth media was then transferred back to the clear acrylic tubes which were wrapped in heavy duty aluminium foil up to a height of 50 cm, the tubes were placed on plant pot bases 25cm in diameter. The water potential of the growth media was measured using a WP4C® Dewpoint PotentiaMeter (Degacon Devices, Pullman, WA, USA), the accuracy of the measurements were ensured by equilibrating the sample and chamber temperatures using an Aqua Lab temperature equilibration plate (Decagon Devices) and the water potential meter with standards supplied by the manufacturer (Degacon Devices). The water potential for the well-watered growth media

was -0.03 ± 0.008 MPa and growth media for the water-deprived plants had a water potential of -0.35 ± 0.03 MPa.

Maize seeds (*Zea Mays* L. cv. CAP9001) were surface-sterilized in 0.35% sodium hypochlorite (Sigma-Aldrich, St Louis, MO, USA) containing 1% Tween-20 (Sigma-Aldrich) for 10 minutes, then rinsed several times in sterile distilled H_2O to remove the sodium hypochlorite and the surfactant. The seeds were then imbibed in 10 mM $CaSO_4$ (Sigma-Aldrich) for 16, hours during which the solution was continuously aerated using an aquarium air pump (Tetra ASP100). This was done as priming seed in $CaSO_4$ prior to germination has been shown to enhance germination rates (Afzal, Rauf *et al.* 2008). After imbibing, the seeds were transferred to a container lined with layers of moist paper towel, the seeds were covered with another set of layers of moist paper towel and allowed to germinate. Germination was carried out in the absence of light at ± 23°C (room temperature) until radicles emerged from the seeds, this occurred ± 48 hours after imbibing. At this point all the seed with emerged radicles were transferred to the clear acrylic tubes containing the prepared growth media. The germinated seeds were covered with growth media at a depth of approximately 8 cm. The tops of the tubes were sealed with cling film to limit water loss from the growth media by evaporation. The cling film was punctured several times to allow gaseous exchange.

The seedlings were grown in a temperature-controlled growth room at 25°C/19°C day/night temperature cycle under a 16/8 hour light/dark cycle with a photosynthetic photon flux density of 300 µmol photons.m^{-2}.s^{-1}. The seedlings were planted in growth media with a water potential for -0.03 ± 0.008 MPa (well-watered) -0.35 ± 0.003 MPa (water-deprived) as such water

deprivation started at the beginning of cultivation in the growth media. Once the seedlings reached the V1 stage (the first fully extended leaf, with a leaf collar is present), plants of the same phenological stage and the same height were selected as representatives for well-watered plants and water-deprived plants. The seedlings were allowed to grow for a minimum 10 days before harvesting. Ten plants for each growth conditions were selected and the primary roots and second youngest leaves were separated from the rest of the plant. Another ten plants were harvested in the same way, however the roots from these plants were divided in to root tip (the first 3 cm section from the tip of the primary root) and mature root (a section 5 cm away from the root tip until the root/stem junction), while the leaves were divided into base (the first 5 cm section from the leaf collar), middles (5 cm section from the centre of the leaf) and tips (the first 5 cm sections from the tip of the leaf). Fresh whole organs (roots and leaves) were used to measure relative water content and cell viability. The rest of the material was ground in liquid nitrogen and stored at -80°C.

3.2.2. Measurement of Relative Water Content

Relative water content was measured in triplicate using the 2nd youngest leaves and primary roots of well-watered and water-deprived plants. This was accomplished by cutting a 10 cm section from the tip of each leaf and root with a sharp pair of scissors. The plant cuttings were weighed to determine their fresh weights. The leaves were then placed in beakers containing distilled H_2O and incubated under ambient light for 4 hours to allow water uptake to full turgor, followed by weighing to determine turgid weight after removal (with paper towel) of any surface

H_2O on the leaves. The leaves were then dried in an oven at 80 °C for 48 hours, immediately placed in a desiccator and weighed to determine their dry weights.

3.2.3. Measurement of Cell Viability

Cell viability was evaluated in the 2nd youngest leaves and primary roots of well-watered and water-deprived plants, using an assay described by Sanevas *et al.*(2007). Fresh tissue of 1 cm^2 in area from the broadest part of the 2nd youngest leaf and a 3 cm section of the centre of the primary roots was collected at harvest. The cuttings were stained with 0.25 % (w/v) Evans Blue for 15 min at room temperature. The Evans Blue was removed by pipetting, followed by three rinse cycles of 10 min each in distilled water. The distilled water was removed and 1 % (w/v) SDS was added to the samples. The samples were incubated for 1 h at 55 °C, then cooled at room temperature for 15 min. The samples were centrifuged at 3000 *g* for 1 min. Aliquots of 200 µl of the supernatant were then pipetted (in triplicate) into a 96 well-plate and absorbance at 600 nm was measured (with 1 % SDS used as a blank for which its $A_{600\ nm}$ values were subtracted from the $A_{600\ nm}$ values of the samples in order to obtain the final $A_{600\ nm}$ values of the samples).

3.2.4. Determination of H_2O_2 and Malondialdehyde Contents

H_2O_2 and malondialdehyde (MDA) contents were measured in the 2nd youngest leaves and primary roots of well-watered and water-deprived plants. The leaves and roots were ground into fine powder in liquid nitrogen using a mortar and pestle that had been pre-cooled with the liquid nitrogen. The ground plant material (500 mg) was then homogenized with 1 ml of cold 6 % (w/v) trichloroacetic acid (TCA), followed by centrifugation at 12,000 *g* for 30 min at 4 °C. The TCA

extract was used for measurement (in triplicates) of H_2O_2 as described by Velikova *et al.*(2000) and MDA as described by Buege *et al.*(1978).

H_2O_2 content was assayed by homogenising 50 µl of TCA extract with 150 µl of reaction buffer containing 5 mM K_2HPO_4, pH 5.0 and 0.5 M KI. Reactions were incubated at 25°C for 20 min, followed by recording of absorbance readings in triplicate at 390 nm. H_2O_2 content was calculated using a standard curve constructed with the absorbance of H_2O_2 standards read at an absorbance of 390 nm. The MDA assay was performed by coalescing 250 µl of TCA extract with 1 ml of 0.5 % 2-thiobarbituric acid (w/v) that had been prepared in 20 % TCA. The homogenate was incubated for 30 min at 95°C and then cooled on ice for 10 min. The thiobarbituric acid reactive substances (TBRAS), reflective of MDA, were detected by reading their absorbance at 532 nm and subtracting nonspecific absorbance at 600 nm. The amount of MDA was calculated using a molar extinction coefficient of 155 $mM^{-1}cm^{-1}$.

3.2.5. Evaluation of the effect of water deficit stress on the transcript accumulation of ZmRD22A and ZmRD22B

3.2.5.1. Total RNA isolation

Turnover of the mRNA transcripts for ZmRD22A and ZmRD22B in response to water deficit stress was investigated in the 2nd youngest leaves and primary roots of maize CAP9001 seedlings by semi-quantitative reverse transcription polymerase chain reaction (Semi-q-RT-PCR). Powdered plant material generated by grinding plant tissue in liquid nitrogen (see section above on H2O2 and MDA measurements for description of the generation of powdered plant material in liquid nitrogen) was used to isolate total RNA. Total RNA was isolated using the Direct-zol™ RNA mini-

prep kit (Zymo Research, Irvine, CA, USA) according to the instructions of the manufacturer. RNase-free DNase I (Zymo Research) was used to remove DNA from the isolated RNA as specified by the manufacturer and RiboLock® RNase Inhibitor (Thermo Scientific, Waltham, MA, USA) was added to prevent RNase-mediated degradation of the RNA.

3.2.5.2. First strand cDNA synthesis

First strand cDNA synthesis was accomplished using 500 ng of total RNA from leaves and roots of well-watered and water-deprived plants. The total RNA was mixed with Oligo (dT)18 universal primers (Thermo Scientific) at a final concentration of 100 pmol, this was then made up to 12.5 µl with nuclease-free water. To this, a reaction buffer and dNTP Mix (Thermos Scientific) was added to a final concentration of 1X and 1 mM respectively. RNA degradation was prevented by the adding 20U of RiboLock® (Thermo Scientific), and then 200U of RevertAid™ Reverse Transcriptase (Thermo Scientific) were used to synthesize 1st strand cDNA from the total RNA. The reaction was carried out at 42 °C for 60 minutes after which the reaction was terminated by incubation at 70°C for 10 minutes as described by the manufactures' instructions.

3.2.5.3. Semi-quantitative PCR analysis of ZmRD22A and ZmRD22B transcript accumulation

Polymerase chain reaction (PCR) was carried out independently for ZmRD22A and ZmRd22B using 2 µl of 1st strand cDNA as template. A negative control in which all components were included except that the 1st strand cDNA was replaced with 2 µl of nuclease-free water was set up to rule out false positive results. The PCR contained the following reagents at the specified concentrations: 400 µM of dNTPs, 0.4 µM of gene-specific forward primer for ZmRD22A (5'-GCG

GGC GGG CGG CGG GCG CCT G-3') or ZmRD22B (5'- CGA CGA CGA CGG CCG GGT CGT G -3') and 0.4 µM of gene specific reverse primer ZmRD22A (5'-TCA GCCGCC GCG GGT CCAGAC GAC G-3') or ZmRD22B (5'- TCA GCC GCT GCG GGT CCA GAC GAC GTG -3'). Amplification was done using 1.25 Units of TrueStart™ Hot Start Taq DNA Polymerase (Thermo Scientific) in the presence of 1.5 mM $MgCl_2$ and 1X TrueStart™ Hot Start Taq buffer. A similar PCR was also set up in order to amplify Zm18S rRNA (forward primer: 5'-CCA TCC CTC CGT AGT TAG CTT CT -3'; reverse primer: 5'-CCT GTC GGC CAA GGC TAT ATA C-3') from the same 1st strand cDNA samples. The PCR was carried out at an initial denaturation temperature of 95 °C for 2 min, followed by 25 cycles of denaturation at 94 °C for 30 sec, primer annealing at 58 °C for 30 seconds and extension at 72 °C for 2 min. Once the 25 cycles were complete, final extension was done at 72 °C for 7 min. In order to determine whether 25 cycles falls within the PCR exponential phase, PCR reactions were also set up under the same conditions as above but with 15, 20 and 30 cycles. The use of cycle gradients allow the earliest cycle number to be identified at which differences in transcript numbers are detectable. The PCR products were size-fractionated on a 1% agarose gel in the presence of 1X GelRed™ (Biotium, Hayward, CA, USA) for DNA staining and images were captured with an AlphaEaseFC (Alpha Innotech Corporation, Miami, FL, USA) UV gel documentation system. Individual gels from three independent experiments were used for expression analysis on the basis of densitometry analysis done using the Spot Denso tool (AlphaEase FC Imaging Software, Alpha Innotech Corporation). Transcript accumulation expressed as ratios relative to the values of the control samples, with densitometry-derived values of 18S rRNA as the reference.

3.2.5.4. Quantitative real-time PCR analysis of ZmRD22A and ZmRD22B transcript accumulation in relation to Zm 18s rRNA and Zm Actin

Quantitative measurement of ZmRD22A and ZmRD22B transcript level changes in response to water deficit stress was carried out independently using quantitative RT-PCR (qRT-PCR). The qRT-PCRs for well-watered and water-deprived plants were completed in triplicate and contained 2 µl of 1st strand cDNA template (as used in the Semi-q-RT-PCR), 0.3 µM gene-specific forward and reverse primers (as described in section 3.2.5.2) and 1X Luminaris Color HiGreen™ Low ROX qPCR master mix (Thermo Scientific). The qRT-PCRs were carried out using a three-step cycling protocol which had a UDG pre-treatment at 50°C for 2 min. An initial denaturation step at 95°C for 10 min was followed by 40 cycles of denaturation at 95°C for 15 sec, annealing at 60°C for 30 sec and extension at 72°C for 30 sec. Data acquisition was set to occur during extension periods. A melting curve step was included after the PCR steps to verify primer specificity and identify the PCR products. Similar qRT-PCR reactions were set up for three internal control genes, maize 18s rRNA (primers sequences provided above), maize Actin (forward primer 5'- GTG ACA ATG GCA CTG GAA TG -3', reverse primer 5'- GAC CTG ACC ATC AGG CAT CT -3') and maize β-tubulin (forward primer 5'- AGC CCG ATG GCA CCA TGC CCA GTG ATA CCT -3', reverse primers 5'- AAC ACC AAG AAT CCC TGC AGC CCA GTG C -3'). Transcript accumulation levels were expressed as ratios relative to the values of the control samples, with the transcript accumulation levels of the internal control genes as the reference.

Transcript levels for ZmRD22A and ZmRD22B were also measured in sections (tip, middle and base as described in section 3.2.1 for generation of sections from the 2nd youngest leaves) from

the 2nd youngest leaves of plants which were well-watered and water-deprived. This was carried out as explained above for the quantitative analysis of transcript levels in whole organs.

3.2.6. Statistical analysis of results

The statistical validity of all the data was tested by means of a One-way Analysis of Variance (ANOVA) and the Tukey-Kramer test at 5% level of significance was completed to compare the means using GraphPad Prism 6.01 software.

3.3. Results

3.3.1. Morphological comparison between maize seedlings grown in well-watered and water-deprived conditions

The morphology of maize seedlings grown in water-deprived and well-watered conditions were examined after three weeks of growth. The seedlings were removed from their growth tubes and photographed. Figure 3.1.A shows the vegetative tissue and root system of a seedling grown in the absence of sufficient water supply. The vegetative tissue of the seedling measured approximately 14.5 cm in length, the 2nd youngest leaf measured approximately 12 cm and the 1st leaf measured approximately 4.5 cm, the youngest leaf was vestigial at the time of harvesting. Aside from the diminutive stature of the seedling, slight curling and a bluish ting can be observed in seedling. The root system of the water deprived seedling was also stunted measuring approximately 15.5 cm from the seed to the tip of the primary root. Three lateral/seminal roots had developed, however no nodal roots had developed. The seedlings grown in well-watered growth media was significantly larger, the vegetative tissue measuring approximately 28 cm in total with the 2nd youngest leaf measuring approximately 21 cm. The seedling grown in well-

watered growth media (Figure 3.1.B) had four leaves at the time of harvesting, which included the 1st leaf and 2nd youngest leaf as in the water-deprived seedling as well as a developed leaf with a collar and a well-developed youngest leaf. The seedling grown with sufficient water supply had a more developed root system, with a primary root measuring ± 27.5 cm in length as well as well-developed lateral/seminal roots and nodal roots. In comparison there was an approximate reduction in vegetative tissue length of 0.51 fold, with a 0.57 fold reduction in the length of the 2nd youngest leaf as a result of water deficit. Similarly when comparing the root systems a 0.56 fold reduction was observed in primary root length, the water-deprived seedling also exhibited less developed lateral/seminal roots and lacked nodal roots.

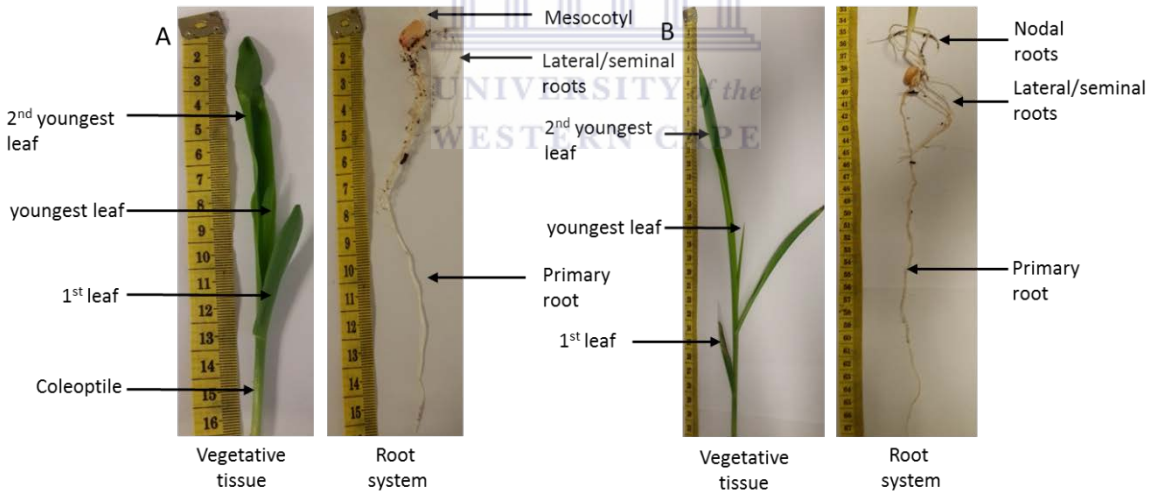

Figure 3.1: Morphological comparison of maize seedling grown in the absence and presence of sufficient water supply. (A) Digital photograph of a maize seedling grown under water-deprived conditions. The photograph on the left shows the vegetative tissue and the roots are shown on the right. (B) Digital imaging of a maize seedling grown with sufficient water supply; the image on the left shows the vegetative tissue and the image on the right shows the root systems. Leaf and root structures are indicated by black arrows and the image scale is provided by the yellow measuring tape.

3.3.2. Measuring relative water content and abiotic stress indicators

Figure 3.2.A-D represents the relative water content (RWC), H_2O_2 content, MDA content and cell viability of the 2nd youngest leaves and primary roots of maize seedlings grown in the presence and absence of sufficient water. Relative water content provides a measure of the water status of a plant. Figure 3.2.A, is a graphic representation of the water status of the leaves and roots of maize seedlings grown with ample water and those grown under water deficit conditions. The RWC in leaves of well-watered maize seedlings was approximately 85% (dark green bar) while in the leaves of maize seedlings deprived of water the RWC was approximately 49% (light green bar), this indicates a decrease of approximately 58% in the RWC of leaves when deprived of water. In the roots a RWC of approximately 84% was observed in seedling which were well-watered (Brown bar), while the RWC in roots of seedlings deprived of water (light brown bar) was measures at approximately 48%, 57% compared to the roots of well-watered seedlings.

Figure 3.2.B represents the changes in hydrogen peroxide content in the leaves and roots of well-watered and water-deprived maize seedling. When the maize plants are supplied with sufficient water, the H_2O_2 content is approximately 14.4 µmol.mg of fresh weight (FW) and approximately 2.97 µmol.mg of FW in the leaves and roots, respectively. In the absence of sufficient water, there is a 2.66-fold increase in leaf H_2O_2, as shown by the light green bar in Figure 3.2.B which indicates 35.7 µmoles H_2O_2 per mg of leaf fresh weight. In the roots, a 3.77-fold increase in H_2O_2 content is observed, as indicated by the light brown bar, which shows a root H_2O_2 content of approximately 11.20 µmoles of H_2O_2 per mg of root fresh weight. Similarly, in figure 3.2.C, there was an increase in both leaf and root MDA content, for which MDA content in the leaves

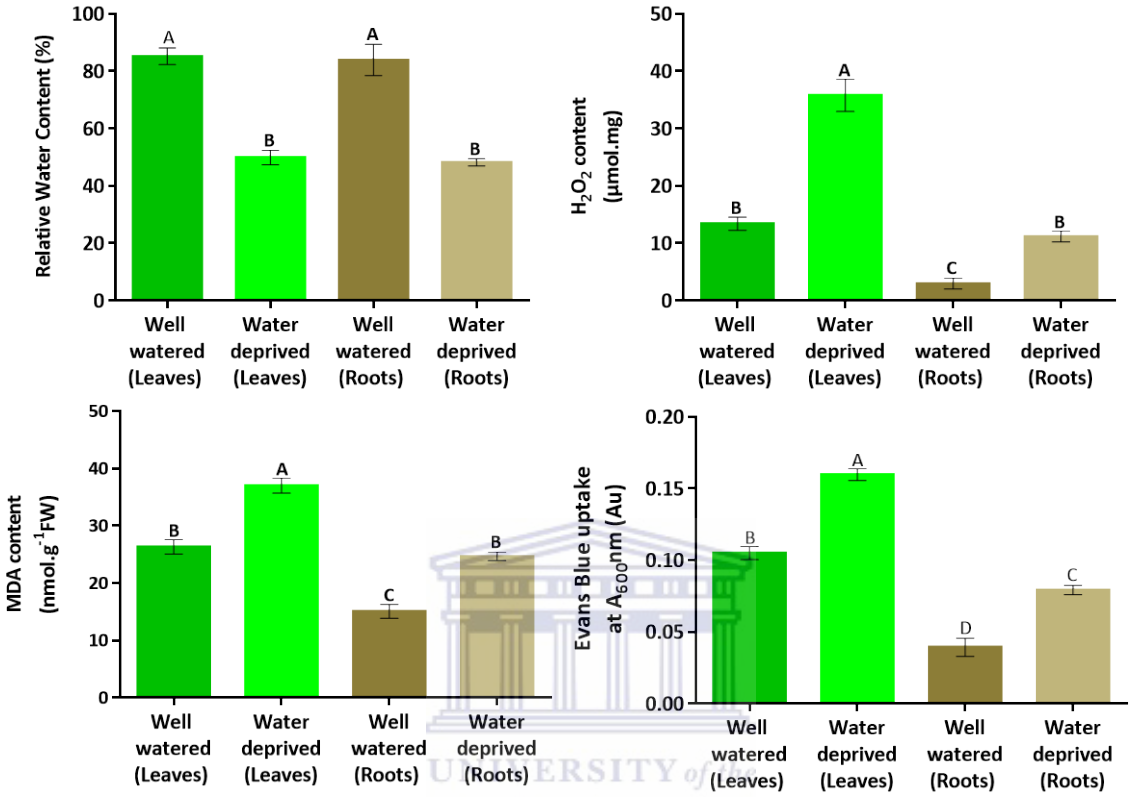

Figure 3.2: The degree of abiotic stress experienced in maize seedling grown under well-watered and water-deprived conditions. (A) Graphic representation of the relative water content (RWC), of the 2nd youngest leaves and primary roots of maize seedling provided with sufficient water and those deprived of water. (B) Hydrogen peroxide (H_2O_2) content in µmol.mg of plant material of maize seedlings which were provided with ample water and those deprived of water during growth. (C) Malondialdehyde (MDA) content expressed as nmol.g^{-1}FW (fresh weight), indication of lipid peroxidation in plants grown in the presence of sufficient water and those grown in the absence of sufficient water. (D) The degree of cell death experienced by maize seedlings, supplied with water and those deprived of water. Cell death was measured absorbance units (Au) as a function of Evan's blue uptake. In all graphs the dark green bars represent the 2nd youngest leaves of well-watered seedling, while the light green bars are representative of the 2nd youngest leaves of water deprived maize seedlings. Similarly the brown bars represent the primary roots of maize seedling provided with sufficient water and the light brown bars are representative of the primary roots of water-deprived maize seedlings. The error bars signify standard deviation, bars with the same letters are statistically similar where $P < 0.05$.

increased 1.40-fold, increasing from 26.35 nmol.g^{-1} FW in well-watered plant leaves (green bar) to 37.03 nmol.g^{-1} FW in water-deprived plant leaves (light green bar). In the roots, there was a 1.55-fold increase in MDA content, going from 15.09 nmol.g^{-1} FW in the roots of well-watered plants to 24.70 nmol.g^{-1} FW in the roots of water-deprived seedlings.

The viability of cells in the leaves and roots of well-watered seedling as compared to water-deprived seedlings is shown in figure 3.2.D, where Evans Blue uptake in the leaf cells of well-watered seedlings is approximately 0.105 Au (green bar), whereas the leaves from water-deprived seedlings took up 1.5-fold more Evans Blue, measuring approximately 0.16 Au (as shown by the light green Bar). A similar trend was observed between the roots of well-watered and water-deprived seedlings, where a 2-fold increase in Evans Blue uptake was observed in water-deprived seedling, corresponding to an increase from approximately 0.04 Au (brown bar) to approximately 0.08 Au (light brown bar).

3.3.3. Semi-quantitative PCR analysis of ZmRD22A and ZmRD22B transcript accumulation levels in response to water deficit stress

The transcript accumulation of ZmRD22A and ZmRD22B genes was measured in relation to the internal control gene Zm 18S rRNA (encoding the 18S rRNA of maize). This was done in well-watered and water-deprived seedlings to examine the effects of water deprivation on the transcript accumulation of these genes. In Figure 3.3.A, which is representative of ZmRD22A transcript accumulation analysis an arbitrary expression level of 0.08 in the leaves of well-watered seedlings was observed. Withholding of water resulted in a 17.5-fold increase in the accumulation of ZmRD22A transcripts, culminating in an arbitrary transcript accumulation level of 1.40. The expression of ZmRD22B is shown in Figure 3.3.B. Here it was shown that, under well-watered conditions, ZmRD22B transcripts accumulate to a level of approximately 0.44 in the leaves. When the seedlings were grown in the absence of water, the transcript accumulation of ZmRD22B increased 2.32-fold to approximately 1.02. In both figures it is clear that the genes are not expressed in the roots under well-watered or water-deprived conditions.

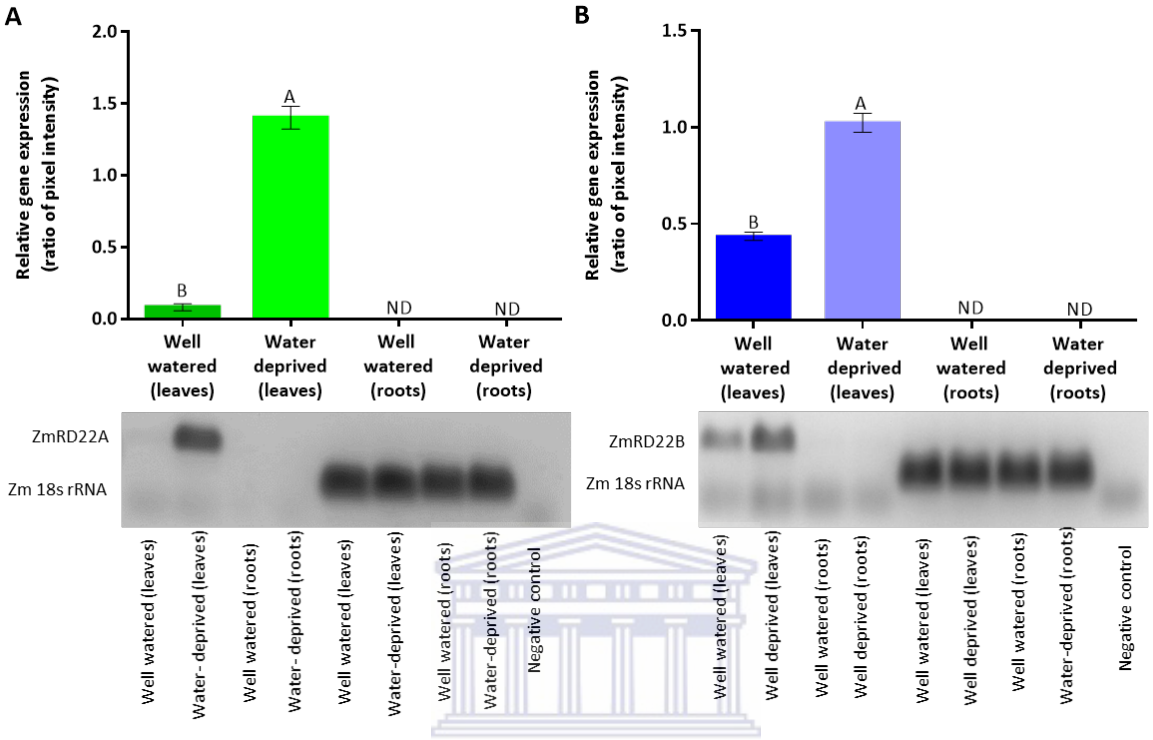

Figure 3.3: Relative gene expression, expressed as the ratio of pixel intensity of the target and reference genes. PCR was used to amplify both the target genes and the reference gene in the leaves and roots of well-watered and water-deprived plants. Gel image A shows the size fractionated ZmRD22A PCR product and gel image B show ZmRD22B. (A) graphic representation of gel image A the dark green bar shows the expression/transcript levels of ZmRD22A in the leaves of well-water plants and the light green bar shows the expression/transcript levels of ZmRD22A in the leaves of water-deprived plants relative to Zm 18s rRNA. (B) Expression/transcript levels of ZmRD22B in relation to Zm 18s rRNA in the leaves of well-watered plants (dark blue bar) and the leaves of water-deprived plants. The error bars signify standard deviation, bars with the same letters are statistically similar where $P < 0.05$.

3.3.4. Relative quantitative RT-PCR analysis of ZmRD22A and ZmRD22B transcript accumulation in response to water deficit stress

Quantitative RT-PCR was carried out to measure the transcript accumulation of ZmRD22A and ZmRD22B in response to water deficit stress. This was accomplished by measuring transcript accumulation in relation to two internal control genes maize (Zm) 18s rRNA and maize (Zm) β-tubulin. From Figure 3.4.A and B, it can be seen that the transcript accumulation of ZmRD22A under conditions of water-deprivation is up-regulated in the leaves as evident by the 16.44 and

26.78-fold increase in transcript accumulation. The accumulation of ZmRD22A transcripts under water deficit stress increased from the arbitrary value of 2.03 to 33.39 relative to Zm 18s rRNA and from 1.29 to 34.55 relative to Zm β-tubulin. When the transcript accumulation relative to the two internal control genes was averaged out it was found that ZmRd22A expression under well-watered conditions was approximately 1.66 but increased 20.44-fold to 33.39 when the seedlings were deprived of water. A similar, all be it less intensive, response to water deprivation is observed in the induction of ZMRD22B transcription in response to water deficit stress (Figure 3.4.C and D). Here, basal transcript accumulation (in leaves of well-watered seedlings) is 0.94 and 1.23 in relation to Zm 18s rRNA and Zm β-tubulin respectively. The basal ZmRd22B transcript accumulation levels increases 3.75 and 1.88-fold in response to water-deprivation. When averaged out the basal transcript accumulation of ZmRD22B is approximately 1.08 while drought increases transcript accumulation 2.7-fold to an expression of approximately 2.92. It is clear from these figures that both ZmRD22A and ZmRD22B are exclusively expressed in the leaves as no transcript accumulation is detected in the roots and remains unchanged even when the seedlings are deprived of water. When comparing the transcript accumulation of the two genes, it appears that transcript accumulation of ZmRD22A is higher in comparison to ZmRD22B. The difference in transcript accumulation in response to water-deprivation stress is more pronounced, with quantitative RT-PCR detecting a divergence of ± 10 fold between the expression of ZmRD22A and ZmRD22B.

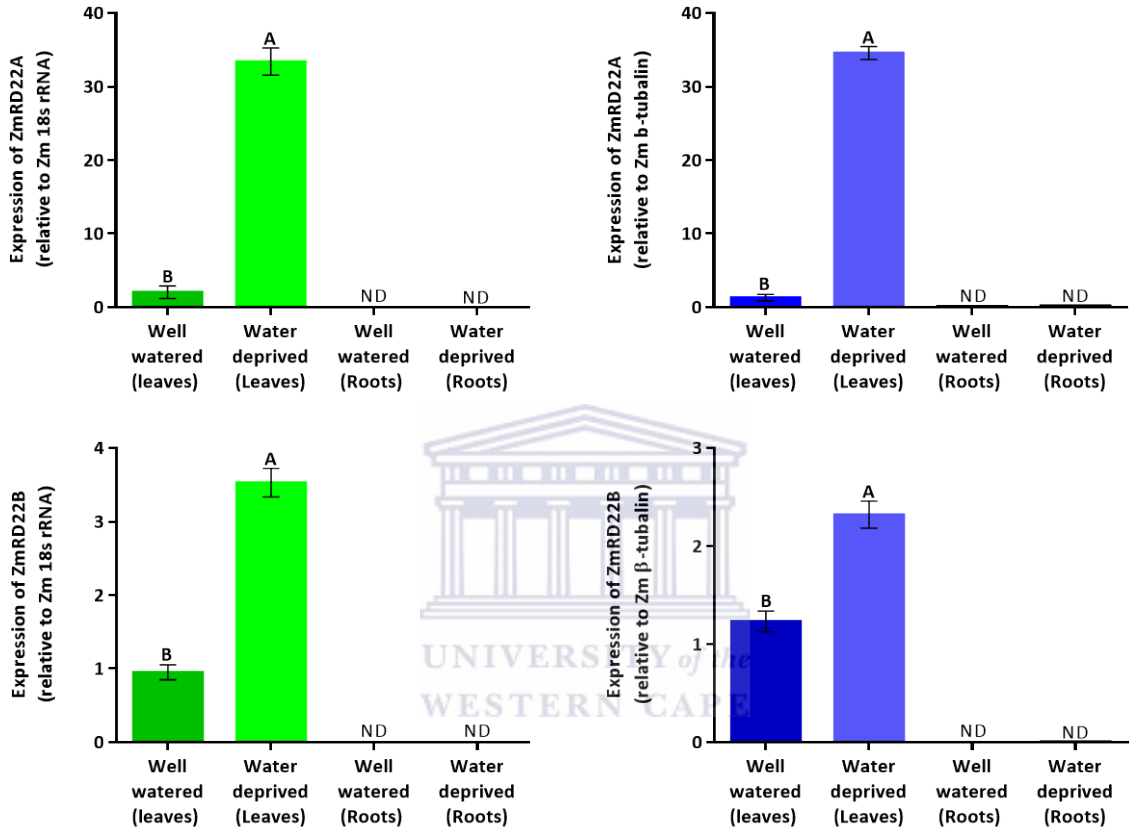

Figure 3.4: Relative quantitative RT-PCR analysis of ZmRD22A and ZmRD22B in relation to Zm 18s rRNA and Zm β-tubulin in response to water-deprivation. (A) The expression of ZmRD22A relative to Zm 18s rRNA, in leaves of seedling supplied with sufficient water is indicated in the dark green bar, while the expression in the leaves of water-deprived plants is shown by the light green bar. (B) Graphic representation of ZmRD22A expression relative to Zm β-tubulin in response to water-deprivation, the bark blue bar shows expression in in the leaves of well-watered seedling and the light blue bar shows the expression in the leaves of seedlings deprived of water. (C) Expression levels of ZmRd22B in relation to Zm 18s rRNA, the dark green bar shows expression under well-watered conditions, the light green bar shows expression under conditions of limited water availability. (D) Graphic representation of ZmRD22B expression in relation to Zm β-tubulin, the dark blue bar shows expression in the leaves of seedling provided with sufficient water, while the light blue bar represents expression levels in the leaves of seedling deprived of water. The error bars signify standard deviation, bars with the same letters are statistically similar where $P < 0.05$.

3.3.5. Relative quantitative RT-PCR analysis of ZmRD22A and ZmRD22B transcript accumulation in response to water deficit stress in defined sections of maize leaves and roots

Total RNA was isolated from three sections of the 2nd youngest leaves of maize seedling which were supplied with sufficient water and those deprived of water. The analysis was completed using two internal control genes, Zm 18s rRNA and Zm β-tubulin. In Figure 3.5.A, it can be seen that the transcript accumulation of ZmRD22A relative to Zm 18s rRNA is approximately 1.74 when the seedlings are supplied with sufficient water. This however changes when the seedlings are deprived of water in the leaf tips (LT) as there is a 7.42-fold increase in the arbitrary value of ZmRD22A transcript accumulation from approximately 1.80 to approximately 13.36. In the middle section of the leaf (LM) the change in ZmRD22A transcript accumulation is less prominent, with a 1.9-fold increase in expression from 1.75 when supplied with sufficient water to 3.35 when deprived of water. The change in ZmRD22A transcript accumulation in relation to Zm 18s rRNA is the most prominent at the base of the leaf (LB) where expression increased 14.44-fold, representing a change in expression from 1.69 when the seedlings were well-watered to 24.41 when they were deprived of water. A similar, less prominent trend in observed in ZmRd22A expression in relation to Zm β-tubulin (Figure 3.4.B) here the transcript accumulation of ZmRD22A is approximately 1.4 when the seedlings have sufficient water supply. When deprived of water, there is a 6.52-fold increase in transcript accumulation of ZmRd22A culminating in a transcript accumulation level of 9.46. Again the effect of water-deprivation on the transcript accumulation of ZmRD22A in the middle section of the leaf is not as prominent. In the middle section of the leaf, ZmRD22A transcript accumulation increased 1.94-fold, increasing transcript

accumulation from a value of 1.37 to 2.66. At the base of the leaf the change in transcript accumulation is again the most pronounced. Here, the expression level change in response to water deficit is 9.98-fold increasing from a meagre 1.38 to 13.78. When the transcript accumulation of ZmRD22A is averaged out over the two internal controls, the transcript accumulation under well-watered conditions was approximately 1.56 across the three sections, while in the 2nd youngest leaves of seedling deprived of water transcript accumulation is 11.41 in the tips, 3.00 in the middle section and 13.09 in the base of the leaf. The transcript accumulation of ZmRD22B was examined in the same way, in figure 3.4.C which shows the expression of ZmRD22B in relation to Zm 18s rRNA expression in the 2nd youngest leaves of well-watered seedlings is approximately 1.7 across all sections of the leaf. When deprived of water there is a positive change in transcript accumulation of ZmRD22B in the leaf tips (LT) as the expression increases from 0.16 to 1.83 an 11.43-fold increase. In the middle section of the leaf (LM), transcript accumulation goes from 0.18 when supplied with sufficient water to 1.34 when deprived of water; a 7.44-fold increase in transcript accumulation in response to water-deprivation. At the base of the leaf (LB), the transcript accumulation of ZmRD22B undergoes a positive change from approximately 0.18 in seedlings grown in well-watered conditions to approximately 2.21 when the seedlings are deprived of water. In comparison, the expression of ZmRD22B in relation to Zm β-tubulin (Figure 3.4.D) exhibits a higher basal transcript accumulation in all sections of the 2nd youngest leaves when supplied with sufficient water; here the transcript accumulation is approximately 0.5 when deprived of water, transcript accumulation is increased to 1.42 at the tips of the leaves (a 2.58-fold increase), 0.85 in the middle section of the leaves (a 1.66-fold increase) and 1.98 at the bases of the leaves (a 3.88-fold

increase). When the expression of ZmRD22B is averaged out over the two internal controls basal expression (well-watered conditions) is approximately 0.35 in all the sections, while in the leaf tip transcript accumulation increases to 1.64, in the leaf middle it increases to 1.09 and at the base it increases to 2.09; with average fold increase of 4.68, 3.11 and 5.97-fold in LT, LM and LB respectively.

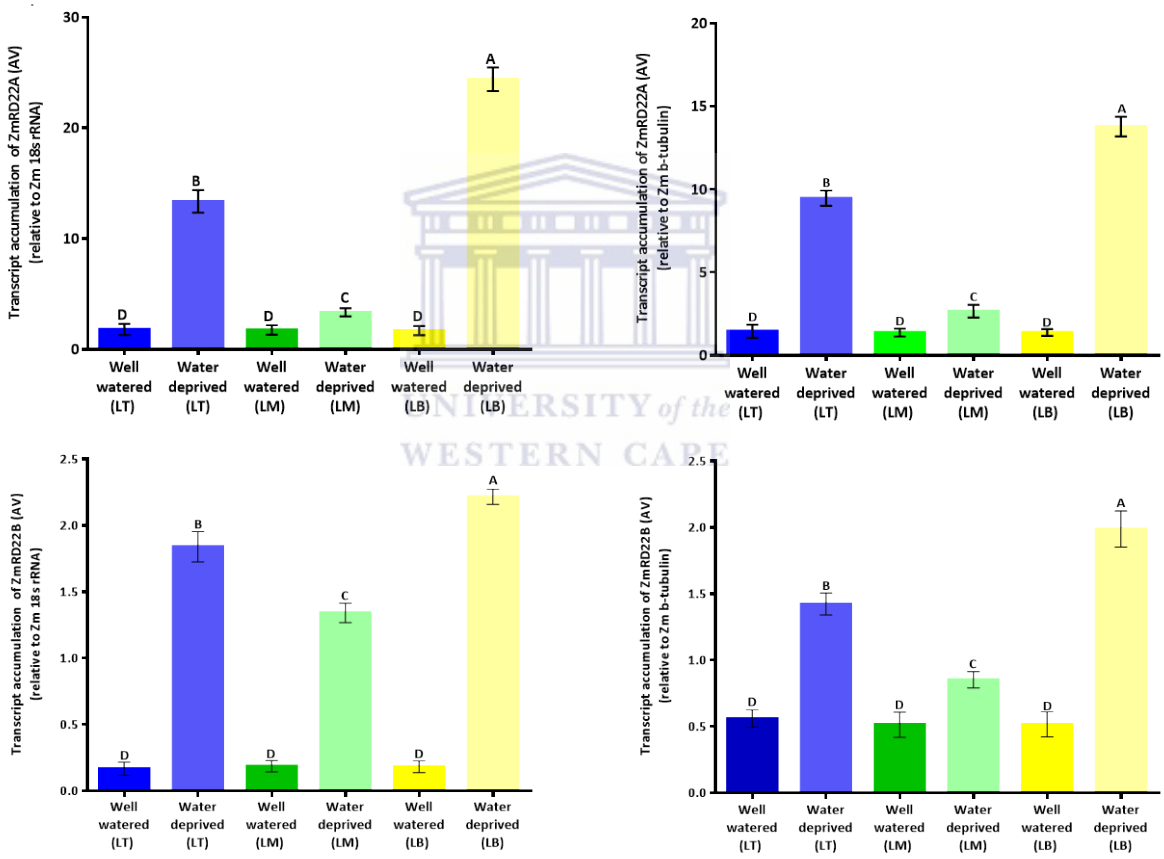

Figure 3.5: Relative RT-PCR quantification of ZmRD22A and ZmRd22B expression in leaf section in response to drought stress. (A) Expression of ZmRD22A relative to Zm 18s rRNA in response to water-deficit stress. (B) Relative expression of ZmRD22A in relation to Zm β-tubulin in response to water-deficit stress. (C) The expression of ZmRD22B relative to Zm 18s rRNA in response to water-deficit stress. (D) Quantitative measure to ZmRD22B expression in relation to Zm β-tubulin in response to water-deficit stress. LT (Leaf tip) well-watered (blue bar), water-deprived (pale blue bar), LM (leaf middle) well-watered (green bar) water-deprived (pale green bar), LB (leaf base) well-watered (yellow bar) water-deprived (pale yellow bar). The error bars signify standard deviation, bars with the same letters are statistically similar where $P < 0.05$.

3.4. Discussion

Plant growth rates are reduced when they are grown in soil with a limited water supply. Plants use physical changes such as rolling of the leaves to limit water loss. It has also been observed that, in conditions of limited water, plants restrict growth of the vegetative tissue in favour of developing more extensive root networks in an attempt to access water which may be in deeper soil layers (Davies, Bacon *et al.* 2000). This was observed in the maize seedlings which were grown in water-deprived soil, as is evident by the stunted vegetative tissue and more developed primary and lateral/seminal root systems. This stunting of growth is evident when a comparison is made to the well-watered plants which had 0.51 and 0.56-fold larger vegetative tissue and root systems, respectively, than the water-deprived plants. The water-deprived seedlings also exhibited leaf rolling and had a blueish tinge to the leaves (Figure 3.1). This is attributed to the degradation of chlorophyll during drought stress conditions and the plant pigment anthocyanin becoming more dominant (Steyn, Wand *et al.* 2002) . The reduction in chlorophyll content suffered during drought stress in another contributing factor in growth reduction. Aside from the physical difference between plants grown in the presence of sufficient water and those deprived of water, there are also biochemical differences that include a decrease in relative water content, an increase in H_2O_2 content coupled with a proportional increase in MDA content and a decrease in the number of viable cells in both vegetative and root tissue. Changes in these "drought stress indicators" were observed in the maize seedling subjected to water deficit stress. These seedlings exhibited RWC of approximately 49% and 48% in the leaves and roots, respectively, indicating an approximate decrease in the water content of 0.57-fold in comparison to the RWC of approximately 85% in the leaves and roots of seedlings supplied with sufficient water

(Figure 3.2.A). As explained by Alizade (2002) leaf RWC is a useful measure of drought stress intensity. The relevance to RWC as a measure of drought stress is further supported by work conducted by Arjenaki and Jabbari *et al.*(2012), who showed that wheat genotypes which were drought-sensitive had a much lower RWC when grown under drought conditions in comparison to drought tolerant wheat genotypes. Changes in the H_2O_2 content of plants is another indication of abiotic stress. This is due to over production of ROS (reactive oxygen species), thus it can be stated that the more severe the stress, the larger the build-up of H_2O_2 will be (Jubany-Marí, Munné-Bosch *et al.* 2009). The relationship between increased H_2O_2 content and drought stress provide insight into the 2.66 and 3.77-fold increase in H_2O_2 in the leaves and roots of maize seedlings deprived of water (Figure 3.2.B). The correlation between increased H_2O_2 content and drought stress was also shown by Chugh and Kaur *et al.*(2011) in their study the content of H_2O_2 in maize seedlings increased after the imposition of drought stress. In the same study, a relationship was shown between increased H_2O_2 content and the lipid peroxidation by-product, MDA. Similarly, when the MDA content was measured in well-watered and water-deprived seedlings there was a significant increase in MDA in both the leaves and roots of the water deprived seedlings. MDA content in the water-deprived plants increased 1.44 and 1.55-fold in the leaves and roots respectively (Figure 3.2.C), similarly to results shown is an experiment conducted by Avramova and AbdElgawad *et al.*(2015) who showed that MDA accumulates at different rates in the meristem, elongation and mature zones of maize leaves under drought stress. As MDA is a by-product of lipid peroxidation, it can be assumed that high concentrations of MDA would be indicative of extensive damages to cellular membranes, which inevitably

culminates in cell death. This was observed in the water-deprived seedling, where H_2O_2 and MDA contents increased along with an increase in the number of non-viable cells (figure 3.2.D).

A similar phenomenon was shown to occur when plants are exposed to high temperatures, as illustrated by a study conducted by Hasanuzzaman and Nahar *et al.*(2013). The reduction in RWC and increases in abiotic stress markers provide sufficient evidence that the water-deprived plants experienced water deficit stress. Having established this, it is fair to assume that changes in the transcript accumulation of ZmRD22A and ZmRD22B can be attributed to the effects of water deficit stress. The spatial and temporal accumulation of ZMRd22A and ZmRD22B transcripts was examined using both semi-quantitative and quantitative techniques. Semi-quantitative analysis showed that basal transcript accumulation of both genes is quite low in the leaves and are not detectable in the roots under well-watered growth conditions (as shown in Figure 3.3). The imposition of water-deprivation stress induced the accumulation of both ZmRD22A and ZmRD22B transcripts in the leaves, however ZmRD22A exhibits a stronger response to water-deprivation. Transcript accumulation in the roots remained undetectable and unaffected by the imposition of water deficit stress for both genes, providing a clear indication the ZmRD22A and ZmRD22B are not expressed in the roots under well-watered or water deficit stress conditions. These results were confirmed by quantitative RT-PCR using two house-keeping genes as internal controls. The overall pattern of transcript accumulation was similar between the semi-quantitative and quantitative analyses, where both genes are expressed only in the leaves of well-watered and water-deprived seedlings, providing further indication that ZmRD22A and ZmRD22B are exclusively expressed in the leaves. Similar results were shown in a study conducted by Harshavaedhan and Van Son *et al.*(2014), where semi-quantitative RT-PCR and

quantitative RT-PCR was used to examine the spatial and temporal expression patterns of AtRD22 (a characterised RD22-like protein). In that study, it was also found that the expression of AtRD22 is restricted to the aerial parts of the plants and that the expression of the gene is up-regulated in response to drought. Although the semi-quantitative and quantitative RT-PCR exhibit similar spatial and temporal transcript accumulation patterns the detected degree to which water deficit stress induces the transcript accumulation of the genes differs depending on the analysis method. The semi-quantitative analysis showed that transcript accumulation of the target genes in response to water deficit stress is statistically similar, as seen in Figure 3.3. However when the result of quantitative analysis of transcript accumulation is considered, the accumulation of ZmRD22A transcripts is 10-fold more than that of ZmRD22B. The discrepancy between the two results contradicts the work carried out by Souza and Souza *et al.*(2009), which showed that statistically similar results are obtained when using semi-quantitative and quantitative RT-PCR was used to detect the MYCN gene in neuroblastomas. The contradiction of this study by the work conducted by Souza and Souza *et al.* (2009) could be attributed to the use of different DNA stains: GelRed was used in DNA visualisation in this study while Souza and Souza *et al.*made use of ethidium bromide; another contributing factor could be the use of different visualisation software (AlphaEase in the current study and Kodak 1-D image analysis software in the contradicting study), the method of analysis could also be a contributor to the contradicting results also. In spite of the discrepancy between the degrees of up-regulation by water deficit stress of the target genes, the fact that the genes' transcript accumulations are positively affected by the imposition of water-deprivation provides sufficient evidence that target genes do respond to water deficit stress. Following the analysis of transcript accumulation in whole organs, specific

sections of leaf tissue was used to determine if different zones/regions of the leaves have unique transcript accumulation patterns for the two maize RD22 genes. Regional transcript accumulation in response to water deficit stress for ZmRD22A and ZmRD22B was found to be the highest at the base of the leaf in relation to both internal controls. The region-specific accumulation of gene transcripts was also shown by Hung and Umstead *et al.*(2014). In this study, EaF82a was expressed differentially in Devil's ivy leaves, expression patterns followed the colour of the leaf section (green or yellow). In another study conducted by Pearce and Houlston *et al.*(1998), the expression of three cold-responsive genes was shown to vary in different regions of barley leaves, depending on the importance of the particular leaf section to the survival of the organ. The section-specific accumulation of ZmRD22-like transcripts could be the result of varying degrees of stress experienced at the different leaf regions/section i.e. the base and tips of the leaves could be suffering the effects of the stress to a greater extent than the middle. Similarly, the expression of a rice gene OsRZFP34 exhibits altered degrees of expression in response to temperature stress; here the gene's expression is more up-regulated in warmer parts of the leaf as a result of differing stomatal aperture (Hsu, Liu *et al.* 2014). Taking these studies into consideration, the region specific transcript accumulation of the two maize RD22-like genes could be caused by the increased effects of drought stress at the base and tips of the leaves. It is also possible that ZmRD22-like transcript accumulation is highest at the base of the leaves due to it being the actively growing part of the leaf making it vital for the continuation of growth once the stress has passed. Conclusively it can be stated that the aims of this study have been met as transcript accumulation was successfully measured using both quantitative and semi-quantitative PCR, these results however do not completely agree with the hypothesised out

comes as transcript accumulation of ZmRD22A and ZmRD22B were only up-regulated by water-deficit stress in the leaves and not in the roots as well as predicted.

Chapter 4: Examining the spatial and temporal expression pattern of GRMZM2G446170 and GRMZM5G800586 in response to exogenous ABA application

4.1. Introduction

The damaging effects of drought stress on crop yield and quality is a limiting factor to the global agricultural industry (Gornall, Betts *et al.* 2010). Developing an understanding of plant functioning under drought conditions is therefore important in the cultivation of crop plants which are more tolerant of abiotic stresses. It is known that plants express a wide range of defence genes in response to drought stress. Along with this the biosynthesis of several plant hormones is up-regulated in response to drought stress signals. These include abscisic acid (ABA), salicylic acid, cytokinins, brassionstreiods and auxins (Mittler 2002, Mahajan and Tuteja 2005, Peleg and Blumwald 2011). Abscisic acid, which is a 15 carbon weak acid, was first identified in the 1960s and was shown to be involved in the inhibition of growth in abscising cotton fruit and was referred to as "abscisin II" as well as in the photoperiodical induction of dormancy in the leaves of sycamore trees where it was referred to as "dromin" (Cutler, Rodriguez *et al.* 2010, Finkelstein 2013). After extensive study, it is now known that ABA is pivotal in the regulation of stomatal aperture size of guard cells, which aids in limiting water loss via transpiration during periods of drought (Zhang, Zhang *et al.* 2001, Desikan, Griffiths *et al.* 2002). Abscisic acid has also been shown to be involved in the induction of drought-responsive genes in *Arabidopsis thaliana* (Yoshida, Fujita *et al.* 2015), *Oryza sativa* (Rabbani, Maruyama *et al.* 2003) and *Glycine max* (Maruyama, Todaka *et al.* 2012). The induction of drought-responsive genes by ABA signals involves the binding of specific transcription factors to *cis*-acting elements such as AREB (Abscisic

acid Response Element Binding factors) and ABF (Abscisic acid Binding Factors) in the promoter regions of the drought-responsive genes (Fujita, Yoshida *et al.* 2013, Nakashima and Yamaguchi-Shinozaki 2013). However, there are several drought-induced genes which are not responsive to ABA. The induction of these genes are known to involve the binding of specific transcription factors to *cis*-acting elements such as DREB (Drought Response Element Binding factors) (Kidokoro, Watanabe *et al.* 2015). One of the drought-responsive genes which are inducible by ABA signals are the plant-specific RD22-like proteins, these proteins are members of the BURP-domain containing proteins family (Xu, Li *et al.* 2010b), identified in the model plant *Arabidopsis thaliana* (Abe, Urao *et al.* 2003), *Brassica napus* (Shunwu, Zhang *et al.* 2004) and G*lycine max* (Granger, Coryell *et al.* 2002). Two putative RD22-like proteins encoded by GRMZM2G446170 and GRMZM5G800586 have been identified and designated ZmRD22A and ZmRD22B, respectively. This study is aimed at elucidating the effect of exogenously applied ABA on the transcript accumulation of these genes, using semi-quantitative and quantitative methods. *In silico* analysis of the two genes completed in a previous study has revealed characteristics of the genes promoter regions which indicate that GRMZM2G446170 (ZmRD22A) is induced in an ABA-independent manner. As such, it is hypothesised that transcript accumulation of ZmRD22A will be unaffected by the exogenous application of ABA while the transcript accumulation of ZmRD22B will be positively affected by the same treatment since its putative promoter region contains AREB-like binding sites.

4.2. Methods and materials

4.2.1. Plant growth and exogenous ABA treatment

Promix media was prepared and placed in acrylic tubes as described in section 3.2.1. The water potential of the growth media was measured using the WP4C® as described in section 3.2.1. A water potential of -0.03 ± 0.008 MPa was used for the growth of the maize seedlings. Maize seeds (*Zea Mays* L. cv. CAP9001) were prepared and grown as described in section 3.2.1.

Once the seedling reached the V3 stage (when the plant has developed three leaves with leaf collars) of vegetative growth, they were treated with 50 µM abscisic acid (ABA). Two separate subsets were supplied with water and 0.05% methanol to act as a controls since the ABA was prepared in methanol and treatments with ABA in this set of experiments result in a final methanol concentration of 0.05%. The seedlings were treated in this way every 24 hours for a total of 72 hours, after which plants of similar height and developmental stage were selected to act as representatives of the 50 µM ABA treatment as well as the 0.05% methanol control and water control. Ten plants for each treatment was selected and the 2nd youngest leaves were separated from the rest of the plant. Another ten plants were harvested in the same way. However their leaves were divided into base (5 cm region at the base of the leaf), middle (5 cm section from the middle of the leaf) and tips (5 cm region from the tip of the leaf). Fresh whole organs were used to assay cell viability, the rest of the material was ground in liquid nitrogen and stored at -80°C.

4.2.2. Measurement of Cell Viability

Cell viability was evaluated in the 2nd youngest leaves of seedling treated with 50 µM ABA, 0.05% methanol or water using an assay described by Sanevas *et al.*(2007). Fresh tissue of 1 cm^2 in area from the broadest part of the 2nd youngest leaf was stained with 0.25 % (w/v) EvansBlue for 15 min at room temperature. The Evan's Blue was removed by pipetting, followed by three rinse cycles in distilled water of 10 min each time. The distilled water was removed and 1 % (w/v) SDS was added to the samples. The samples were incubated for 1 h at 55 °C, then cooled at room temperature for 15 min. The samples were centrifuged at 3000 *g* for 1 min, and 200 µl aliquots of the supernatant was then pipetted (in triplicate) into a 96 well-plate and absorbance at 600 nm was measured (with 1 % SDS used as a blank for which its $A_{600\ nm}$ values were subtracted from the $A_{600\ nm}$ values of the samples in order to obtain the final $A_{600\ nm}$ values of the samples).

4.2.3. Determination of H_2O_2 and Malondialdehyde Contents

H_2O_2 and Malondialdehyde (MDA) contents were measured in the 2nd youngest leaves treated with either 50 µM ABA, 0.05% methanol or water. The leaves were ground into fine powder in liquid nitrogen using a mortar and pestle that had been pre-cooled with the liquid nitrogen. The ground leaf material (500 mg) was then homogenized with 1 ml of cold 6 % (w/v) trichloroacetic acid (TCA), followed by centrifugation at 12,000 *g* for 30 min at 4 °C. The TCA extract was used for measurement (in triplicates) of H_2O_2 as described by Velikova *et al.*(2000) and MDA as described by Buege *et al.*(1978).

H_2O_2 content was assayed by homogenising 50 µl of TCA extract with 150 µl of reaction buffer containing 5 mM K_2HPO_4, pH 5.0 and 0.5 M KI. Reactions were incubated at 25 °C for 20 min,

followed by recording of absorbance readings in triplicate at 390 nm. H_2O_2 content was calculated using a standard curve constructed with the absorbance of H_2O_2 standards read at an absorbance of 390 nm. The MDA assay was performed by coalescing, 250 µl of TCA extract with 1 ml of 0.5 % 2-thiobarbituric acid (w/v) that had been prepared in 20 % TCA. The homogenate was incubated for 30 min at 95 °C, then cooled on ice for 10 min. The thiobarbituric acid reactive substances (TBRAS), reflective of MDA, were detected by reading their absorbance at 532 nm and subtracting nonspecific absorbance at 600 nm. The amount of MDA was calculated using a molar extinction coefficient of 155 $mM^{-1}cm^{-1}$.

4.2.4. Lignin content assay

The lignin content in the 2nd youngest leaves of maize seedling treated with 50 µM ABA, 0.05% methanol or water was measured using the acetyl bromide method as described by Moreira-Vilar and Siqueira-Soares *et al.*(2014). This was accomplished by first making a protein-free cell wall preparation by homogenising 300 mg of leaf material from the treated seedlings with 7 ml of 50 mM potassium phosphate buffer (PPB) at pH7. The solution was centrifuged at 1 400 *g* for 5 min to pellet the leaf material, after which the pellet was washed twice with 50 mM PPB (pH7). The pellet was then washed thrice in a solution of 50 mM PPB (pH7) and 1% (V/V) Triton X-100, followed by two washes in 1M NaCl made up with 50 mM PPB (pH7). The pellet was then rinsed twice with distilled H_2O and twice with acetone, after which it was dried at 60 °C for 24 hours. The material was pelleted by centrifugation at 1400 *g* for 5 min between each step. The lignin content in the leaf material was then assayed by homogenising 20 mg of the protein-free cell wall preparation in 500 µl of 25% (V/V) acetyl bromide in glacial acetic acid. The homogenate was incubated for 30 min at 70 °C and then cooled on ice for 5 min. To the cooled mixture 900 µl of

2M NaOH, 100 µl of 5 M Hydroxylamine-HCl and 6 ml glacial acetic acid was added. The solution was centrifuged at 1400 *g* for 5 min and the absorbance was measured at 280 nm in triplicate, a blank was prepared containing all of the assay components excluding the protein-free cell wall preparation. Lignin content was calculated using a standard curve of alkali lignin (Sigma-Aldrich) and the result were expressed as *mg* of lignin per *g* of cell wall.

4.2.5. Evaluation of the effect of exogenous ABA applications on the transcript accumulation of ZmRD22A and ZmRD22B

4.2.5.1. Total RNA isolation

Turnover of the mRNA transcripts for ZmRD22A and ZmRD22B in response to exogenous ABA application was investigated in the 2nd youngest leaves of maize CAP9001 seedlings by semi-quantitative reverse transcription polymerase chain reaction (Semi-q-RT-PCR). Powdered plant material generated by grinding plant tissue in liquid nitrogen was used to isolate total RNA from leaf tissue. Total RNA was isolated using the Direct-zol™ RNA mini-prep kit (Zymo Research) according to the instructions of the manufacturer. RNase-free DNase I (Zymo Research) was used to remove DNA from the isolated RNA as specified by the manufacturer. RiboLock® RNase Inhibitor (Thermo Scientific) was added to prevent RNase-mediated degradation of the RNA.

4.2.5.2. First strand cDNA synthesis

First strand cDNA synthesis was accomplished using 500 ng of total RNA from the 2nd youngest leaves of seedling treated with either 50 µM ABA, 0.05% methanol or water. The total RNA was mixed with Oligo (dT)18 universal primers (Thermo Scientific) at a final concentration of 100 pmol, and then made up to 12.5 µl with nuclease-free water. To this, reaction buffer and dNTP Mix (thermos Scientific) was added to a final concentration of 1X and 1 mM respectively. RNA

degradation was prevented by the adding 20 U of RiboLock®. For 1st strand cDNA synthesis 200 U of RevertAid™ Reverse Transcriptase (Thermo Scientific) was used. The reaction was carried out at 42 °C for 60 minutes after which the reaction was terminated by incubation at 70 °C for 10 minutes as described by the manufactures' instructions.

4.2.5.3. Semi-quantitative PCR analysis of ZmRD22A and ZmRD22B transcript levels

PCR was carried out independently for ZmRD22A and ZmRD22B. This was done using 2 µl of 1st strand cDNA (synthesised from the plants treated with ABA and their controls) as template. A negative control containing 2 µl of nuclease-free water was included to rule out false positive results. PCR was done as described in section 3.2.5.3. The PCR products were size-fractionated on a 1% agarose gel and analysed as described in section 3.2.5.3.

4.2.5.4. Quantitative PCR analysis of ZmRD22A and ZmRD22B transcript levels

Quantitative measurement of ZmRD22A and ZmRD22B transcript level changes in response to ABA treatment was carried out as described in section 3.2.5.4, using cDNA made from RNA isolated from the leaves of ABA-treated plants together with their corresponding controls. Expression levels were expressed as ratios relative to the values of the control samples, with expression levels of the internal control genes as the reference.

4.2.6. Statistical analysis of results

The statistical validity of all the data was tested by means of a One-way analysis of variance (ANOVA) and the Tukey-Kramer test at 5% level of significance was completed to compare the means using GraphPad Prism 6.01 software.

4.3. Results

4.3.1. Examining the effect of exogenous ABA application of the stress status of maize seedlings

The effect of exogenous ABA application on the abiotic stress status of maize seedlings were measured by assaying four molecular indictors of water deficit stress. These stress indicators include changes in cellular H_2O_2 content, lipid peroxidation measured by as MDA (a lipid peroxidation by-product) content, changes in cell viability and the lignin content of the cell walls of treated seedlings. As shown in Figure 4.1.A, it was found that the water control and methanol control had the same effect on H_2O_2 content, measured at approximately 10 µmol.mg^{-1} of leaf material. When cellular H_2O_2 was measured in the 2nd youngest leaves of maize seedling subjected to the exogenous application of 50 µM ABA, a 1.89-fold increase in H_2O_2 was detected. As with the H_2O_2 measurement both the water control and methanol control had similar MDA content. A significant response to the ABA treatment was detected in which MDA content was measured at 27.59 nmol.g^{-1} of leaf material (Figure 4.1.B), a 1.49-fold increase in MDA content in comparison to the control treatments. The number of non-viable cells was assayed by Evans Blue staining, a dye which is only able to cross cell membranes which have been damaged. These results are shown in Figure 4.1.C and from the graph it can be seen that water and 0.05% methanol had an insignificant effect on the seedling's cell viability. ABA, however increased the number of non-viable cells in the tissue of the 2nd youngest leaves of maize seedlings, to a level 2-fold higher than in the seedling treated with water or 0.05% methanol. The final indicator of water deficit stress to be measured was the lignin content in the cell wall of the cells making up

the tissue of the 2nd youngest leaves of the studied seedlings. Here it was found that none of the treatments had an effect on cell wall lignin content (Figure 4.1.D).

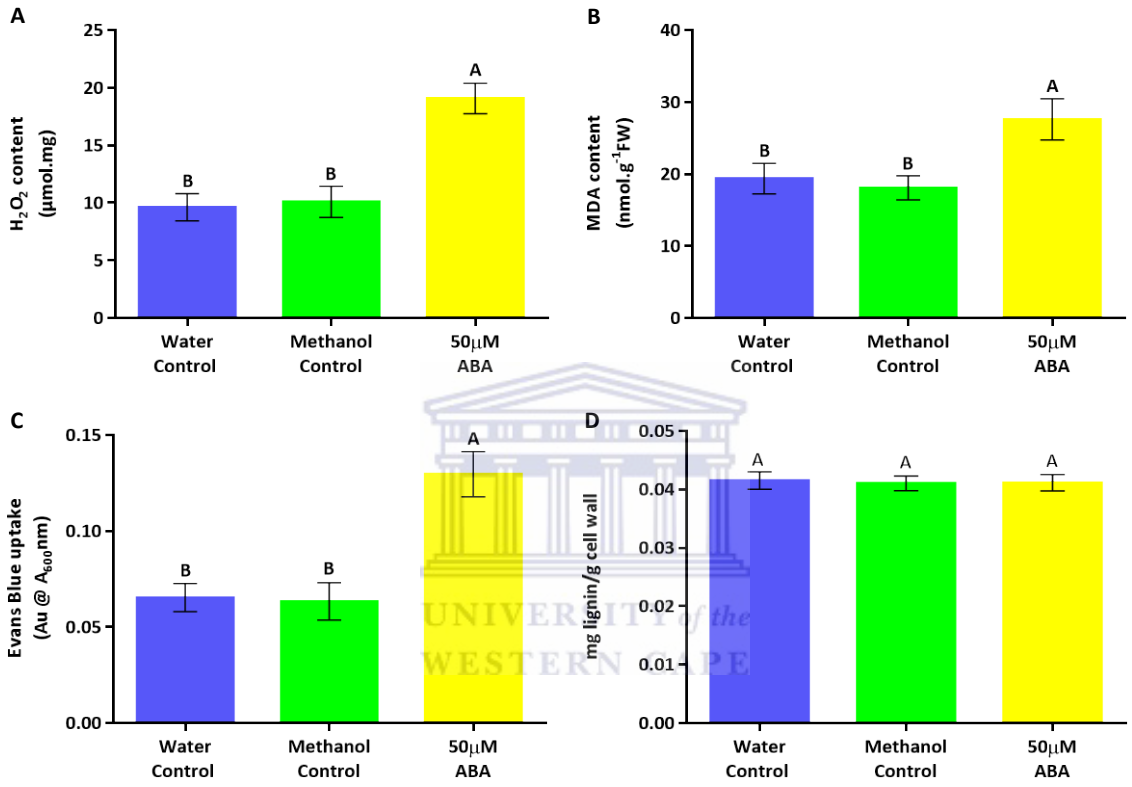

Figure 4.1: Measuring the stress status of maize seedlings after exogenous application of 50 µM ABA. (A) Measure of cellular H_2O_2 in µmol.mg of plant material, after the exogenous application of ABA to maize seedlings. (B) Changes in plasma membrane lipid peroxidation was a measure of cellular MDA content (measured in nmol.g^{-1} of fresh weight. (C) Evaluation of cell viability by Evans Blue uptake measured in Absorbance units (Au) at 600 nm. (D) Cell wall lignin content of maize seedlings subjected to water treatments, measured in *mg* of lignin per *g* of cell wall. In all the graphs the water control is represented by the blue bar, while the green and yellow bars represent the methanol control and ABA treatment respectively. The error bars signify standard deviation, bars with the same letters are statistically similar where $P < 0.05$.

4.3.2. Semi-quantitative RT-PCR analysis of the effect of exogenous ABA application on GRMZM2G446170 and GRMZM5G800586 transcript accumulation

Semi-quantitative RT-PCR analysis was conducted to examine the effect exogenously applied ABA has on the accumulation of ZmRD22A (GRMZM2G446170) and ZmRD22B (GRMZM5G800586) transcripts. In Figure 4.2.A, the gel image shows that there is no change in ZmRD22A transcript accumulation in response to the application of ABA. This is indicated by the similarity in intensity of the first three bands on the gel. When the transcript accumulation in measured in relation to Zm 18s rRNA (internal control gene) as indicated by the graph, still no change is observes. As shown by the graph at Figure 4.2.A transcript accumulation of ZmRB22A is an arbitrary value of approximately 0.09. The transcript accumulation of ZmRD22B was measured in the same way as shown in figure 4.2.B, where a positive change in transcript accumulation is seen in relation to the water and methanol controls. This change in ZmRD22B transcript accumulation is indicated by the increased intensity of the third band on the gel image as well as by the 4.52-fold increase inZmRD22B transcript accumulation from approximately 0.14 to 0.62 relative to Zm 18s rRNA as shown by the graph in Figure 4.2.B.

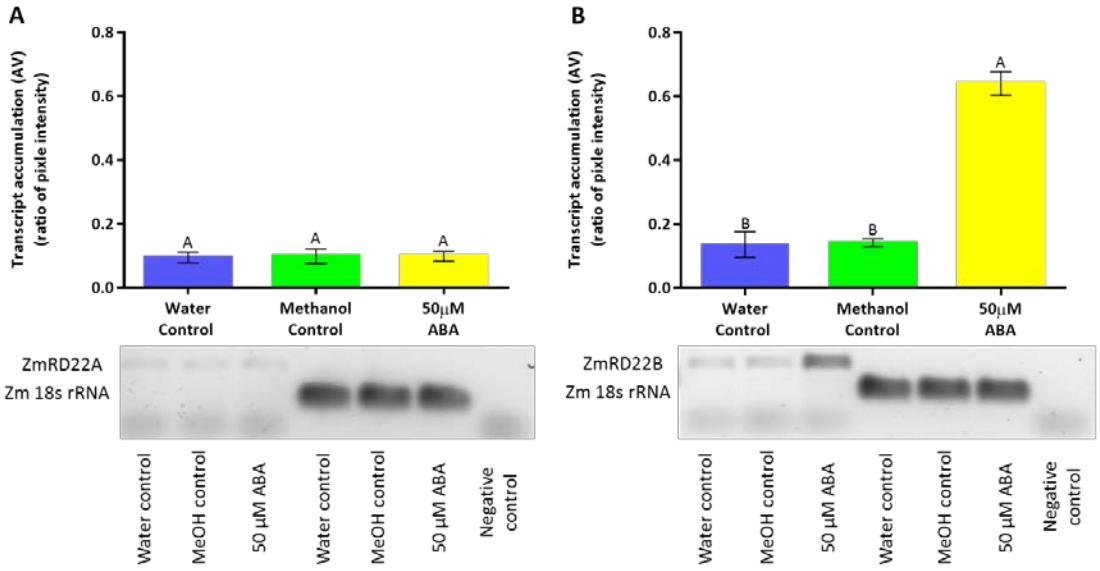

Figure 4.2: Semi-quantitative RT-PCR analysis of the effect exogenous ABA application has on transcript accumulation of ZmRD22A and ZmRD22B in the 2nd youngest leaves of maize seedlings. (A) Graph and gel image repressing the transcript accumulation of ZmRD22A in response to ABA application. Controls are indicated by the blue bar (water control) and the green bar (methanol control) and ABA treatment by the yellow bar. (B) Transcript accumulation of ZmRD22B in response to exogenous ABA application represented as a graph and a gel image. In the graph the controls are shown by the blue and green bars (water and methanol controls respectively) and the ABA treatment is shown by the yellow bar. Transcript accumulation is measured in arbitrary values. The error bars signify standard deviation, bars with the same letters are statistically similar where $P < 0.05$.

4.3.3. Quantitative RT-PCR analysis of GRMZM2G446170 and GRMZM5G800586 transcript accumulation in response to exogenous ABA application

The accumulation of ZmRD22A and ZMRD22B transcripts in response to exogenous ABA treatment was measured using relative qRT-PCR. This was done in relation to two maize internal control genes Zm 18s rRNA and Zm β-tubulin. The accumulation of ZmRD22A transcripts was found to be non-responsive to the exogenous application of ABA. This is shown in figures 4.3.A and B. Here, the transcript accumulation of ZmRD22A is shown to be statistically similar across the water/methanol controls and the ABA treatment, relative to Zm 18s rRNA transcript accumulation was approximately 1.32, while in relation to Zm β-tubulin it was approximately 1.55. Transcript accumulation of ZmRD22B was responsive to the ABA treatments, as seen in Figure 4.3.C, which provides a graphic view of ZmRD22B transcript accumulation relative to Zm

18s rRNA. Basal levels of ZmRD22B were approximately 2.4. In the 2nd youngest leaves of the seedlings treated with 0.05% methanol, ZmRD22B transcript accumulation was determined to be 1.99, the water control resulted in a statistically similar ZmRD22B transcript accumulation. When ABA was applied to maize seedlings the transcript accumulation of ZmRD22B increased 12.5-fold in relation to the control treatments, relative to Zm 18s rRNA. A similar trend in ZmRD22B transcript accumulation was observed relative to Zm β-tubulin in the 2nd youngest leaves of maize seedlings exposed to ABA as seen in Figure 4.3.D. In relation to Zm β-tubulin, basal ZmRD22B transcript levels (water control) were approximately 2.28 while transcript accumulation in response to the methanol control was 2.03. When measuring ZmRD22B transcript accumulation in response to ABA treatment, an increase of 11.5-fold was observed compared to basal transcript accumulation levels, relative to Zm β-tubulin.

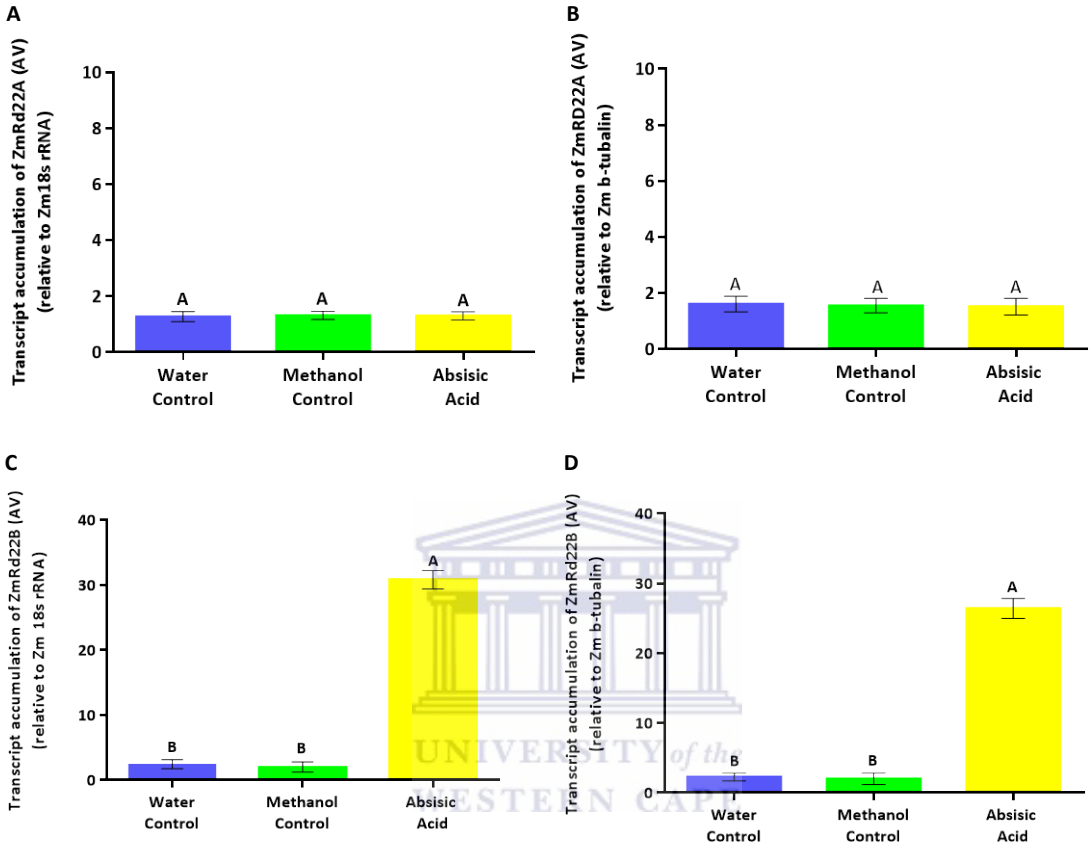

Figure 4.3: Quantitative RT-PCR analysis of ZmRD22A and ZmRD22B transcript accumulation in response to the exogenous application of ABA. (A) ZmRD22A transcript accumulation relative to Zm 18s rRNA in the 2nd youngest leaves of maize seedlings treated with ABA.(B) Graphic representation of ZmRD22A transcript accumulation, calculated in relation to Zm β-tubulin in response to exogenous treatment of maize seedlings with ABA. (C) Effect of ABA on transcript accumulation of ZmRD22B relative to Zm 18s rRNA in response to the application of ABA to maize seedlings. (D) ZmRD22B transcript accumulation relative to Zm β-tubulin in the 2nd youngest leaves of maize seedlings treated with ABA. In all the graphs, the water control is indicated by the blue bar, the methanol control by the green bar and the ABA treatment by the yellow bar. All measurements are given as arbitrary values. The error bars signify standard deviation, bars with the same letters are statistically similar where $P < 0.05$.

4.3.4. Determination of spatial and temporal changes in the transcript accumulation of GRMZM5G800586 in leaf regions by Quantitative RT-PCR in response to exogenous ABA treatments

As ZmRD22A seemed to be non-responsive to exogenous ABA treatments, the effect of ABA application on ZmRD22A transcript accumulation was not measured in different section of the leaf. As such, Figure 4.4.A and B show transcript accumulation of ZmRD22B in response to exogenous ABA application at the base of the leaves, in the middle of the leaves and at the tip of the leaves. In Figure 4.4.A, which is a representation of ZmRD22B transcript accumulation relative to Zm18s rRNA in response to ABA application. It can be seen that average transcript accumulation in response to the water control and methanol control was approximately 2.25 and 2.16 respectively in all three leaf regions. In the 2nd youngest leaves of maize seedling treated with ABA, ZmRD22B transcript accumulation levels were found to be approximately 18.11 at the tip of the leaves, 23.00 in the middle of the leaves and 27.52 at the base of the leaves. This implies that a 9.25, 9.50 and 11.46-fold increase in transcript accumulation occurs in response to the ABA treatments at the tip, middle and base region of the leaves, respectively. Transcript accumulation of ZmRD22B in relation to Zm β-tubulin and in response to ABA treatment exhibited a similar trend. However in relation to Zm β-tubulin, the response of ZmRD22B is less intense. As seen in Figure 4.4.B, the basal transcript accumulation and that in response to the 0.05% methanol control treatments remains the same throughout the leaf sections. Basal transcript accumulation in all leaf regions examined here was found to be approximately 1.73, while transcript levels in response to the methanol control treatment was approximately 1.58 across all leaf sections. In response to ABA treatment, a 5.18, 6.09 and 7.91-fold increase in ZmRD22B transcripts accumulation levels was observed at the tip, middle and base of the leaves, respectively.

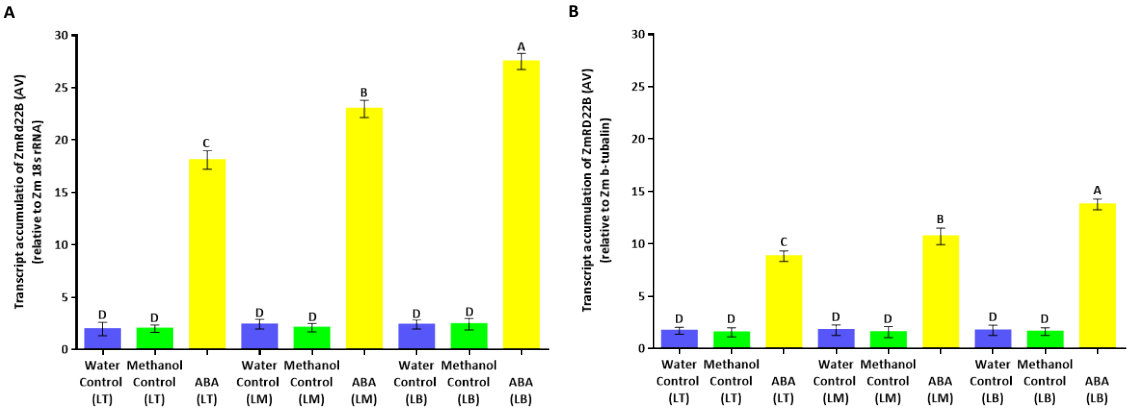

Figure 4.4: qRT-PCR measurement of ZmRD22B transcript accumulation in leaf sections in response to ABA treatments. (A) Spatial transcript accumulation of ZmRD22B transcripts relative to Zm 18s rRNA in the 2nd youngest leaves of maize seedlings exogenously treated with ABA. (B) Transcript accumulation of ZmRD22B relative to Zm β-tubulin in various leaf regions of the 2nd youngest leaves of ABA-treated maize seedlings. The water control is represented by the blue bar, the green bar represents the methanol control and the yellow bar indicates the ABA treatment. The leaf regions examined are as follows: leaf tips (LT), leaf middle (LM) and leaf base (LB). The error bars signify standard deviation, bars with the same letters are statistically similar where $P < 0.05$.

4.4. Discussion

In the previous chapter, the induction of ZmRD22A and ZmRD22B was shown to be responsive to drought. In the current chapter, the induction of these genes was examined in response to ABA signals. As such it was important to ensure that the seedlings used in this study were not suffering from drought stress. This was accomplished by assaying H_2O_2 content, MDA content, cell viability and lignin content. These stress indicator assays showed that the seedling which were supplied with water and methanol were not suffering from drought stress as leaf H_2O_2 content and MDA content were similar to those of seedlings not suffering from drought stress. As a result of the low H_2O_2 and MDA content in these seedling, Evans Blue uptake was low, which indicates that a large number of cells remained viable. When the same assays were carried out in maize seedlings treated, with 50 µM ABA, an increase in stress indicators was observed. This is attributed to the increased production of H_2O_2 in response to ABA application. The induction of H_2O_2 production

in response to ABA was shown by Pei and Murata *et al.*(2000) in a study which examined the involvement of ABA-induced H_2O_2 biosynthesis in stomatal guard cell aperture size in response to drought stress. An increase in Evan's blue uptake was observed, this may be perceived as ABA having a negative effect on cell viability. However Evan's blue uptake in ABA treated seedlings remain lower than in water-deprived seedlings as seen in chapter 3. The increase in Evan's blue uptake could be attributed to cell damage due to physical damage during sample preparation of the assay. In an attempt to determine whether the exogenous application of ABA was causing the seedlings to suffer stress, a cell wall lignin content assay was conducted. This was done as cell wall lignin content has been shown to increase in response to abiotic stress as shown in studies conducted by Hu and Li *et al.*(2009) as well as Le Gall and Philippe *et al.*(2015). The maize seedlings which were treated with ABA showed statistically similar cell wall lignin content, indicating that the seedling are not suffering abiotic stress. Having established that any gene response would be as a result of the exogenous ABA application and not abiotic stress, the transcript accumulation of ZmRD22A and ZmRd22B were measured via semi-qRT PCR. The results of the semi-qRT PCR shows that ZmRD22A is not responsive to ABA as the transcript accumulation of this gene remains statically similar across the treatments. The unresponsiveness of ZmRD22A is another indication that the seedling exposed to ABA were not suffering drought stress as it was shown in the previous chapter that ZmRD22A transcript accumulation increases when the seedlings are suffering the effects of water deficit. The unresponsive nature of ZmRD22A to ABA is not unheard of, because RD29A, a gene responsive to dehydration, isolated from *Arabidopsis thaliana* by Yamaguchi-Shinozaki and Shinozaki (1994) was shown to be up-regulated in response to drought stress but unresponsive to ABA. Other examples of genes which are drought-

responsive and expressed in an ABA-independent manner are COR78 and LTI78. These gene were shown by Nakashima and Yamaguchi-Shinozaki (2009) to be expressed in ABA-deficient Arabidopsis mutants in response to drought stress. When transcript accumulation of ZmRD22B was examined, an increase in transcripts was observed, in response to exogenous ABA application. The responsiveness of RD22-like genes to ABA stimuli has been shown in Arabidopsis and maize in separate studies conducted in Arabidopsis by Yamaguchi-shinozaki and Shinozaki (1993) and Wang and Zhou *et al.*(2012) respectively. The results obtained from semi-qRT PCR analysis was confirmed by qRT-PCR analysis. Here ZmRD22A was shown to be unresponsive to exogenous ABA application in relation to both Zm 18s rRNA and Zm β-tubulin. Examining the accumulation of ZmRD22B transcripts in response to exogenous ABA revealed a significant increase in comparison to the water and methanol controls relative to both Zm 18s rRNA and Zm β-tubulin. Similarly when ZmRD22B transcript accumulation was examined at the tips of leaves, in the middle of leaves and at the base of leaves, it was found that exogenous ABA application increased transcript accumulation. This experiment showed that ZmRD22B transcripts accumulate mostly at the base of the 2nd youngest leaves in response to exogenous ABA application, while the second highest level of ZmRD22B transcript accumulation is the middle of the leaves while the tips show the lowest ZmRD22B transcript accumulation.

Chapter 5: General conclusion

In light of global climate change and the resulting altered rainfall patterns, it is important to understand how crop plants respond to abiotic stress. The low rainfall received during the drought period currently being experienced in South Africa, is proving to be devastating to the 2015/2016 maize crop. To prevent a similar situation in the future, developing more drought tolerant maize cultivars is important. This can be accomplished by studying the changes maize plants undergo when grown in water-deprived conditions. Towards this goal, this study was aimed at the characterization of two putative maize RD22-like proteins designated ZmRD22A and ZmRD22B. This was done by conducting a bioinformatic analysis of ZmRD22A and ZmRD22B in reference to three experimentally characterized RD22-like proteins. The proteins were characterized based on the spatial and temporal transcript accumulation patterns. Transcript accumulation was studied in response to exposure to water deficit stress and exogenous ABA treatments using both semi-quantitative and quantitative analysis.

Upon completion of *in silico* analysis of the putative maize RD22-like proteins, it was found that they have several defining characteristics in common with the three experimentally characterised RD22-like proteins. Both the maize proteins have the domain organization of members of the RD22-like subfamily proteins, i.e. an N-terminal signal peptide, a highly conserved region followed by a variable region containing several TxV repeat units and most definitively a C-terminal BURP domain. The maize proteins were also shown, by *in silico* analysis, to be localized in the apoplast as occurs in the experimentally characterised RD22-like proteins. The shared sequence and domain similarities of these maize proteins to the characterised RD22-like proteins

suggest that the two maize proteins are BURP domain-containing proteins belonging to the RD22 subfamily. The *in silico* analysis is indicative of similar functionality between the maize proteins and the reference proteins based on their sequence features and subcellular localization. However, the exact function of this protein subfamily is yet to be elucidated.

Semi-quantitative RT-PCR and quantitative RT-PCR analyses have shown that ZmRD22A and ZmRD22B are expressed only in the aerial parts of the plants. Transcript accumulation of ZmRD22A and ZmRD22B were shown to be up-regulated in response to water deprivation. This suggests that the function is specific to the defence of the vegetative tissue against the effects of water deficit stress. Region-specific transcript accumulation of the two putative RD22-like genes in maize leaves is likely due to the differences in water relations at these regions or specific differences in expression of transcription factors regulating the expression of these RD22-like genes. The base of the leaf is the active growth region, which can be associated with higher water demand. Consequently, the effects of water deprivation would be more severe at the base and induction of defence protein expression may occur here before the rest of the leaf. Expression of RD22-like proteins at the tip of the leaves maybe an attempt at protecting it against the extensive water loss that may occur in this region because of less ability to retain water at this position due to the age of tissue at this region. However, experiments to demonstrate enhanced aging-related senescence and increased water loss in this region compared to the other regions need to be done to verify this speculation. Seedlings treated with ABA did not exhibit any symptoms of water deficit stress. Therefore, changes in ZmRD22A and ZmRD22B transcript accumulation in the ABA treatment experiment are due to the effect of exogenous application of ABA on the expression

of these two genes. These results suggest that ZmRD22A expression is induced in an ABA-independent manner while the expression of ZmRD22B is dependent on ABA.

It can be concluded from all the data collected from these experiments that ZmRD22A (GRMZM2G446170) and ZmRD22B (GRMZM5G800586) encode BURP domain-containing proteins of the RD22 subfamily. The expression of these proteins is confined to the vegetative tissue and the proteins are potentially active in defence against the effects of water deprivation stress. This is shown by their low basal transcript accumulation levels under well-watered conditions and up-regulation in response to water deficit stress and/or ABA (for which biosynthesis is induced by drought). Their spatial expression patterns suggest that their expression differs in various regions of the leaves, with high expression at the base rather than the tip in response to both ABA and drought.

The results obtained in this study provide insight into the regulation of ZmRD22A and ZmRD22B expression by water deficit. However, the function of the genes during water deficit stress has not been elucidated. As such, further study is required for functional characterization. In spite of this, the objectives of this study having been met. Functional characterisation can be undertaken in the future to establish the mechanism by which these proteins contribute to maize responses to drought and their potential as tools for enhancing maize drought tolerance. This could involve protein binding assays to determine if the function of these RD22-like proteins involves interaction with other proteins, and if so which proteins they interact with. This would involve the isolation of maize apoplastic proteins and the use of far Western blots to determine which proteins are involved in the interaction. Furthermore, as it has been shown that ZmRD22A and ZmRD22B are induced by water deficit stress, and thus the effects of up-regulating the expression

of these genes on the drought tolerance of maize plants can be studied alongside with the effects of down-regulation of the genes. This could lead to the development of maize cultivars with enhanced drought tolerance and deeper understanding of the mechanisms involved in the role of these proteins in drought responses of maize.

Chapter 6: References

Abe, H., Urao, T., Ito, T., Seki, M., Shinozaki, K. & Yamaguchi-Shinozaki, K. 2003. Arabidopsis AtMYC2 (bHLH) and AtMYB2 (MYB) Function as Transcriptional Activators in Abscisic Acid Signaling. *The Plant Cell Online,* 15**,** 63-78.

Abe, H., Yamaguchi-Shinozaki, K., Urao, T., Iwasaki, T., Hosokawa, D. & Shinozaki, K. 1997. Role of arabidopsis MYC and MYB homologs in drought- and abscisic acid-regulated gene expression. *The Plant Cell Online,* 9**,** 1859-68.

Afzal, I., Rauf, S., Basra, S. & Murtaza, G. 2008. Halopriming improves vigor, metabolism of reserves and ionic contents in wheat seedlings under salt stress. *Plant Soil Environ,* 54**,** 382-388.

Alizade A 2002. *Soil, Water and Plant Relationship* Mashhad, Iran Emam Reza University Press.

Almagro, L., Gómez Ros, L. V., Belchi-Navarro, S., Bru, R., Ros Barceló, A. & Pedreño, M. A. 2009. Class III peroxidases in plant defence reactions. *Journal of Experimental Botany,* 60**,** 377-390.

Anjum, N., Sofo, A., Scopa, A., Roychoudhury, A., Gill, S., Iqbal, M., Lukatkin, A., Pereira, E., Duarte, A. & Ahmad, I. 2015. Lipids and proteins—major targets of oxidative modifications in abiotic stressed plants. *Environmental Science and Pollution Research,* 22**,** 4099-4121.

Anjum, S. A., Xie, X.-Y., Wang, L.-C., Saleem, M. F., Man, C. & Lei, W. 2011. Morphological, physiological and biochemical responses of plants to drought stress. *African Journal of Agricultural Research,* 6**,** 2026-2032.

Arjenaki, F. G., Jabbari, R. & Morshedi, A. 2012. Evaluation of drought stress on relative water content, chlorophyll content and mineral elements of wheat (Triticum aestivum L.) varieties. *International Journal of Agriculture and Crop Sciences,* 4**,** 726-729.

Asada, K. 1999. THE WATER-WATER CYCLE IN CHLOROPLASTS: Scavenging of Active Oxygens and Dissipation of Excess Photons. *Annual Review of Plant Physiology and Plant Molecular Biology,* 50**,** 601-639.

Asada, K. 2006. Production and Scavenging of Reactive Oxygen Species in Chloroplasts and Their Functions. *Plant Physiology,* 141**,** 391-396.

Atkinson, N. J. & Urwin, P. E. 2012. The interaction of plant biotic and abiotic stresses: from genes to the field. *Journal of Experimental Botany*.

Avramova, V., Abdelgawad, H., Zhang, Z., Fotschki, B., Casadevall, R., Vergauwen, L., Knapen, D., Taleisnik, E., Guisez, Y., Asard, H. & Beemster, G. T. S. 2015. Drought Induces Distinct Growth Response, Protection, and Recovery Mechanisms in the Maize Leaf Growth Zone. *Plant Physiology,* 169**,** 1382-1396.

Banzai, T., Sumiya, K., Hanagata, N., Dubinsky, Z. & Karube, I. 2002. Molecular cloning and characterization of genes encoding BURP domain-containing protein in the mangrove, Bruguiera gymnorrhiza. *Trees,* 16**,** 87-93.

Bassüner, R., Bäumlein, H., Huth, A., Jung, R., Wobus, U., Rapoport, T., Saalbach, G. & Müntz, K. 1988. Abundant embryonic mRNA in field bean (Vicia faba L.) codes for a new class of seed proteins: cDNA cloning and characterization of the primary translation product. *Plant Molecular Biology,* 11**,** 321-334.

Batchelor, A., Boutilier, K., Miller, S., Hattori, J., Bowman, L., Hu, M., Lantin, S., Johnson, D. & Miki, B. 2002. SCB1, a BURP-domain protein gene, from developing soybean seed coats. *Planta,* 215**,** 523-532.

Bäumlein, H., Boerjan, W., Nagy, I., Bassfüner, R., Montagu, M., Inzé, D. & Wobus, U. 1991. A novel seed protein gene from Vicia faba is developmentally regulated in transgenic tobacco and Arabidopsis plants. *Molecular and General Genetics MGG,* 225**,** 459-467.

Bhattacharjee, S. 2012. The Language of Reactive Oxygen Species Signaling in Plants. *Journal of Botany,* 2012**,** 22.

Bita, C. E. & Gerats, T. 2013. Plant tolerance to high temperature in a changing environment: scientific fundamentals and production of heat stress-tolerant crops. *Frontiers in Plant Science,* 4.

Boerjan, W., Ralph, J. & Baucher, M. 2003. Lignin biosynthesis. *Annu Rev Plant Biol,* 54**,** 519-46.

Boudet, A.-M. 2000. Lignins and lignification: Selected issues. *Plant Physiology and Biochemistry,* 38**,** 81-96.

Bray, E. A. 1997. Plant responses to water deficit. *Trends in Plant Science,* 2**,** 48-54.

Bray, E. A. 2002. Abscisic acid regulation of gene expression during water-deficit stress in the era of the Arabidopsis genome. *Plant, Cell & Environment,* 25**,** 153-161.

Brummell, D. & Harpster, M. 2001. Cell wall metabolism in fruit softening and quality and its manipulation in transgenic plants. *In:* Carpita, N. C., Campbell, M. & Tierney, M. (eds.) *Plant Cell Walls.* Springer Netherlands.

Buege, J. A. & Aust, S. D. 1978. Microsomal lipid peroxidation. *Methods in enzymology,* 52**,** 302-310.

Burton, R. A., Zhang, X.-Q., Hrmova, M. & Fincher, G. B. 1999. A Single Limit Dextrinase Gene Is Expressed Both in the Developing Endosperm and in Germinated Grains of Barley. *Plant Physiology,* 119**,** 859-872.

Castro-Concha, L. A., Escobedo, R. M. & De Miranda-Ham, M. L. 2006. Measurement of cell viability in in vitro cultures. *Plant Cell Culture Protocols.* Springer.

Chang, W.-C., Chen, M.-H. & Lee, T.-M. 1999. 2, 3, 5-Triphenyltetrazolium reduction in the viability assay of Ulva fasciata (Chlorophyta) in response to salinity stress. *Botanical Bulletin of Academia Sinica,* 40.

Chaves, M. M., Pereira, J. S., Maroco, J., Rodrigues, M. L., Ricardo, C. P. P., Osório, M. L., Carvalho, I., Faria, T. & Pinheiro, C. 2002. How Plants Cope with Water Stress in the Field? Photosynthesis and Growth. *Annals of Botany,* 89**,** 907-916.

Chugh, V., Kaur, N. & Gupta, A. K. 2011. Evaluation of oxidative stress tolerance in maize (Zea mays L.) seedlings in response to drought. *Indian J Biochem Biophys,* 48**,** 47-53.

Cutler, S. R., Rodriguez, P. L., Finkelstein, R. R. & Abrams, S. R. 2010. Abscisic acid: emergence of a core signaling network. *Annu Rev Plant Biol,* 61**,** 651-79.

Dat, J., Vandenabeele, S., Vranova, E., Van Montagu, M., Inze, D. & Van Breusegem, F. 2000. Dual action of the active oxygen species during plant stress responses. *Cell Mol Life Sci,* 57**,** 779-95.

Davies, K. J. A. 2000. Oxidative Stress, Antioxidant Defenses, and Damage Removal, Repair, and Replacement Systems. *IUBMB Life,* 50**,** 279-289.

Davies, W. J., Bacon, M. A., Stuart Thompson, D., Sobeih, W. & González Rodríguez, L. 2000. Regulation of leaf and fruit growth in plants growing in drying soil: exploitation of the plants' chemical signalling system and hydraulic architecture to increase the efficiency of water use in agriculture. *Journal of Experimental Botany,* 51**,** 1617-1626.

Del Río, L. A., Sandalio, L. M., Corpas, F. J., Palma, J. M. & Barroso, J. B. 2006. Reactive Oxygen Species and Reactive Nitrogen Species in Peroxisomes. Production, Scavenging, and Role in Cell Signaling. *Plant Physiology,* 141**,** 330-335.

Desikan, R., Cheung, M. K., Bright, J., Henson, D., Hancock, J. T. & Neill, S. J. 2004. ABA, hydrogen peroxide and nitric oxide signalling in stomatal guard cells. *Journal of Experimental Botany,* 55**,** 205-212.

Desikan, R., Griffiths, R., Hancock, J. & Neill, S. 2002. A new role for an old enzyme: nitrate reductase-mediated nitric oxide generation is required for abscisic acid-induced stomatal closure in Arabidopsis thaliana. *Proceedings of the National Academy of Sciences,* 99**,** 16314-16318.

Ding, X., Hou, X., Xie, K. & Xiong, L. 2009. Genome-wide identification of BURP domain-containing genes in rice reveals a gene family with diverse structures and responses to abiotic stresses. *Planta,* 230**,** 149-163.

Emanuelsson, O., Nielsen, H., Brunak, S. & Von Heijne, G. 2000. Predicting Subcellular Localization of Proteins Based on their N-terminal Amino Acid Sequence. *Journal of Molecular Biology,* 300**,** 1005-1016.

Fam, S. S. & Morrow, J. D. 2003. The Isoprostanes: Unique Products of Arachidonic Acid Oxidation-A Review. *Current Medicinal Chemistry,* 10**,** 1723-1740.

Fan, L., Linker, R., Gepstein, S., Tanimoto, E., Yamamoto, R. & Neumann, P. M. 2006. Progressive Inhibition by Water Deficit of Cell Wall Extensibility and Growth along the Elongation Zone of Maize Roots Is Related to Increased Lignin Metabolism and Progressive Stelar Accumulation of Wall Phenolics. *Plant Physiology,* 140**,** 603-612.

Finkelstein, R. 2013. Abscisic Acid Synthesis and Response. *The Arabidopsis Book / American Society of Plant Biologists,* 11**,** e0166.

Finkelstein, R. R. & Rock, C. D. 2002. Abscisic Acid biosynthesis and response. *Arabidopsis Book,* 1**,** e0058.

Fujii, H., Verslues, P. E. & Zhu, J.-K. 2011. Arabidopsis decuple mutant reveals the importance of SnRK2 kinases in osmotic stress responses in vivo. *Proceedings of the National Academy of Sciences,* 108**,** 1717-1722.

Fujita, Y., Nakashima, K., Yoshida, T., Katagiri, T., Kidokoro, S., Kanamori, N., Umezawa, T., Fujita, M., Maruyama, K. & Ishiyama, K. 2009. Three SnRK2 protein kinases are the main positive regulators of abscisic acid signaling in response to water stress in Arabidopsis. *Plant and Cell Physiology,* 50**,** 2123-2132.

Fujita, Y., Yoshida, T. & Yamaguchi-Shinozaki, K. 2013. Pivotal role of the AREB/ABF-SnRK2 pathway in ABRE-mediated transcription in response to osmotic stress in plants. *Physiologia Plantarum,* 147**,** 15-27.

Gan, D., Jiang, H., Zhang, J., Zhao, Y., Zhu, S. & Cheng, B. 2011. Genome-wide analysis of BURP domain-containing genes in Maize and Sorghum. *Molecular Biology Reports,* 38**,** 4553-4563.

Garg, N. & Manchanda, G. 2009. ROS generation in plants: Boon or bane? *Plant Biosystems - An International Journal Dealing with all Aspects of Plant Biology,* 143**,** 81-96.

Gechev, T., Minkov, I. & Hille, J. 2005. Hydrogen Peroxide-induced Cell Death in Arabidopsis: Transcriptional and Mutant Analysis Reveals a Role of an Oxoglutarate-dependent Dioxygenase Gene in the Cell Death Process. *IUBMB Life,* 57**,** 181-188.

Gechev, T. S., Van Breusegem, F., Stone, J. M., Denev, I. & Laloi, C. 2006. Reactive oxygen species as signals that modulate plant stress responses and programmed cell death. *Bioessays,* 28**,** 1091-1101.

Ghezzi, P. & Bonetto, V. 2003. Redox proteomics: Identification of oxidatively modified proteins. *PROTEOMICS,* 3**,** 1145-1153.

Gill, S. S. & Tuteja, N. 2010. Reactive oxygen species and antioxidant machinery in abiotic stress tolerance in crop plants. *Plant Physiology and Biochemistry,* 48**,** 909-930.

Gornall, J., Betts, R., Burke, E., Clark, R., Camp, J., Willett, K. & Wiltshire, A. 2010. Implications of climate change for agricultural productivity in the early twenty-first century. *Philosophical Transactions of the Royal Society of London B: Biological Sciences,* 365**,** 2973-2989.

Gough, D. R. & Cotter, T. G. 2011. Hydrogen peroxide: a Jekyll and Hyde signalling molecule. *Cell Death and Dis,* 2**,** e213.

Granger, C., Coryell, V., Khanna, A., Keim, P., Vodkin, L. & Shoemaker, R. C. 2002. Identification, structure, and differential expression of members of a BURP domain containing protein family in soybean. *Genome,* 45**,** 693-701.

Grether-Beck, S., Bonizzi, G., Schmitt-Brenden, H., Felsner, I., Timmer, A., Sies, H., Johnson, J. P., Piette, J. & Krutmann, J. 2000. *Non-enzymatic triggering of the ceramide signalling cascade by solar UVA radiation*.

Guiltinan, M., Marcotte, W. & Quatrano, R. 1990. A plant leucine zipper protein that recognizes an abscisic acid response element. *Science,* 250**,** 267-271.

Harshavardhan, V. T., Seiler, C., Junker, A., Weigelt-Fischer, K., Klukas, C., Altmann, T., Sreenivasulu, N., Bäumlein, H. & Kuhlmann, M. 2014. AtRD22 and AtUSPL1, Members of the Plant-Specific BURP Domain Family Involved in Arabidopsis thaliana Drought Tolerance.

Harshavardhan, V. T., Van Son, L., Seiler, C., Junker, A., Weigelt-Fischer, K., Klukas, C., Altmann, T., Sreenivasulu, N., Bäumlein, H. & Kuhlmann, M. 2014. AtRD22 and AtUSPL1, Members of the Plant-Specific BURP Domain Family Involved in Arabidopsis thaliana Drought Tolerance. *PLoS ONE,* 9**,** e110065.

Hasanuzzaman, M., Nahar, K., Alam, M. M., Roychowdhury, R. & Fujita, M. 2013. Physiological, Biochemical, and Molecular Mechanisms of Heat Stress Tolerance in Plants. *International Journal of Molecular Sciences,* 14**,** 9643-9684.

Hattori, J., Boutilier, K. A., Campagne, M. M. L. & Miki, B. L. 1998. A conserved BURP domain defines a novel group of plant proteins with unusual primary structures. *Molecular and General Genetics MGG,* 259**,** 424-428.

Hayashi, M., Nito, K., Takei-Hoshi, R., Yagi, M., Kondo, M., Suenaga, A., Yamaya, T. & Nishimura, M. 2002. Ped3p is a Peroxisomal ATP-Binding Cassette Transporter that might Supply Substrates for Fatty Acid β-Oxidation. *Plant and Cell Physiology,* 43**,** 1-11.

Hirai, N., Yoshida, R., Todoroki, Y. & Ohigashi, H. 2000. Biosynthesis of abscisic acid by the non-mevalonate pathway in plants, and by the mevalonate pathway in fungi. *Biosci Biotechnol Biochem,* 64**,** 1448-58.

Hodges, D. M., Delong, J. M., Forney, C. F. & Prange, R. K. 1999. Improving the thiobarbituric acid-reactive-substances assay for estimating lipid peroxidation in plant tissues containing anthocyanin and other interfering compounds. *Planta,* 207**,** 604-611.

Hofmann, N. R. 2011. The Evolution of Photorespiratory Glycolate Oxidase Activity. *The Plant Cell Online,* 23**,** 2805.

Hsu, K. H., Liu, C. C., Wu, S. J., Kuo, Y. Y., Lu, C. A., Wu, C. R., Lian, P. J., Hong, C. Y., Ke, Y. T., Huang, J. H. & Yeh, C. H. 2014. Expression of a gene encoding a rice RING zinc-finger protein, OsRZFP34, enhances stomata opening. *Plant Molecular Biology,* 86**,** 125-37.

Hu, Y., Li, W. C., Xu, Y. Q., Li, G. J., Liao, Y. & Fu, F. L. 2009. Differential expression of candidate genes for lignin biosynthesis under drought stress in maize leaves. *J Appl Genet,* 50**,** 213-23.

Hung, C. Y., Umstead, M. L., Chen, J., Holliday, B. M., Kittur, F. S., Henny, R. J., Burkey, K. O. & Xie, J. 2014. Differential expression of a novel gene EaF82a in green and yellow sectors of variegated Epipremnum aureum leaves is related to uneven distribution of auxin. *Physiol Plant,* 152**,** 749-62.

Ingram, J. & Bartels, D. 1996. THE MOLECULAR BASIS OF DEHYDRATION TOLERANCE IN PLANTS. *Annual Review of Plant Physiology and Plant Molecular Biology,* 47**,** 377-403.

Iuchi, S., Kobayashi, M., Taji, T., Naramoto, M., Seki, M., Kato, T., Tabata, S., Kakubari, Y., Yamaguchi-Shinozaki, K. & Shinozaki, K. 2001. Regulation of drought tolerance by gene manipulation of 9-cis-epoxycarotenoid dioxygenase, a key enzyme in abscisic acid biosynthesis in Arabidopsis. *Plant J,* 27**,** 325-33.

Iwasaki, T., Yamaguchi-Shinozaki, K. & Shinozaki, K. 1995. Identification of a cis-regulatory region of a gene in Arabidopsis thaliana whose induction by dehydration is mediated by abscisic acid and requires protein synthesis. *Molecular and General Genetics MGG,* 247**,** 391-398.

Jacyn Baker, C. & Mock, N. 1994. An improved method for monitoring cell death in cell suspension and leaf disc assays using evans blue. *Plant Cell, Tissue and Organ Culture,* 39**,** 7-12.

Jamoussi, R. J., Elabbassi, M. M., Jouira, H., Hanana, M., Zoghlami, N., Ghorbel, A. & Mliki, A. 2014. Physiological responses of transgenic tobacco plants expressing the dehydration-responsive RD22 gene of Vitis vinifera to salt stress. *Turk J Bot,* 38**,** 268-280.

Joshi, C. P. 1987. An inspection of the domain between putative TATA box and translation start site in 79 plant genes. *Nucleic Acids Research,* 15**,** 6643-6653.

Jubany-Marí, T., Munné-Bosch, S., López-Carbonell, M. & Alegre, L. 2009. Hydrogen peroxide is involved in the acclimation of the Mediterranean shrub, Cistus albidus L., to summer drought. *Journal of Experimental Botany,* 60**,** 107-120.

Kasahara, H., Takei, K., Ueda, N., Hishiyama, S., Yamaya, T., Kamiya, Y., Yamaguchi, S. & Sakakibara, H. 2004. Distinct isoprenoid origins of cis- and trans-zeatin biosyntheses in Arabidopsis. *J Biol Chem,* 279**,** 14049-54.

Kidokoro, S., Watanabe, K., Ohori, T., Moriwaki, T., Maruyama, K., Mizoi, J., Myint Phyu Sin Htwe, N., Fujita, Y., Sekita, S. & Shinozaki, K. 2015. Soybean DREB1/CBF-type transcription factors function in heat and drought as well as cold stress-responsive gene expression. *The Plant Journal,* 81**,** 505-518.

Kim, J.-S., Mizoi, J., Yoshida, T., Fujita, Y., Nakajima, J., Ohori, T., Todaka, D., Nakashima, K., Hirayama, T. & Shinozaki, K. 2011. An ABRE promoter sequence is involved in osmotic stress-responsive expression of the DREB2A gene, which encodes a transcription factor regulating drought-inducible genes in Arabidopsis. *Plant and Cell Physiology,* 52**,** 2136-2146.

Kotchoni, S. O., Kuhns, C., Ditzer, A., Kirch, H.-H. & Bartels, D. 2006. Over-expression of different aldehyde dehydrogenase genes in Arabidopsis thaliana confers tolerance to abiotic stress and protects plants against lipid peroxidation and oxidative stress. *Plant, Cell & Environment,* 29**,** 1033-1048.

Krieger-Liszkay, A., Fufezan, C. & Trebst, A. 2008. Singlet oxygen production in photosystem II and related protection mechanism. *Photosynthesis Research,* 98**,** 551-564.

Lam, E. 2004. Controlled cell death, plant survival and development. *Nat Rev Mol Cell Biol,* 5**,** 305-315.

Le Gall, H., Philippe, F., Domon, J.-M., Gillet, F., Pelloux, J. & Rayon, C. 2015. Cell Wall Metabolism in Response to Abiotic Stress. *Plants,* 4**,** 112-166.

Levine, A., Tenhaken, R., Dixon, R. & Lamb, C. 1994. H2O2 from the oxidative burst orchestrates the plant hypersensitive disease resistance response. *Cell,* 79**,** 583-593.

Liu, N., Ding, Y., Fromm, M. & Avramova, Z. 2014. Different gene-specific mechanisms determine the 'revised-response' memory transcription patterns of a subset of A. thaliana dehydration stress responding genes. *Nucleic Acids Research,* 42**,** 5556-5566.

Mahajan, S. & Tuteja, N. 2005. Cold, salinity and drought stresses: An overview. *Archives of Biochemistry and Biophysics,* 444**,** 139-158.

Makino, A., Miyake, C. & Yokota, A. 2002. Physiological Functions of the Water–Water Cycle (Mehler Reaction) and the Cyclic Electron Flow around PSI in Rice Leaves. *Plant and Cell Physiology,* 43**,** 1017-1026.

Maruyama, K., Todaka, D., Mizoi, J., Yoshida, T., Kidokoro, S., Matsukura, S., Takasaki, H., Sakurai, T., Yamamoto, Y. Y. & Yoshiwara, K. 2012. Identification of cis-acting promoter elements in cold-and dehydration-induced transcriptional pathways in Arabidopsis, rice, and soybean. *DNA research,* 19**,** 37-49.

Matus, J. T., Aquea, F., Espinoza, C., Vega, A., Cavallini, E., Dal Santo, S., Cañón, P., De La Guardia, A. R.-H., Serrano, J. & Tornielli, G. B. 2014. Inspection of the Grapevine BURP Superfamily Highlights an Expansion of RD22 Genes with Distinctive Expression Features in Berry Development and ABA-Mediated Stress Responses.

Menkens, A. E., Schindler, U. & Cashmore, A. R. 1995. The G-box: a ubiquitous regulatory DNA element in plants bound by the GBF family of bZIP proteins. *Trends in Biochemical Sciences,* 20**,** 506-510.

Merlot, S., Mustilli, A.-C., Genty, B., North, H., Lefebvre, V., Sotta, B., Vavasseur, A. & Giraudat, J. 2002. Use of infrared thermal imaging to isolate Arabidopsis mutants defective in stomatal regulation. *The Plant Journal,* 30**,** 601-609.

Mittler, R. 2002. Oxidative stress, antioxidants and stress tolerance. *Trends in Plant Science,* 7**,** 405-410.

Moller, I. M. 2001. PLANT MITOCHONDRIA AND OXIDATIVE STRESS: Electron Transport, NADPH Turnover, and Metabolism of Reactive Oxygen Species. *Annu Rev Plant Physiol Plant Mol Biol,* 52**,** 561-591.

Møller, I. M., Jensen, P. E. & Hansson, A. 2007. Oxidative Modifications to Cellular Components in Plants. *Annual Review of Plant Biology,* 58**,** 459-481.

Montillet, J.-L., Chamnongpol, S., Rustérucci, C., Dat, J., Van De Cotte, B., Agnel, J.-P., Battesti, C., Inzé, D., Van Breusegem, F. & Triantaphylidès, C. 2005. Fatty Acid Hydroperoxides and H(2)O(2) in the Execution of Hypersensitive Cell Death in Tobacco Leaves. *Plant Physiology,* 138**,** 1516-1526.

Moreira-Vilar, F. C., Siqueira-Soares, R. D. C., Finger-Teixeira, A., De Oliveira, D. M., Ferro, A. P., Da Rocha, G. J., Ferrarese, M. D. L. L., Dos Santos, W. D. & Ferrarese-Filho, O. 2014. The Acetyl Bromide Method Is Faster, Simpler and Presents Best Recovery of Lignin in Different Herbaceous Tissues than Klason and Thioglycolic Acid Methods. *PLoS ONE,* 9**,** e110000.

Morimoto, K., Mizoi, J., Qin, F., Kim, J.-S., Sato, H., Osakabe, Y., Shinozaki, K. & Yamaguchi-Shinozaki, K. 2013. Stabilization of Arabidopsis DREB2A is required but not sufficient for the induction of target genes under conditions of stress.

Nakashima, K., Ito, Y. & Yamaguchi-Shinozaki, K. 2009. Transcriptional regulatory networks in response to abiotic stresses in Arabidopsis and grasses. *Plant Physiology,* 149**,** 88-95.

Nakashima, K. & Yamaguchi-Shinozaki, K. 2013. ABA signaling in stress-response and seed development. *Plant cell reports,* 32**,** 959-970.

Nakashima, K., Yamaguchi-Shinozaki, K. & Shinozaki, K. 2014. The transcriptional regulatory network in the drought response and its crosstalk in abiotic stress responses including drought, cold, and heat. *Frontiers in Plant Science,* 5**,** 170.

Navrot, N., Collin, V., Gualberto, J., Gelhaye, E., Hirasawa, M., Rey, P., Knaff, D. B., Issakidis, E., Jacquot, J.-P. & Rouhier, N. 2006. Plant Glutathione Peroxidases Are Functional Peroxiredoxins Distributed in Several Subcellular Compartments and Regulated during Biotic and Abiotic Stresses. *Plant Physiology,* 142**,** 1364-1379.

Olczak, M. & Wątorek, W. 2003. Two subfamilies of plant purple acid phosphatases. *Physiologia Plantarum,* 118**,** 491-498.

Pearce, R. S., Houlston, C. E., Atherton, K. M., Rixon, J. E., Harrison, P., Hughes, M. A. & Alison Dunn, M. 1998. Localization of Expression of Three Cold-Induced Genes, blt101, blt4.9, and blt14, in Different Tissues of the Crown and Developing Leaves of Cold-Acclimated Cultivated Barley. *Plant Physiology,* 117**,** 787-795.

Pei, Z.-M., Murata, Y., Benning, G., Thomine, S., Klusener, B., Allen, G. J., Grill, E. & Schroeder, J. I. 2000. Calcium channels activated by hydrogen peroxide mediate abscisic acid signalling in guard cells. *Nature,* 406**,** 731-734.

Peleg, Z. & Blumwald, E. 2011. Hormone balance and abiotic stress tolerance in crop plants. *Current Opinion in Plant Biology,* 14**,** 290-295.

Pennell, R. I. & Lamb, C. 1997. Programmed Cell Death in Plants. *The Plant cell,* 9**,** 1157-1168.

Petersen, T. N., Brunak, S., Von Heijne, G. & Nielsen, H. 2011. SignalP 4.0: discriminating signal peptides from transmembrane regions. *Nat Methods,* 8**,** 785-6.

Pinto, E., Sigaud-Kutner, T. C. S., Leitão, M. a. S., Okamoto, O. K., Morse, D. & Colepicolo, P. 2003. Heavy metal-induced oxidative stress in algae. *Journal of Phycology,* 39**,** 1008-1018.

Qin, F., Sakuma, Y., Tran, L.-S. P., Maruyama, K., Kidokoro, S., Fujita, Y., Fujita, M., Umezawa, T., Sawano, Y. & Miyazono, K.-I. 2008. Arabidopsis DREB2A-interacting proteins function as RING E3 ligases and negatively regulate plant drought stress–responsive gene expression. *The Plant cell,* 20**,** 1693-1707.

Quin, X. & Zeevaart, J. a. D. 1999. The 9-cis-epoxycarotenoid cleavage reaction is the key regulatory step of abscisic acid biosynthesis in water-stressed bean. *Proceedings of the National Academy of Sciences,* 96**,** 15354-15361.

Rabbani, M. A., Maruyama, K., Abe, H., Khan, M. A., Katsura, K., Ito, Y., Yoshiwara, K., Seki, M., Shinozaki, K. & Yamaguchi-Shinozaki, K. 2003. Monitoring Expression Profiles of Rice Genes under Cold,

Drought, and High-Salinity Stresses and Abscisic Acid Application Using cDNA Microarray and RNA Gel-Blot Analyses. *Plant Physiology,* 133**,** 1755-1767.

Rautengarten, C., Steinhauser, D., Büssis, D., Stintzi, A., Schaller, A., Kopka, J. & Altmann, T. 2005. Inferring Hypotheses on Functional Relationships of Genes: Analysis of the Arabidopsis thaliana Subtilase Gene Family. *PLoS Computational Biology,* 1**,** e40.

Rhoads, D. M., Umbach, A. L., Subbaiah, C. C. & Siedow, J. N. 2006. Mitochondrial Reactive Oxygen Species. Contribution to Oxidative Stress and Interorganellar Signaling. *Plant Physiology,* 141**,** 357-366.

Rinalducci, S., Murgiano, L. & Zolla, L. 2008. Redox proteomics: basic principles and future perspectives for the detection of protein oxidation in plants. *Journal of Experimental Botany,* 59**,** 3781-3801.

Rogé, P. & Astier, M. 2015. Changes in Climate, Crops, and Tradition: Cajete Maize and the Rainfed Farming Systems of Oaxaca, Mexico. *Human Ecology***,** 1-15.

Sakuma, Y., Maruyama, K., Osakabe, Y., Qin, F., Seki, M., Shinozaki, K. & Yamaguchi-Shinozaki, K. 2006a. Functional analysis of an Arabidopsis transcription factor, DREB2A, involved in drought-responsive gene expression. *Plant Cell,* 18**,** 1292-309.

Sakuma, Y., Maruyama, K., Qin, F., Osakabe, Y., Shinozaki, K. & Yamaguchi-Shinozaki, K. 2006b. Dual function of an Arabidopsis transcription factor DREB2A in water-stress-responsive and heat-stress-responsive gene expression. *Proceedings of the National Academy of Sciences,* 103**,** 18822-18827.

Sanevas, N., Sunohara, Y. & Matsumoto, H. 2007. Characterization of reactive oxygen species-involved oxidative damage in Hapalosiphon species crude extract-treated wheat and onion roots. *Weed biology and management,* 7**,** 172-177.

Schwartz, S. H., Qin, X. & Zeevaart, J. a. D. 2003. Elucidation of the Indirect Pathway of Abscisic Acid Biosynthesis by Mutants, Genes, and Enzymes. *Plant Physiology,* 131**,** 1591-1601.

Seo, M. & Koshiba, T. 2002. Complex regulation of ABA biosynthesis in plants. *Trends in Plant Science,* 7**,** 41-48.

Shao, H.-B., Chu, L.-Y., Jaleel, C. A., Manivannan, P., Panneerselvam, R. & Shao, M.-A. 2009. Understanding water deficit stress-induced changes in the basic metabolism of higher plants–biotechnologically and sustainably improving agriculture and the ecoenvironment in arid regions of the globe. *Critical reviews in biotechnology,* 29**,** 131-151.

Sharma, P., Jha, A. B., Dubey, R. S. & Pessarakli, M. 2012. Reactive Oxygen Species, Oxidative Damage, and Antioxidative Defense Mechanism in Plants under Stressful Conditions. *Journal of Botany,* 2012**,** 26.

Shen, Q. & Ho, T. H. 1995. Functional dissection of an abscisic acid (ABA)-inducible gene reveals two independent ABA-responsive complexes each containing a G-box and a novel cis-acting element. *The Plant Cell Online,* 7**,** 295-307.

Shinozaki, K. & Yamaguchi-Shinozaki, K. 1997. Gene Expression and Signal Transduction in Water-Stress Response. *Plant Physiology,* 115**,** 327-334.

Shinozaki, K. & Yamaguchi-Shinozaki, K. 2000. Molecular responses to dehydration and low temperature: differences and cross-talk between two stress signaling pathways. *Current Opinion in Plant Biology,* 3**,** 217-223.

Shinozaki, K. & Yamaguchi-Shinozaki, K. 2007. Gene networks involved in drought stress response and tolerance. *Journal of Experimental Botany,* 58**,** 221-227.

Shulaev, V. & Oliver, D. J. 2006. Metabolic and Proteomic Markers for Oxidative Stress. New Tools for Reactive Oxygen Species Research. *Plant Physiology,* 141**,** 367-372.

Shunwu, Y., Zhang, L., Zuo, K., Li, Z. & Tang, K. 2004. Isolation and characterization of a BURP domain-containing gene BnBDC1 from Brassica napus involved in abiotic and biotic stress. *Physiologia Plantarum,* 122**,** 210-218.

South African Weather Services. 2015. *Historical rain maps* [Online]. Available: http://www.weathersa.co.za/climate/historical-rain-maps [Accessed November 16 2015].

Souza, A. C. M. F., Souza, D. R. V., Sanabani, S. S., Giorgi, R. R. & Bendit, I. 2009. The performance of semi-quantitative differential PCR is similar to that of real-time PCR for the detection of the MYCN gene in neuroblastomas. *Brazilian Journal of Medical and Biological Research,* 42**,** 791-795.

Steyn, W., Wand, S., Holcroft, D. & Jacobs, G. 2002. Anthocyanins in vegetative tissues: a proposed unified function in photoprotection. *New Phytologist,* 155**,** 349-361.

Tang, Y., Ou, Z., Qiu, J. & Mi, Z. 2014. Putative signal peptides of two BURP proteins can direct proteins to their destinations in tobacco cell system. *Biotechnology Letters,* 36**,** 2343-2349.

Taulavuori, E., Hellström, E. K., Taulavuori, K. & Laine, K. 2001. Comparison of two methods used to analyse lipid peroxidation from Vaccinium myrtillus (L.) during snow removal, reacclimation and cold acclimation. *Journal of Experimental Botany,* 52**,** 2375-2380.

Tuteja, N., Singh, M. B., Misra, M. K., Bhalla, P. L. & Tuteja, R. 2001. Molecular Mechanisms of DNA Damage and Repair: Progress in Plants. *Critical Reviews in Biochemistry and Molecular Biology,* 36**,** 337-397.

Usda. 2004. *South Africa corn* [Online]. Available: http://www.usda.gov/oce/weather/pubs/Other/MWCACP/Graphs/South_Africa/South%20AfricaCorn.pdf [Accessed November 25

2015].

Van Breusegem, F. & Dat, J. F. 2006. Reactive Oxygen Species in Plant Cell Death. *Plant Physiology,* 141**,** 384-390.

Van Son, L., Tiedemann, J., Rutten, T., Hillmer, S., Hinz, G., Zank, T., Manteuffel, R. & Bäumlein, H. 2009. The BURP domain protein AtUSPL1 of Arabidopsis thaliana is destined to the protein storage vacuoles and overexpression of the cognate gene distorts seed development. *Plant Molecular Biology,* 71**,** 319-329.

Vatansever, F., De Melo, W. C. M. A., Avci, P., Vecchio, D., Sadasivam, M., Gupta, A., Chandran, R., Karimi, M., Parizotto, N. A., Yin, R., Tegos, G. P. & Hamblin, M. R. 2013. Antimicrobial strategies centered around reactive oxygen species – bactericidal antibiotics, photodynamic therapy, and beyond. *FEMS Microbiology Reviews,* 37**,** 955-989.

Velikova, V., Yordanov, I. & Edreva, A. 2000. Oxidative stress and some antioxidant systems in acid rain-treated bean plants: Protective role of exogenous polyamines. *Plant Science,* 151**,** 59-66.

Wang, H., Zhou, L., Fu, Y., Cheung, M. Y., Wong, F. L., Phang, T. H., Sun, Z. & Lam, H. M. 2012. Expression of an apoplast-localized BURP-domain protein from soybean (GmRD22) enhances tolerance towards abiotic stress. *Plant Cell Environ,* 35**,** 1932-47.

Wasilewska, A., Vlad, F., Sirichandra, C., Redko, Y., Jammes, F., Valon, C., Frey, N. F. D. & Leung, J. 2008. An Update on Abscisic Acid Signaling in Plants and More …. *Molecular Plant,* 1**,** 198-217.

Xiong, L., Lee, H., Ishitani, M. & Zhu, J.-K. 2002. Regulation of Osmotic Stress-responsive Gene Expression by theLOS6/ABA1 Locus inArabidopsis. *Journal of Biological Chemistry,* 277**,** 8588-8596.

Xiong, L., Schumaker, K. & Zhu, J. 2001. Cell signaling during cold, drought, and salt stress. *The Plant cell,* 14**,** S165-83.

Xiong, L. & Zhu, J.-K. 2003. Regulation of Abscisic Acid Biosynthesis. *Plant Physiology,* 133**,** 29-36.

Xu, B., Gou, J.-Y., Li, F.-G., Shangguan, X.-X., Zhao, B., Yang, C.-Q., Wang, L.-J., Yuan, S., Liu, C.-J. & Chen, X.-Y. 2013. A Cotton BURP Domain Protein Interacts With α-Expansin and Their Co-Expression Promotes Plant Growth and Fruit Production. *Molecular Plant,* 6**,** 945-958.

Xu, H., Li, Y., Yan, Y., Wang, K., Gao, Y. & Hu, Y. 2010a. Genome-scale identification of Soybean BURP domain-containing genes and their expression under stress treatments. *BMC Plant Biology,* 10**,** 197.

Xu, H., Li, Y., Yan, Y., Wang, K., Gao, Y. & Hu, Y. 2010b. Genome-scale identification of soybean BURP domain-containing genes and their expression under stress treatments. *BMC Plant Biol,* 10**,** 197.

Yamaguchi-Shinozaki, K. & Shinozaki, K. 1993. The plant hormone abscisic acid mediates the drought-induced expression but not the seed-specific expression of rd22, a gene responsive to dehydration stress in Arabidopsis thaliana. *Molecular and General Genetics MGG,* 238**,** 17-25.

Yamaguchi-Shinozaki, K. & Shinozaki, K. 1994. A novel cis-acting element in an Arabidopsis gene is involved in responsiveness to drought, low-temperature, or high-salt stress. *The Plant cell,* 6**,** 251-264.

Yamaguchi-Shinozaki, K. & Shinozaki, K. 2006. Transcriptional regulatory networks in cellular responses and tolerance to dehydration and cold stresses. *Annu. Rev. Plant Biol.,* 57**,** 781-803.

Yang, L., Wang, C. C., Guo, W. D., Li, X. B., Lu, M. & Yu, C. L. 2006. Differential expression of cell wall related genes in the elongation zone of rice roots under water deficit. *Russian Journal of Plant Physiology,* 53**,** 390-395.

Yang, W., Liu, X.-D., Chi, X.-J., Wu, C.-A., Li, Y.-Z., Song, L.-L., Liu, X.-M., Wang, Y.-F., Wang, F.-W., Zhang, C., Liu, Y., Zong, J.-M. & Li, H.-Y. 2011. Dwarf apple MbDREB1 enhances plant tolerance to low temperature, drought, and salt stress via both ABA-dependent and ABA-independent pathways. *Planta,* 233**,** 219-229.

Yoshida, T., Fujita, Y., Maruyama, K., Mogami, J., Todaka, D., Shinozaki, K. & Yamaguchi-Shinozaki, K. 2015. Four Arabidopsis AREB/ABF transcription factors function predominantly in gene expression downstream of SnRK2 kinases in abscisic acid signalling in response to osmotic stress. *Plant, Cell & Environment,* 38**,** 35-49.

Yoshida, T., Mogami, J. & Yamaguchi-Shinozaki, K. 2014. ABA-dependent and ABA-independent signaling in response to osmotic stress in plants. *Current Opinion in Plant Biology,* 21**,** 133-139.

Yoshimura, K., Masuda, A., Kuwano, M., Yokota, A. & Akashi, K. 2008. Programmed proteome response for drought avoidance/tolerance in the root of a C(3) xerophyte (wild watermelon) under water deficits. *Plant Cell Physiol,* 49**,** 226-41.

Yu, C. S., Chen, Y. C., Lu, C. H. & Hwang, J. K. 2006. Prediction of protein subcellular localization. *Proteins: Structure, Function, and Bioinformatics,* 64**,** 643-651.

Zhang, X., Zhang, L., Dong, F., Gao, J., Galbraith, D. W. & Song, C. P. 2001. Hydrogen peroxide is involved in abscisic acid-induced stomatal closure in Vicia faba. *Plant Physiol,* 126**,** 1438-48.

Zheng, L., Heupel, R. C. & Dellapenna, D. 1992. The beta subunit of tomato fruit polygalacturonase isoenzyme 1: isolation, characterization, and identification of unique structural features. *The Plant Cell Online,* 4**,** 1147-56.

Zhu, J.-K. 2002. Salt and drought stress signal transduction in plants. *Annual Review of Plant Biology,* 53**,** 247.

UNIVERSITY of the
WESTERN CAPE